UNIVERZITA KARLOVA V PRAZE

2. LÉKAŘSKÁ FAKULTA
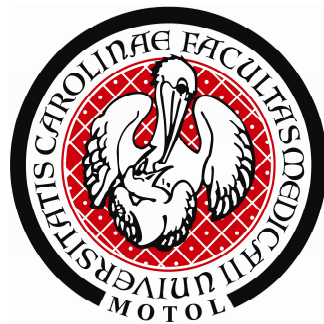
DIZERTAČNÍ PRÁCE

Funkce adaptorových molekul
v procesu leukemogenezy

MUDr. Karel Švojgr

školitel: doc. MUDr. Jan Zuna, PhD.

Praha 2012

Prohlášení:

Prohlašuji, že jsem závěrečnou práci zpracoval samostatně a že jsem uvedl všechny použité informační zdroje. Současně dávám svolení k tomu, aby tato závěrečná práce byla archivována v Ústavu vědeckých informací 2. lékařské fakulty Univerzity Karlovy v Praze a zde užívána ke studijním účelům. Za předpokladu, že každý, kdo tuto práci použije pro svou přednáškovou nebo publikační aktivitu, se zavazuje, že bude tento zdroj informací řádně citovat.

Souhlasím se zpřístupněním elektronické verze mé práce v Digitálním repozitáři Univerzity Karlovy v Praze (http://repozitar.cuni.cz). Práce je zpřístupněna pouze v rámci Univerzity Karlovy v Praze

V Praze, 4.6.2012

MUDr. Karel Švojgr

Poděkování:

Největší poděkování patří mému školiteli, doc. MUDr. Janu Zunovi, Ph.D., za profesionální vedení, cenné zkušenosti, které mi předal, a za možnost podílet se na vědecky zajímavých projektech. Dále děkuji prof. MUDr. Janu Trkovi, Ph.D. za možnost pracovat v laboratořích s velmi dobrým zázemím a celému kolektivu CLIP za více než přátelskou atmosféru. Velký dík patří doc. MUDr. Tomáši Kalinovi, Ph.D., za jeho kritické myšlení a přístup při řešení vědeckých experimentů. V neposlední řadě bych chtěl poděkovat mé ženě MUDr. Andree Švojgrové a dětem Markétce a Františkovi za trpělivost a toleranci.

Předmluva:

Předkládaná dizertační práce se věnuje především objasnění vlivu signalizačních adaptorových molekul na léčebnou odpověď u dětské akutní lymfoblastické leukémie. Pomocí metod kvantitativní polymerázové řetězové reakce, průtokové cytometrie a Western blotu byla stanovena exprese adaptorových molekul u hlavních podtypů akutní lymfoblastické leukémie a u nemaligních buněčných prekurzorů. Ukázali jsme, že molekula NTAL u T-akutní lymfoblastické leukémie potencuje glukokortikoidy indukovanou apoptózu. Na buněčném modelu v *in-vitro* experimentu jsme ověřili pozorovování a objasnili biologickou podstatu tohoto jevu. V záverečné části naší práce jsme ve fyziologických lidských prekurzorech T-lymfocytů definovali expresi signalizační molekuly CD148.

Obsah

Abstrakt:

Leukémie jsou nejčastějším nádorovým onemocněním u dětí. Na leukemogenezi se podílí faktory vrozené i získané a mimo jiné i aberantní buněčná signalizace. Transmembránové signalizační adaptorové molekuly by mohly být kauzální příčinou vzniku a propagace leukémie.

V první části naší práce jsme pomocí kvantitativní polymerázové řetězové reakce analyzovali expresi adaptorových molekul PAG, LAT a NTAL ve fyziologických lymfocytárních prekurzorech a v diagnostických vzorcích kostní dřeně dětských pacientů s akutní lymfoblastickou leukémií (ALL). V průběhu lymfocytárního vývoje se exprese většiny adaptorových molekul významně mění (vzestup LAT a pokles NTAL v průběhu vývoje T-lymfocytů; pokles PAG při vývoji B-lymfocytů). Obdobně se exprese adaptorových molekul velmi liší i v hlavních podtypech ALL. Především TEL/AML1 pozitivní akutní lymfoblastické leukémie mají unikátní profil exprese adaptorových molekul (vysoká exprese PAG a LAT, nízké exprese molekuly NTAL). V T-akutní lymfoblastické leukémii můžeme pomocí molekuly NTAL identifikovat 2 skupiny pacientů – ti, kteří příznivě odpoví na iniciální předléčbu prednisonem, mají většinou vysokou expresi molekuly NTAL. Na druhou stranu pacienti, kteří na iniciální předléčbu prednisonem odpoví špatně, mají většinou hladinu molekuly NTAL nízkou.

V druhé části naší práce jsme modelovali v *in-vitro* experimentech vliv molekuly NTAL na glukokortikoidy mediovanou apoptózu u T-akutní lymfoblastické leukémie. Použili jsme buněčnou linii Jurkat (T-akutní lymfoblastická leukémie, která neexprimuje protein NTAL) (Jurkat/wt) a vytvořili jsme buněčnou linii Jurkat/NTAL+, kam byl vnesen konstrukt stabilně produkující protein NTAL. Buněčnou smrt a buněčnou signalizaci jsme studovali pomocí průtokové cytometrie, Western blotu a kvantitativní polymerázové řetězové reakce. Při inkubaci buněčných linií Jurkat/wt a Jurkat/NTAL+ s methylprednisolonem je buněčná linie Jurkat/NTAL+ citlivější na podávaný kortikosteroid. Obdobně, po stimulaci T-buněčného receptoru, jsme pozorovali nižší procento přežívajících buněk u linie Jurkat/NTAL+ než u linie Jurkat/wt. Po stimulaci T-buněčného receptoru má Jurkat/NTAL+ linie vyšší hladinu fosforylované formy molekuly ERK a exprimuje na svém povrchu více aktivačního markeru CD69. Chemický inhibitor ERK molekuly U0126 téměř kompletně zastaví apoptózu po stimulaci T-buněčného receptoru. Především ale potlačí senzitizující efekt molekuly NTAL na kortikosteroidy indukovanou apoptózu. Molekula NTAL je tedy zřejmě tumor supresorem zvyšujícím citlivost leukemických buněk na podávané kortikosteroidy a molekula ERK je zodpovědná za tento proces.

V poslední části naší práce jsme se věnovali expresi signalizační molekuly CD148 v průběhu fyziologického thymocytárního vývoje. Na lidských thymech, za pomoci průtokové cytometrie, jsme detailně popsali změnu exprese CD148 v průběhu zrání T-lymfocytu. Nejvyšší expresi jsme nalezli v posledním stádiu vývoje T-lymfocytu, krátce před tím, než nezralý T-lymfocyt opouští thymus.

Abstract:

Acute lymphoblastic leukaemia is the most common malignancy in childhood. Various acquired and congenital factors are involved in leukemogenesis including aberrant cell signaling. Transmembrane adaptor molecules could play an important role in development and propagation of leukemia.

In a first part of our study, we analyzed an expression of adaptor molecules PAG, LAT and NTAL in physiological lymphocyte precursors and in diagnostic samples of different subtypes of childhood acute lymphoblastic leukemia (ALL). In physiological lymphocyte development the expression of adaptor molecules has significant dynamics (increase of LAT and decrease of NTAL in T-lymphocyte development; decrease of PAG in B-lymphocyte development). Similarly, in subtypes of childhood ALL the expression of adaptor molecules is very different. Especially, TAL/AML1 positive acute lymphoblastic leukemia has a unique expression profile of adaptor molecules (high expression of PAG and LAT, low expression of molecule NTAL). In T-cell acute lymphoblastic leukemia the expression of NTAL molecule identifies two groups of patients – those, who respond favourably to initial prednisone treatment, have higher level of NTAL comparing to patients, who respond to prednisone unfavourably. Those patients have low level of NTAL molecule expression.

In a second part of our study, we examined the role of NTAL molecule to glucocorticoid induced cell death in *in-vitro* experiments. We used T-cell acute lymphoblastic leukemia cell line Jurkat (Jurkat/wt) and we derived Jurkat cell line with stable NTAL expression (Jurkat/NTAL+). Cell signalling and cell death after methylprednisolone treatment and after T-cell receptor stimulation were analysed using flow cytometry, Western blot and quantitative polymerase chain reaction. Jurkat/NTAL+ cell line was more sensitive to glucocorticoid treatment than Jurkat/wt cell line. Similarly, after stimulation of T-cell receptor, we observed lower percentage of surviving Jurkat/NTAL+ cells than Jurkat/wt. Moreover, after T-cell receptor stimulation Jurkat/NTAL+ cells showed significantly higher level of ERK phosphorylation and of CD69 activation marker compared to Jurkat/wt. The ERK inhibitor U0126 almost completely abrogated T-cell receptor induced cell death and, importantly, reversed the sensitizing effect of the NTAL protein to methylprednisolone induced cell death.We conclude that NTAL is a tumor suppressor enhancing proximal signaling of leukemic blasts. ERK that is the key molecule responsible for increasing cell sensitivity to methylprednisolone induced cell death.

In a last part of our study, we focused on the expression of CD148 molecule during physiological thymocyte development. Using flow cytometry, we described in detail the change of CD148 expression during T-lymphocyte maturation. We found the highest expression of CD148 in the last stage of T-lymphocyte development, shortly before immature T-lymphocytes exit the thymus.

Akutní leukémie dětského věku

Nádorová onemocnění jsou po úrazech druhou nejčastější příčinou úmrtí v dětském věku [1]. Nejčastějším nádorovým onemocněním u dětí jsou v rozvinutých zemích leukémie [2]. Leukémie je zhoubnou klonální proliferací nezralých maligních lymfoidních či myeloidních buněk, kdy je jejich přirozený vývoj zablokovaný v určité fázi vývoje a klonální buňky se před tímto blokem hromadí [3]. Jinak řečeno, spíše než o rychlejší proliferaci maligních blastů, dochází při vzniku leukémie k bloku vyzrávání a k potlačení buněčné smrti (apoptózy). Maligní blastické buňky infiltrují kostní dřeň a parenchymové orgány, což vede k dysfunkci těchto tkání. Při masivním vyplavení blastů do periferní krve můžeme ve zkumavce pozorovat bílý prstenec tvořený nádorovými buňkami – obraz leukémie. Podle buněčné řady, ze které pocházejí, dělíme leukémie na lymfoblastické a myeloidní a dále na akutní a chronické. Nejčastějším podtypem leukémie, vyskytujícím se v dětském věku, je akutní lymfoblastická leukémie, která tvoří 75-80% případů. Zbytek tvoří akutní myeloidní leukémie a chronická myeloidní leukémie. Chronická lymfoblastická leukémie je v dětském věku extrémně vzácná [4]. V naší práci se dále budeme zabývat pouze akutní lymfoblastickou leukémií (ALL).

1. Akutní lymfoblastická leukémie

V České republice je diagnostikováno každým rokem přibližně 65 nových případů ALL [5] a přestože se může vyskytnout v kterémkoliv věku, její incidence je nejvyšší mezi batolaty a mladšími předškoláky [6]. Před rokem 1960 byl osud pacientů s ALL uniformně fatální [7]. První klinická studie léčby ALL byla vedena na počátku šedesátých let v USA [8] a od té doby se přežití dětí s ALL dramaticky zlepšilo. V současné době při použití moderních terapeutických postupů je ALL relativně dobře léčitelným maligním onemocněním, kdy v dlouhodobém horizontu žije přes 80% pacientů [2,5,8,9]. Tyto mimořádné výsledky byly dosaženy díky poznání etiopatogeneze ALL, použití a zapojení nových terapeutických postupů, znalosti optimálního dávkování a kombinace cytostatik a v neposlední řadě pomocí zlepšení podpůrné péče. I dnešní léčba ALL je však spojena s mnohými časnými i pozdějšími nežádoucími účinky. Úspěch léčby je tedy závislý i na znalosti prognostických faktorů ALL a co nejpřesnější stratifikaci pacientů do různých rizikových skupin, protože ne každý pacient potřebuje stejně intenzivní a tedy i stejně toxickou léčbu.

1.1 Etiopatogeneze

1.1.1 Genetické faktory a faktory vnějšího prostředí

Etiopatogeneze ALL je komplexní, roli hrají faktory jak genetické tak faktory vnějšího prostředí. Vrozené genetické syndromy jsou pravděpodobně zodpovědné za méně než 5% případů ALL. Mezi syndromy se zvýšeným rizikem ALL patří Downův syndrom [10], syndromy se zvýšenou chromozomální fragilitou (Fanconiho anémie, Bloomův syndrom, Nijmegen breakage syndrom), Li-Fraumeni syndrom a ataxia-teleangiektasia a neurofibromatóza [11]. Ovšem u většiny pacientů se na vzniku leukémie podílí mutace vzniklá de-novo. Z faktorů vnějšího prostřední je znám vyšší výskyt leukémie po expozici ionizujícího záření [12]. Jiné další potenciální noxy zodpovědné za vznik leukémie nebyly prokázány [13].

1.1.2 Prenatální původ ALL

Ke vniku leukémie jsou nejspíše zapotřebí alespoň dva zásahy. První vede ke vzniku takzvaného preleukemického klonu. Tento klon bývá často charakterizován přítomností specifického fúzního genu [13]. Preleukemický klon může vzniknout již v průběhu intrauterinního života [14,15], buňky tohoto klonu mají jistou proliferační výhodu, ale nevytváří obraz leukémie. Vznik preleukemického klonu je pravděpodobně relativně častý fenomén. Přibližně v 1-3% pupečníkových krví zdravých novorozenců byl nalezen fúzní gen TEL/AML1 [16,17], což je ovšem asi 100x více než skutečná incidence TEL/AML1 pozitivní ALL. Faktorem, který způsobí změnu preleukemického

klonu na kmen leukemický, je pravděpodobně dosud blíže nepopsaná abnormální imunologická odpověď na bakteriální či virové onemocnění [13,18]. Tato teorie vysvětluje významný vzestup incidence ALL mezi 2. až 5. rokem věku u dětí; pozdní expozice imunitního systému běžné infekci způsobí neadekvátní imunologickou reakci organismu, což pravděpodobně vede ke vzniku genetických změn zodpovědných za druhý zásah [13].

1.2. Klasifikace akutní lymfoblastické leukémie

1.2.1 Morfologie

Morfologicky se akutní lymfoblastické leukémie dělí podle FAB (francouzsko – americko – britské) klasifikace na leukémie s malými, homogenními L1 lymfoblasty, s L2 lymfoblasty různé velikosti, které mají často viditelná jadérka a s L3 lymfoblasty se silně bazofilní cytoplasmou a četnou vakuolizací. Kromě L3 lymfoblastů, které jsou patognomické pro zralou B-ALL, toto morfologické rozdělení nekoreluje s imunofenotypickou či cytogenetickou klasifikací a nelze ho použít k rizikové stratifikaci ALL [4,19].

1.2.2. Imunofenotyp

Díky monoklonálním protilátkám s navázanými imunoflorescenčními barvami a rozšíření průtokové cytometrie zažila v posledních letech velký rozmach imunofenotypická klasifikace ALL (klasifikace založená na stanovení povrchových a intracelulárních znaků). Pomocí průtokové cytometrie můžeme

v horizontu několika hodin od odběru kostní dřeně zpravidla říci, jestli se u pacienta skutečně jedná o maligní onemocnění a pokud ano, jedná-li se o ALL či o jiný typ hemoblastózy. Tato velmi rychlá informace je důležitá a obvykle dostačující k potvrzení maligního onemocnění, zařazení pacienta do léčebného protokolu a zahájení protinádorové léčby. Průtoková cytometrie je dále schopna určit, zda buňky ALL pocházejí z prekurzorů B či T-lymfocytů a rozlišit leukemické buňky podle zralosti. Maligní blasty totiž exprimují na svém povrchu antigeny, které odpovídají původnímu vývojovému stadiu, ze kterého vzešly. Dále se na nich vyskytují tak zvané aberantní antigeny – antigeny z jiného stupě zralosti lymfocytu či antigeny charakteristické pro jinou vývojovou linii. Příkladem aberantních antigenů je přítomnost myeloidních antigenů v B-prekurzorové ALL (BCP-ALL) [20,21]. Tyto aberantní antigeny mohou mít prognostický význam a zároveň pomáhají k lepší identifikaci leukemického klonu při sledování hladiny minimální (submikroskopické) zbytkové nemoci v kostní dřeni či periferní krvi [22-24]. V současné době se používá imunologická charakteristika ALL podle skupiny EGIL (European Group for Immunological characterisation of Leukemia) [25,26] a tato klasifikace je v rámci léčebných protokolů používána i v České republice. BCP-ALL se dělí na nejméně zralé pro-B-ALL, common-ALL a nejvíce zralé pre-B-ALL. ALL pocházející z prekurzorů T-lymfocytů (T-ALL) se dělí podle zralosti na pro, intermediate a zralé T-ALL a nově zařazenou skupinu early T-cell precursor (ETP) ALL [27]. Toto rozdělení má prognostický význam, obecně méně zralé leukémie (pro B-ALL, pro T-ALL a ETP-ALL) mají horší prognózu než leukémie pocházející ze zralejších prekurzorů [28].

1.2.3. Cytogenetika

V rámci stratifikace ALL do rizikových podskupin je zcela zásadní cytogenetické a molekulárně genetické vyšetření maligních blastů. Numerické či strukturální chromozomální změny jsou popisovány u 80 až 90% leukémií [19]. Mezi nejčastější numerické chromozomální změny patří hyperdiploidie, kterou diagnostikujeme u 25% pacientů s ALL. Hyperploidní leukemická buňka obsahuje mezi 53 až 58 chromozómy. Tento typ leukémie patří mezi podtypy s nejlepší prognózou. Naopak pacienti s hypodiploidií (počtem chromozomů pod 45) mají nízkou šanci na dlouhodobé přežití [29]. Zatímco klasické cytogenetické vyšetření trvá obvykle několik týdnů, informaci o ploidii ALL blastů máme nyní velmi rychle k dispozici pomocí průtokové cytometrie, která změří obsah DNA v buňce a výsledek se porovná s množstvím DNA v normální diploidní buňce. Výsledek je udáván jako DNA index. ALL s DNA indexem mezi 1,16 až 1,6 jsou ALL hyperdiploidní, naopak ALL s DNA indexem nižším než 1,0 jsou ALL hypodiploidní [4].

Strukturální genetické abnormality jsou u ALL velice časté a řada z nich se podílí na vzniku leukémie. Mezi nejčastější kauzální genetické změny patří translokace, delece, amplifikace a inverze, které v důsledku vedou k zástavě buněčné diferenciace a vzniku leukémie. Translokace t(12;21) (TEL-AML1, podle nové nomenklatury ETV6-RUNX1) se vyskytuje u jedné čtvrtiny pacientů s ALL a je tak nejčastější strukturální chromozomální změnou u ALL v dětském věku. Tato chromozomální translokace je takzvaně kryptická, není detekovatelná klasickým cytogenetickým vyšetřením. Nejčastěji ji dokazujeme molekulárně genetickým vyšetřením nebo metodou FISH (fluorescence in situ

13

hybridization). ALL s TEL/AML1 translokací mají velmi dobrou prognózu [30,31]. Druhou nejčastější strukturální chromozomální translokací vyskytující se přibližně u 5% ALL je translokace t(1;19) (E2A-PBX1), tato translokace ale v současných léčebných protokolech svůj prognostický význam ztratila. Mezi další časté chromozomální translokace s prognostickým významem patří BCR-ABL1 a translokace genu MLL, řadící BCP-ALL do vysokého rizika. Translokaci t(9;22) (BCR-ABL1) nese přibližně 5% pacientů a tato translokace vede k upregulaci tyrozinové kinázy ABL [32] a dysregulaci buněčné signalizace. Součástí moderní léčby BCR-ABL1 pozitivní leukémie jsou tyrozin kinázové inhibitory [33,34]. Strukturální abnormality lokusu 11q23 (obsahujícího MLL gen) mají především kojenecké leukémie a leukémie sekundární, celkově se na skladbě ALL podílí přibližně 5%. MLL gen má více jak 100 fúzních partnerů mezi nejčastěji se vyskytující translokace patří t(4;11)(q21;q23) a dále t(11;19)(q23;p13.3) a t(9;11)(p22;q23) [35].

Na etiopatogenezi T-ALL se také podílejí rekurentní chromozomální aberace, translokace a delece [36,37]. Na podkladě chromozomálních translokací a expresního profilování můžeme T-ALL rozdělit do několika skupin. Toto rozdělení ovšem prozatím není v léčebných protokolech zohledněno, byť se jednotlivé skupiny prognózou liší [38,39]. První skupina je charakterizována vysokou expresí genů TAL a LMO, kdy jsou tyto onkogeny translokovány do blízkosti silného promotoru T-buněčného receptoru (TCR). Do druhé skupiny patří aberace genu TLX1 (HOX11) a to především translokace t(10;14) a t(7;10). Třetí skupinu charakterizuje translokace TLX3 (HOX11L2). Ve čtvrté

skupině jsou různé aberace vedoucí k ektopické expresi HOXA skupiny genů [36,37,40,41].

CRFL2 overexpression 6%

Hyperdiploidy > 50 chromosomes 25%

ERG deletion 7%

iAMP21 2%

Others 7%

BCR-ABL1 t(9;22) 3%

MLL rearrangements e.g., t(4;22), t(11;19), t(9;11) 8%

HOX11L2 5q35 2.5%

LYL1 19p13 1.5%

TAL1 1p32 7%

HOX11 10q24 0.3%

MLL-ENL 0.3%

E2A-PBX1 t(1;19) 5%

MYC t(8;14), t(2;8), t(8;22) 2%

ETV6-RUNX1 t(12;21), 25%
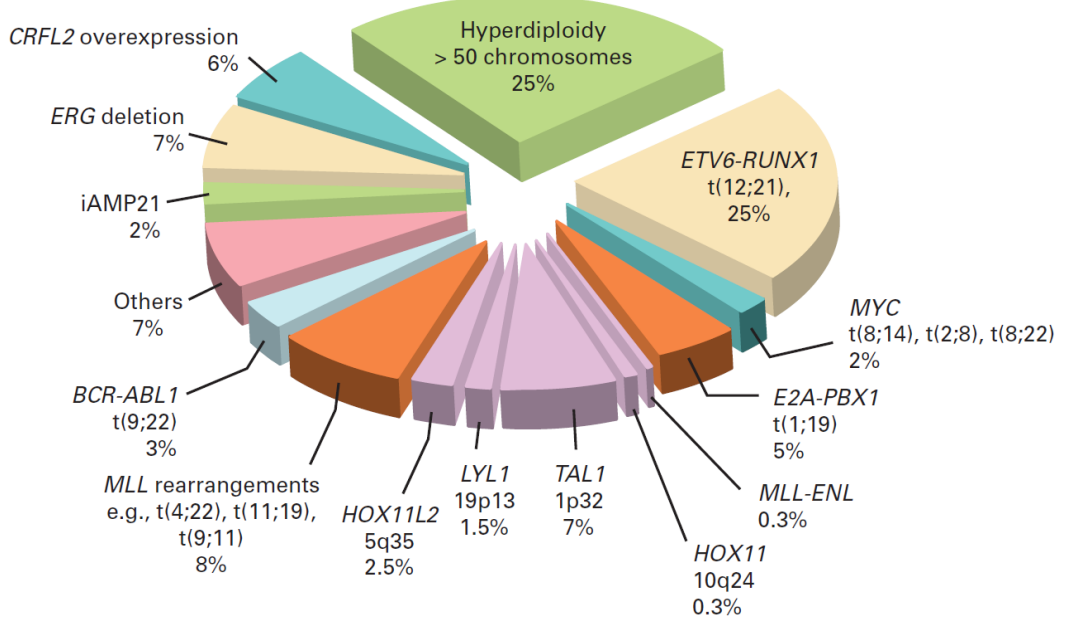
Obr. 1 Zastoupení specifických genových abnormalit dětských ALL [28]

1.2.4. Molekulární genetika

V nedávné době došlo díky rozvoji rozvoji moderních molekulárně genetických technik k nalezení nových genetických alterací u ALL. Byly nalezeny změny v tumor supresorových genech a v genech regulujících buněčný cyklus (CDKN2A/B, PTEN, RB1), transkripčních faktorech a kofaktorech (IKZF1, PAX5, ETV6, ERG, TBL1XR1), v genech, které jsou zapojeny v lymfoidní maturaci a signalizaci (JAK1/2, CRLF2, BTLA, TOX) a také v genech zodpovědných za odpověď na léčbu (například glukokortikoidní receptor NR3C1). Některé z těchto dříve nepopsaných změn, jejichž funkční

ani prognostický význam není často ještě zcela známý, byl nalezen u dvou třetin BCP-ALL [42].

Alterace genu PAX5 se vyskytuje u 30% B-prekurzorových ALL (BCP-ALL) a zdá se, že nemá prognostický význam. Mutace genu IKZF1 (IKAROS), která se nachází u 15% BCP-ALL, je negativním prognostickým faktorem, ale zřejmě jen u některých ALL [43-46]. Tyto transkripční faktory jsou zodpovědné za nasměrování vývoje hematopoetické kmenové buňky do lymfoidní linie [47,48], proto mutace těchto transkripčních faktorů mohou být zodpovědné za blok v maturaci lymfocytu [49,50]. Monoalelické, dominantně negativní mutace genu IKZF1 se vyskytují až u 50% BCR-ABL pozitivních ALL a jsou spojeny se špatnou odpovědí na léčbu tyrozin kinázovými inhibitory [43]. Funkční signalizace pre-B-buněčného receptoru společně s intaktním genem IKZF1 fungují jako silné tumor supresory při vzniku BCR-ABL pozitivní ALL [51]. Mutace IKZF1 se také vyskytují u skupiny BCP-ALL bez rekurentních chromozomálních změn, ovšem jejich genový profil je podobný BCR-ABL1 pozitivním ALL. Tato skupina se nazývá „BCR-ABL1 like" ALL a má velmi špatnou prognózu [52].

Přibližně u 10% BCP-ALL nacházíme vysoce exprimovaný gen CRLF2, což je způsobeno nejčastěji IgH-CRLF2 translokací nebo chimérickou fúzí P2RYR-CRLF2 a často se vyskytuje u BCP-ALL asociovaných s Downovým syndromem [53,54]. V leukémiích není funkce tohoto genu ještě do detailu popsána, ale pravděpodobně je spojena s aktivačními mutacemi JAK kináz, což vede k aberantní aktivaci JAK-STAT signalizační dráhy [55]. Na myším modelu tyto dvě aberantní změny kooperují při rozvoji leukémie [56].

Dalším zcela recentním objevem odhaleným díky použití metod sekvenování nové generace bylo nalezení velkého množství kryptických chromozomálních translokací a strukturálních mutací aktivující různé tyrozin kinázové dráhy, postihující například geny ABL, JAK2, PDGFRB, EPOR [42].

V neposlední řadě v nízkém procentu případů BCP-ALL nacházíme intrachromozomální amplifikace chromozomu 21 [57], mutace genu EGR a mutace genu CREBBP. Mutace genu CREBPP jsou často nacházeny v relapsu ALL a vedou k abnormální acetylaci histonů [58] a dalším cytogenetickým a molekulárně genetickým změnám.

Genetické změny, které sjednocují větší část T-ALL, a výskytují se napříč jednotlivými genetickými skupinami, jsou aberace genu NOTCH1, jehož aktivace je nalézána u více než 50% T-ALL [59,60]. NOTCH1 je fyziologicky důležitým regulátorem diferenciace, proliferace, apoptózy a adheze T-lymfocytu. U T-ALL může být NOTCH1 velmi vzácně aktivován mechanismem chromozomální translokace t(7;9) k TCRbeta lokusu [61]. Ovšem nejčastěji je molekula NOTCH1 aktivována mutacemi v heterodimerizační (HD) nebo PEST doméně genu, což vede k vysoké aktivitě intracelulární domény NOTCH1 [62]. V nedávné době bylo popsáno, že mutace v genu FBXW7 vedou ke snížené degradaci aktivní formy NOTCH1 a tím tato mutace přispívá k NOTCH1 mediované leukemogenezi [63]. Aktivace genu NOTCH1 u T-ALL vede ke zvýšené expresi mnoha různých genů (HES1, DTX1, PTCRA, NOTCH3, MYC) [64].

Mezi další časté genetické změny vedoucí k propagaci T-ALL patří mutace či hypermetylace promotorů regulátorů buněčného cyklu p15 a p16

(CDKN2A/B), které se vyskytují až v 70% případů [37] a genetické defekty v signalizační dráze T-buněčného receptoru a pre-T-buněčného receptoru [41]. V průběhu fyziologického vývoje T-lymfocytu je signalizace generovaná z pre-TCR komplexu důležitá pro jeho správný vývoj. Tato signalizace vede k aktivaci RAS-MAPK dráhy, PI3K dráhy a několika dalších signalizačních drah [65,66]. U T-ALL jsou některé části těchto signalizačních drah často mutovány [41]. Mezi nejdůležitější patří aktivační mutace RAS genu, které byly nalezeny u 10% T-ALL [67] a homozygozytní PTEN mutace, které byly nalezeny u 17% T-ALL [68]. U T-ALL bývají dále nalézány mutace dalších tyrozin kinázových genů, například translokace NUP214-ABL1 (6% případů T-ALL) [69] a mutace a translokace genu JAK [70].

Všechny tyto nálezy implikují, že alterovaná buněčná signalizace je charakteristickým rysem ALL a že v budoucnu by mohly být určité podtypy leukémií léčeny specificky pomocí biologických preparátů (například tyrosin-kinázovými inhibitory).

1.3. Léčba a stratifikace do rizikových skupin

Principem moderní léčby akutní lymfoblastické leukémie je při dostatečné účinnosti minimalizovat její toxicitu. ALL je v České republice léčena podle mezinárodních protokolů skupiny BFM (Berlin-Frankfurt-Münster) [5]. Pro správnou léčbu je důležité stratifikovat pacienty do rizikových skupin, protože jednotlivé podtypy ALL se svým fenotypem, genotypem a šancí na dlouhodobé přežití velmi liší [2]. Do jednotlivých rizikových skupin (standardní, střední a

vysoké riziko), se pacienti řadí podle cytogeneticko-imunofenotypicko-molekulární charakteristiky leukemických buněk a podle iniciální odpovědi na léčbu.

V průběhu prvních sedmi dnů terapie ALL jsou pacienti uniformně léčeni pomocí glukokortikoidů a jedné dávky intratékálního metotrexátu. Pacienti, kteří zredukují počet blastů pod 1000 v 1 mikrolitru periferní krve, jsou označeni jako pacienti s dobrou odpovědí na prednison (prednisone good responders - PGR). Ti, jejichž blasty neklesly pod arbitrážní hranici, reagovali na léčbu prednisonem špatně (prednisone poor responders - PPR) [71]. Odpověď na prednison je jedním z nejdůležitějších prognostických faktorů léčby dětské ALL.

Když počet blastů v kostní dřeni klesne pod úroveň rozeznatelnou světelným mikroskopem (pod 5% blastů), mluvíme o takzvané minimální reziduální nemoci (MRN). Informaci o MRN nám může poskytnout vyšetření kostní dřeně průtokovou cytometrií, ovšem zlatý standard je hodnocení kvantifikace klonálně-specifických imunoglobulinových a T-buněčných receptorů pomocí kvantitativní polymerázové řetězové reakce [72-75].

Hodnocení MRN slouží k hodnocení účinnosti terapie. Dynamika poklesu minimální zbytkové nemoci je nově zařazena do léčebných protokolů a pacienti, u kterých MRN klesá zpomaleně, jsou indikováni k intenzifikaci léčby.

2. Adaptorové molekuly a signalizace

Fosforylace protein tyrozinových zbytků hraje důležitou roli v přenosu mnoha buněčných signálů. V imunitních buňkách signalizace z povrchu buňky do nitra probíhá jako kaskáda jednotlivých fosforylačních a defosforylačních kroků [76]. Konečným efektorem těchto kroků bývá transkripční faktor, který umožní stimulaci či naopak potlačení transkripce různých genů. Alterovaná buněčná signalizace je charakteristickým znakem leukémií.

Důležitou kauzální roli v etiopatogenezi ALL by mohly hrát transmembránové adaptorové molekuly (TRAPs). Jedná se o signalizační molekuly, které nemají enzymatickou funkci. Jejich úlohou je vytvoření „lešení" (scaffold) a umožnění alostericky přesné lokalizace a interakce signalizačním molekulám s kinázovou aktivitou, což vede k propagaci signálu dále do buňky. TRAPs mají krátkou extracelulární doménu, palmitoylovanou transmembránovou doménu a relativně dlouhou intracelulární část, která obsahuje různé množství tyrozinových signalizačních motivů [77,78]. V současné době je známo minimálně 7 transmembránových adaptorových molekul. Čtyři z těchto molekul (linker for activation of T-cells (LAT); non T-cell activation linker (NTAL); phosphoprotein associated with glycosphingolipid enriched microdomains (PAG); Lck interacting transmembrane adaptor (LIME)) jsou lokalizovány v "glycolipid-enriched membrane microdomains" (GEMs), někdy taky označované jako tzv. „lipidové rafty" („lipid rafts"). GEMs jsou submikroskopické okrsky buněčné membrány, které charakterizuje vysoký obsah cholesterolu a sfingolipidů a unikátní proteinové složení. Právě v GEMs dochází k důležité interakci mezi imunoreceptory, adaptorovými proteiny a

dalšími signalizačními molekulami, což vede k propagaci signálu dále do nitra buňky [79,80].
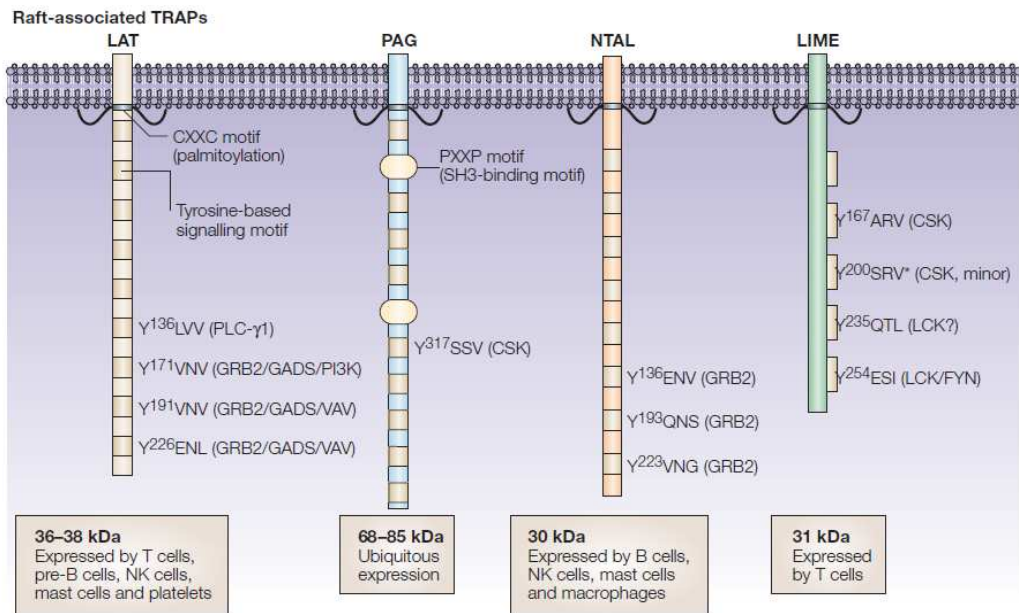
Obr. 2 Struktura transmembránových adaptorových preteinů [76].

V naší práci jsme se především zabývali molekulami PAG, LAT a NTAL.

PAG, též nazývaný Csk binding protein (CBP), váže tyrosin kinázu CSK, která je hlavním inhibitorem SRC kináz [81]. V signalizaci fyziologických T a B-lymfocytů je role molekuly PAG pravděpodobně odlišná. V klidových T-lymfocytech je molekula PAG jedním z nejvíce fosforylovaných proteinů, což vede k potlačení SRC kináz LCK a FYN. Lokalizace v lipidovém raftu je pro inhibiční funkci PAG klíčová [82]. Po aktivaci T-buněčného receptoru (TCR) dochází k defosforylaci PAG, k porušení PAG-CSK vazby a tím k odstranění CSK mediované inhibice LCK a FYN [77]. Naproti tomu v B-lymfocytech po aktivaci B-buněčného receptoru (BCR) dochází ke zvýšené fosforylaci PAG [78]. To pravděpodobně poukazuje na fakt, že ve fyziologické B-lymfocytární

signalizaci jsou SRC kinázy zapojeny spíše v negativní regulaci signalizace, kdy SRC kináza LYN fosforyluje nejenom aktivační tyrosinové motivy, ale i inhibiční tyrosinové motivy signalizačních molekul [83]. PAG je dále vysoce exprimován v buňkách germinálních center folikulárního lymfomu a to do té míry, že by mohl být použit jako diagnostický imunohistochemický marker těchto lymfomů [84]. Na molekule PAG byla poprvé prokázána možná spojitost s leukémií. U skotu parasit Theileria parva snižuje fosforylaci molekuly PAG, což vytváří u svého hostitele „leukemický" obraz krvetvorby (proliferace bez exogenně přidaných růstových faktorů v in-vitro podmínkách). Po odstranění parazita pomocí chemoterapeutik dochází k opětovné fosforylaci PAG a návratu lymfocytů k normálnímu fenotypu [85].

LAT se fyziologicky vyskytuje pouze v T-lymfocytech a v nezralých pre B-lymfocytech [78]. Pro vývoj a správnou funkci T-lymfocytů je LAT zcela zásadní [86], protože tato molekula je nezbytná pro přenos signálu od imunoreceptoru do nitra buňky. LAT -/- myším chybějí zralé T-lymfocyty, neboť T-lymfocytární prekurzory se nevyvinou přes stádium „double-negative" (DN) [78]. LAT je zapojen také v buněčném vývoji pre B-lymfocytů. LAT -/- myši mají méně zralých B-lymfocytů a v jejich hematopoetické tkáni je nacházeno více pre-B-buněk [87]. LAT tedy může v B-řadě fungovat jako tumor supresor indukující fyziologickou diferenciaci B-lymfocytů [88].

NTAL, také nazývaný LAB či WBSRC5, je podle nové nomenklatury pojmenován LAT2. V naší práci používáme původní označení této molekuly NTAL. Protein NTAL je fyziologicky přítomen v B, NK a myeloidních buňkách, není exprimován v klidových T-lymfocytech. NTAL má velice podobnou

struktruru jako molekula LAT, postrádá pouze vazebné místo pro fosfolipázu C-gama [89]. Na NTAL deficientní myši prokázali Wang et al. lepší Ca2+ influx a lepší proliferaci B-buněk po antigenní stimulaci [90]. NTAL se ovšem nezdá být ekvivalentem LAT v B-lymfocytech, protože je zapojen spíše do prolongovaného než časného zvýšení množství intracelulárního vápníku po aktivaci imunoreceptoru [91]. NTAL není exprimován v klidových T-lymfocytech, po antigenní stimulaci je jeho exprese vysoce upregulována, což snižuje míru fosforylace molekul ERK a Akt [92]. V aktivovaných T-lymfocytech by NTAL mohl hypoteticky působit jako inhibitor signalizace kompeticí s LAT o místo v lipidovém raftu. NTAL má tedy schopnost působit jako aktivátor nebo inhibitor lymfocytární signalizace podle jednotlivých lymfocytárních subtypů.

Centrální serine/threonin kináza ERK1/2 je exprimována ve většině tkání těla a je aktivována širokou škálou extracelulárních signálů. RAS dependentní signalizační dráha se podílí na kontrole diferenciace, proliferace a osudu buňky. V T-lymfocytech je ERK aktivována po aktivaci TCR sekvenční fosforylací RAS-RAF-MEK-ERK signální kaskády. ERK je vlivem dalšího buněčného kontextu v T-lymfocytech zapojen v často opačných biologických jevech – v zablokování buněčného cyklu i v podpoře progrese v buněčném cyklu [93]; v buněčné smrti i v podpoře přežívání buňky [94]. V průběhu fyziologického vývoje T-lymfocytu, v T-lymfocytárních prekursorech v thymu, se ERK podílí na pozitivní a negativní selekci lymfocytů. Časná a vysoká fosforylace ERK vede k buněčné smrti lymfocytárních prekurzorů (negativní selekce) a naopak při pomalu nastupující fosforylaci ERK buňky přežijí (pozitivní selekce) [95].

3. Cíle práce

Hlavním cílem našeho projektu bylo objasnit úlohu adaptorových molekul u dětské akutní lymfoblastické leukémie.

- Stanovit expresi adaptorových molekul v průběhu fyziologického lymfocytárního vývoje a u hlavních podtypů dětské ALL.

- V *in-vitro* podmínkách a za použití leukemických buněčných linií objasnit funkci vybraných adaptorových molekul u ALL.

- Ve spolupráci s kolegy z Akademie věd České republiky stanovit expresi signalizační molekuly CD148 u lidských prekurzorů T-lymfocytů.

4.1. Exprese adaptorových molekul v průběhu fyziologického vývoje lymfocytů a u dětských leukémií

Příloha 1 (vědecká publikace)

Adaptor molecules expression in normal lymphopoiesis and in childhood leukemia, <u>Karel Švojgr</u>, Tatiana Burjanivová, Martina Vášková, Tomáš Kalina, Jan Starý, Jan Trka, Jan Zuna Immunology Letters 2009;122:185-192, IF: 2,858

<u>Úvod a metodika</u>

Důležitou roli by při vzniku leukémie mohly hrát signalizační adaptorové molekuly. V naší práci jsme se nejprve věnovali popsání dynamiky exprese adaptorových molekul NTAL, LAT a PAG v rámci fyziologického lymfocytárního vývoje B a T-lymfocytů a následně u dětské akutní lymfoblastické leukémie. Na

úrovni m-RNA jsme expresi zkoumali pomocí kvantitativní reverzně-transkriptázové polymerázové řetězové reakce (qRT-PCR) a na úrovni proteinů za použití průtokové cytometrie. Vývoj B-lymfocytárních prekurzorů byl studován na vzorcích kostní dřeně dětí bez známek maligního onemocnění (u pacientů více než 1 rok po transplantaci kmenových buněk krvetvorby a u pacientů, kterým byla vyšetřována kostní dřeň k vyloučení hematologické malignity), celkem jsme vyšetřili 16 vzorků. T-lymfocytární vývoj byl zkoumán na vzorcích thymů dětí podstupujících kardiologickou operaci (celkem 16 thymů). Devět vzorků periferní krve zdravých dárců bylo použito k analýze zralých fyziologických B a T-lymfocytů.

Diagnostické vzorky kostní dřeně 75 dětí s akutní lymfoblastickou leukémií jsme použili k analýze exprese adaptorových molekul v maligních blastech. Z této skupiny mělo 36 pacientů B-prekurzorovou leukémii (BCP-ALL): 15 pacientů TEL-AML1 pozitivní, 5 MLL-AF4 pozitivní, 8 hyperdiploidní a 8 BCP-ALL bez TEL-AML1 translokace, bez hyperdiploidie či MLL-AF4 translokace. Z 39 pacientů s T-ALL mělo 7 pacientů pre T-ALL, 13 intermediální a 19 zralou T-ALL.

Abychom mohli stanovit expresi m-RNA adaptorových molekul v analyzovaných vzorcích metodou qRT-PCR, roztřídili jsme (sorting) nejprve za pomoci průtokové cytometrie (FACS Aria) nemaligní B a T-prekurzory lymfocytů do frakcí odpovídajících jednotlivým vývojovým stádiím podle imunofenotypu. Při analýze leukemických buněk jsme použili vzorky kostní dřeně s přítomností více než 80% maligních buněk ve vzorku. Ze zkoumaných buněk jsme izolovali RNA a ta byla přepsána do cDNA reverzní transkriptázou.

Všechny qRT-PCR experimenty jsme provedli na přístrojích iCycler iQ System nebo ABI 7700 a za použití primerů, které byly navrženy pomocí Primer Express 2.0 Software a Vector NTI Software. Ke kontrole kvantity a kvality cDNA jsme použili housekeeping gen ABL. Výsledná normalizovaná exprese jednotlivých genů ve vzorku byla definována jako poměr exprese analyzovaného genu (NTAL, LAT, PAG) a exprese genu ABL.

Hladinu proteinu v jednotlivých subpopulacích lymfocytárního vývoje jsme stanovili pomocí mnohobarevné průtokové cytometrie. Nativní vzorky kostní dřeně, periferní krve nebo kryoprezervované tymocytární tkáně byly označeny monoklonálními protilátkami. Povrchové značení sloužilo k identifikaci jednotlivých subpopulací; ke značení intracelulárních adaptorových proteinů jsme buňky permeabilizovali kitem FIX&PERM. Vzorky byly analyzovány na přístrojích FACS Aria, CyAN ADP nebo BD LSR II. Analýza dat z průtokové cytometrie byla provedena pomocí softwaru FlowJo 8.1.1. Exprese molekul NTAL, LAT a PAG je prezentována jako poměr střední intenzity fluorescence k izotopové kontrole v odpovídajícím gatu.

Výsledky a diskuze

V naší práci jsme definovali a porovnali změny v expresi adaptorových molekul na úrovni m-RNA a proteinu v průběhu fyziologického lymfocytárního vývoje s expresí v hlavních podtypech dětské akutní lymfoblastické leukémie. Obecně, hladina i dynamika m-RNA i proteinu korelují velmi dobře. Analýza na úrovni proteinu a m-RNA ukázala, že zatímco některé adaptorové molekuly jsou při vývoji B a T-lymfocytu přítomny v relativně konstantních hladinách, jiné ukazují významnou dynamiku (v průběhu vývoje T-buněk snižování exprese

26

NTAL a zvyšování exprese LAT; při vývoji B řady snižování exprese PAG). Tyto výsledky potvrzují, že v průběhu fyziologického zrání lymfocytů jsou zapojeny rozdílné adaptorové proteiny a aktivovány různé intracelulární signalizační dráhy.

Dalším ze zajímavých výsledků bylo nalezení rozdílu v expresi adaptorových proteinů mezi TEL-AML1 a hyperdiploidními leukémiemi. Ačkoliv tyto leukémie mají velmi podobnou charakteristiku – postihují nejčastěji děti v předškolním věku, mají obdobný imunofenotyp a obvykle velmi dobrou prognózu – přesto se exprese adaptorových molekul mezi těmito podtypy ALL velmi liší (TEL-AML1 mají v porovnání s hyperdiploidími ALL vyšší expresi molekul PAG a nižší NTAL). Tento nález pravděpodobně poukazuje na odlišné biologické pozadí těchto leukémií. TEL-AML1 pozitivní ALL vzniká ve stadiu časného B-progenitoru s vysokou VDJ rekombinázovou aktivitou [96] a právě tento jev může reflektovat vysoká hladina molekuly PAG. PAG dále velmi dobře koreluje s expresí molekuly CD27 na maligních blastech. CD27 je exprimována na buňkách s vysokou aktivitou VDJ rekombinázy [96-98]. Vysoká hladina PAG může vést v maligních blastech k vyšší aktivitě Csk a tím k potlačení aktivity Src kináz. To může způsobit snížení fosforylace inhibičních ITAM motivů, což může vést k vyšší propagaci aktivačního signálu včetně VDJ rekombinantní aktivity

Exprese molekuly LAT se signifikantně zvyšuje se zráním nemaligních i maligních T-buněk, ale množství této molekuly v maligních blastech nedosahuje výše dosažené v periferních T-lymfocytech. Molekula LAT je nezbytná pro aktivaci T-buněk [99] a proto nižší hladina LAT v leukemických

buňkách může znamenat, že maligní buňky nemusí být schopny adekvátně odpovědět na antigenní stimulaci, byť mohou být imunofenotypicky ve stejném maturačním stádiu.

Asi nejzajímavější v této části naší práce je pozorování, že rozdílná exprese NTAL mRNA u T-ALL ovlivňuje odpověď na léčbu a tím i prognózu onemocnění. Nízká hladina NTAL v blastech pacientů s T-ALL signifikantně koreluje se špatnou odpovědí na iniciální léčbu prednisonem, zatímco pacienti s vysokou expresí NTAL v maligních blastech na prednison většinou odpovídají příznivě. Tento poznatek jsme se pokusili modelovat v další části našeho projektu v *in-vitro* experimentech.

4.2. Adaptorový protein NTAL zesiluje proximální signalizaci a potencuje kortikosteroidy indukovanou apoptózu u T-ALL

Příloha 2 (vědecká publikace)

***The adaptor protein NTAL enhances proximal signaling and potentiates corticosteroid-induced apoptosis in T-ALL**, <u>Karel Švojgr</u>, Tomáš Kalina, Veronika Kanderová, Tereza Skopcová, Tomáš Brdička, Jan Zuna, Experimental Hematology 2012;40(5):379-85, IF: 3,198*

<u>Úvod a metodika</u>

Ve druhé části našeho projektu jsme modelovali v *in-vitro* podmínkách pozorování z výše uvedené práce: pacienti příznivě reagující na sedmidenní předléčbu prednisonem (prednison good responders) mají vyšší hladinu NTAL mRNA než pacienti, kteří odpoví špatně. Dále jsme se v naší práci zabývali intracelulárními mechanismy, zodpovědnými za pozorovaný jev.

K *in-vitro* experimentům jsme zvolili buněčnou linii Jurkat. Jedná se o dlouhodobě zavedenou buněčnou linii, která byla získána z periferní krve 14 letého chlapce v prvním relapsu T-ALL. V nativní Jurkat buněčné linii (Jurkat/wt) není NTAL protein detekovatelný a linie exprimuje pouze velmi malé množství NTAL mRNA. Abychom mohli studovat roli molekuly NTAL v maligních T-lymfocytech, transfekovali jsme tuto nativní Jurkat linii expresním vektorem pEFIRES-N produkujícím NTAL protein (Jurkat/NTAL+) [89]. Expresi jsme ověřili pomocí qRT-PCR a Western-blotu. V buněčné kultuře se linie Jurkat/wt i Jurkat/NTAL+ chovají obdobně. Pomocí intracelulární fosfo-specifické průtokové cytometrie a Western-blotu jsme hodnotili buněčnou signalizaci Jurkat/wt a Jurkat/NTAL+ buněk. Buněčná smrt byla hodnocena po obarvení suspense buněk Annexinem V a propidium iodidem, kdy živé buňky byly definovány jako Annexin V negativní, propidium iodide negativní.

Výsledky a diskuze

V našem prvním experimentu se nám podařilo v *in-vitro* podmínkách potvrdit jev pozorovaný na pacientech s T-ALL. Při přidání 1mM koncentrace methylprednisolonu k buněčné kultuře Jurkat/wt a Jurkat/NTAL+ buněk jsme průtokovou cytometrií hodnotili procento přežívajících buněk. Po 48 hodinách inkubace s methylprednisolonem byly Jurkat/wt buňky signifikantně rezistentnější na methylprednisolon než Jurkat/NTAL+ buňky. Tento experiment tedy potvrdil naše *in-vivo* pozorování, že blasty pacientů s T-ALL, které mají vyšší hladinu NTAL mRNA, jsou citlivější na léčbu glukokortikoidy.

Naší prvotní hypotézou bylo, že NTAL by mohl být inhibitorem T-lymfocytární signalizace kompeticí s LAT o místo v lipidovém raftu. Abychom

objasnili roli NTAL molekuly v našem experimentu, stimulovali jsme T-buněčný receptor (TCR) anti-CD3 protilátkou (IgM protilátka C305) a sledovali jsme změny ve fosforylaci klíčových intracelulárních signalizačních molekul: extracelular signal regulated kinase 1/2 (ERK), Jun N-terminal kinace (JNK) a p38 mitogen activated protein kinace (MAPK) pomocí fosfo-specifické průtokové cytometrie a pomocí Western-blotu. V nestimulovaných Jurkat/wt a Jurkat/NTAL+ buňkách je bazální fosforylace ERK, JNK a p38 MAPK obdobná. Krátce po stimulaci došlo k významnému nárůstu fosforylace ERK molekuly a zároveň linie Jurkat/NTAL+ měla v časovém bodě 5 minut 1,5krát vyšší hladinu fosforylovaného ERK než Jurkat/wt. Obdobně linie Jurkat/NTAL+ nesla na svém povrchu za 24 hodin po stimulaci C305 více aktivačního markeru CD69. Na druhou stranu, vzestup fosforylace molekuly JNK byl porovnatelný mezi liniemi Jurkat/wt a Jurkat/NTAL+; fosforylace p38 MAPK se po TCR stimulaci nezměnila. Tato data tedy oproti původní hypotéze ukazují, že NTAL posiluje proximální signalizaci maligního T-lymfocytu, což vede k vyšší hladině fosforyovaného ERK.

Fyziologicky je v thymu rozdílná síla propagace TCR signálu zodpovědná za pozitivní či negativní selekci T-lymfocytárních prekursorů – rychlá a vysoká fosforylace ERK vede buňky k programované buněčné smrti, zatímco anti-apoptoticky působí, pokud fosforylace ERK nastupuje pomaleji a je prolongovaná [94,95]. S těmito poznatky nás tedy logicky dále zajímala úroveň buněčné smrti linií Jurkat/wt a Jurkat/NTAL+ po stimulaci TCR protilátkou C305. Linie Jurkat/NTAL+ byla podle očekávání na TCR indukovanou buněčnou smrt skutečně signifikantně citlivější.

Fosforylace ERK může být velmi úspěšně zablokována chemickým inhibitorem U0126. Po přidání U0126 120 minut před anti-CD3 stimulační protilátkou C305 nedošlo ke skokovému nárůstu fosforylace molekuly ERK v žádném měřeném časovém bodě v Jurkat/wt ani Jurkat/NTAL+ linii. Zároveň při použití ERK inhibitoru U0126 120 min před anti-CD3 protilátkou došlo k téměř úplnému zastavení buněčné smrti, ačkoliv určitý rozdíl mezi liniemi Jurkat/wt a Jurkat/NTAL+ byl zachován. Tento rozdíl může být způsoben nedokonalou inhibicí ERK fosforylace U0126 a nebo jiným, námi neanalyzovaným mechanismem, který se podílí na buněčné smrti v Jurkat/NTAL+ buňkách. Dalším zajímavým poznatkem bylo, že při přidání ERK inhibitoru U0126 až 30 minut po anti-CD3 protilátce C305 dochází pouze k mírnému snížení úrovně buněčné smrti v porovnání s použitím samotné C305 protilátky Tento jev si vysvětlujeme tím, že sekvence intracelulárních změn vedoucích k buněčné smrti je 30 minut po stimulaci buněk již nastartována. Inhibice molekuly ERK tedy potlačuje pozitivní efekt molekuly NTAL v TCR indukované buněčné smrti.

Naše data naznačují, že NTAL zvyšuje citlivost Jurkat/NTAL+ buněk cestou vyšší fosforylace molekuly ERK. Proto jsme se v závěrečném experimentu zaměřili na inhibici fosforylace ERK a její vliv na buněčnou smrt indukovanou glukokortikoidy. K buněčným liniím Jurkat/wt a Jurkat/NTAL+ jsme 30 min před methylprednisolonem přidali ERK inhibitor U0126. Po 48 hod koinkubace jsme (narozdíl od výše popsaného původního experimentu bez inhibitoru) pozorovali identické procento přežívajících buněk v Jurkat/wt i Jurkat/NTAL+ linii.

Výsledkem této části naší studie je tedy experimentálně potvrzené pozorování, že molekula NTAL v T-ALL funguje jako tumor supresor posilující proximální signalizaci leukemických blastů a ERK je klíčovou intracelulární molekulou zodpovědnou za tento proces.

4.3. Stanovení exprese protein-tyrozinové fosfatázy CD148 ve fyziologických prekurzorech T-lymfocytů.

Příloha číslo 3 (vědecká publikace)

Regulation of Src family kinases involved in T cell receptor signaling by protein-tyrosine phosphatase CD148, Ondřej Štěpánek, Tomáš Kalina, Pavel Dráber, Tereza Skopcová, <u>Karel Švojgr,</u> Pavla Angelisová, Václav Hořejší, Arthur Weiss, Tomáš Brdička. Journal of Biological Chemistry 2011;24;288(25):22101-22112, IF: 5,838

<u>Úvod a metodika</u>

Ve třetí části naší práce jsme se věnovali protein-tyrosin fosfatáze CD148. Jedná se o transmembránovou signalizační molekulu, která je exprimována jak v ne-hematopoetické tkáni, tak i v lymfocytech [100]. Ačkoliv role protein-tyrosin fosfatáz v T-buněčné signalizaci bývá obyčejně inhibiční, CD148 má pravděpodobně v řízení lymfocytární signalizace funkci duální, obdobnou jako molekula CD45 [101]. Tyto molekuly se podílejí na inhibici i aktivaci lymfocytární signalizace defosforylací specifických aktivačních, ale i inhibičních fosfotyrosinových zbytků.

Při porovnání lidských a myších lymfocytů existuje v expresi molekuly CD148 velký rozdíl. V lidské periferní krvi je většina leukocytů CD148 pozitivních, naproti tomu myší naivní T-lymfocyty jsou CD148 negativní [102]. Zatímco v lidském thymu byla CD148 pozitivita nalezena pouze na CD3+ buňkách [103], v myších lymfocytárních prekursorech byla CD148 pozitivita nalezena na nejméně zralých buňkách ve stadiu double-negative (CD4-CD8-) [102]. Naším podílem v této práci bylo tedy detailní definování exprese CD148 na prekursorech lidských T-lymfocytů v porovnání s myšími thymocyty. Lidské tkáně thymu byly opět získány od pacientů podstupujících kardiologickou operaci ve FN v Motole (věkové rozmezí pacientů 9 dní – 4 roky). Z tkání byla vymyta suspenze jednotlivých buněk, ty byly označeny monoklonálními protilátkami a expresi CD148 jsme měřili v jednotlivých subpopulacích T-lymfocytárního vývoje pomocí průtokové cytometrie.

Výsledky a diskuze

Prokázali jsme, že exprese CD148 v lidských a myších thymocytech je kompletně inverzní. Zatímco lidské thymocytární prekurzory mají nejvyšší povrchový výskyt molekuly CD148 ve stadiích single pozitivů, u myší je to naopak. Nejvyšší exprese CD148 u myší je v nejranějších stádiích T-lymfocytárního vývoje, ve stadiu double negativu a nezralého single pozitivu. Tranzice ze stadia double pozitivu do stadia single pozitivu není zcela lineární [104]. My jsme v naší práci definovali přechod z časného stadia double pozitivu do nejpozdnějšího single pozitivu pomocí molekul CD44 a CD1a. Tento vývoj je charakterizován počátečním stadiem CD44-CD1a+, přes stadium CD44+CD1a+ do nejpozdějšího stadia CD44+CD1a-. Následně již buňka

přechází do periferní krve jako naivní T-lymfocyt. A právě v nejpozdějším stádiu T-lymfocytární diferenciace CD44+CD1a- je exprese molekuly CD148 nejvyšší. Očekávaně s vysokou expresí CD148 v pozdních fázích lymfocytárního vývoje dobře korelují molekuly CD27 a CD69, markery úspěšné pozitivní selekce T-lymfocytárního prekurzoru.

V další části této práce naši kolegové z Ústavu molekulární genetiky Akademie věd České republiky prokázali, že molekula CD148 má obdobně jako molekula CD45 skutečně aktivační i inhibiční vliv na T-lymfocytární signalizaci.

5. Závěr

Předkládaná práce se věnuje funkci adaptorových molekul u dětské akutní lymfoblastické leukémie. Nejprve jsme se věnovali expresi adaptorových molekul v průběhu fyziologického lymfocytárního vývoje a u hlavních podtypů dětské ALL. Prokázali jsme, že v průběhu lymfocytárního vývoje exprese některých adaptorových molekul vykazuje signifikatní dynamiku zatímco u jiných adaptorů zůstává konstantní. U dětských ALL obsahují rozdílné množství adaptorových molekul především hyperdiploidní a TEL/AML1 pozitivní ALL. Pravděpodobně naším nejzajímavějším nálezem bylo, že vyšší exprese molekuly NTAL zvyšuje citlivost T-ALL na podávané kortikoidy. Tento jev jsme modelovali a potvrdili v *in-vitro* experimentech. Za použití nativní a derivované leukemické buněčné linie jsme objasnili intracelulární mechanismus tohoto děje – molekula NTAL zvyšuje fosforylaci molekuly ERK a to vede k potenciaci kortikoidy indukované buněčné smrti. V závěrečné části naší práce jsme potvrdili naši hypotézu, že exprese molekuly CD148 je kompletně inverzní v lidských a myších prekurzorech T- lymfocytů.

Předkládaná práce poodhalila funkci adaptorových molekul a buněčné signalizace u dětské akutní lymfoblastické leukémie. Naše poznatky mohou být dále využity k detailnímu popisu aberantní buněčné signalizace u dětských akutních leukémií.

6. Seznam zkratek

ALL	akutní lymfoblastická leukémie
ABL	*c-abl oncogene 1*
BCP-ALL	B-prekurzorová akutní lymfoblastická leékemie *(B-cell precursor acute lymphoblastic leukemia)*
BCR	B-buněčný receptor *(B-cell receptor)*
BFM	Berlín - Frankfurt - Münster
BTLA	*B and T-lymphocyte associated*
CD	*Cluster of Differentiation*
CDKN2A/B	*cylin-dependent kinase inhibitor 2 A, B*
CREBBP	*CREB binding protein*
CRLF2	*cytokine receptor-like factor 2*
DN	*double negative*
DTX1	*deltex homolog 1*
EGIL	*European Group for Immunological characterization of Leukemia*
EPOR	*erythropoietin receptor*
ERG	v-*ets erythroblastosis virus E26 oncogene homolog*
ERK	*extracellular signal-regulated kinases*
ETP-ALL	akutní lymfoblastickáleukémie z časných T-*prekurzorů (early T-cell procersor acute lymphoblastic leukemia)*
ETV6	*ets variant 6*
FAB	francouzsko-americko-britský
FISH	fluorescenční in-situ hybridizace
GEMs	*glykolipid-enriched membrane microdomains*
GPI	glykofosfatidylinosit
HOXA	*homeobox A*
HES1	*hairy and enhancer of split 1*
Ig	imunoglobulin
IL	interleukin
IKZF1	*IKAROS family zinc finger 1*

JAK	*Janus kinase 1*
JNK	*c-Jun N-terminal* kinases
LAT	*linker for activation of T-cells*
LIME	*LCK interacting transmembrane adaptor*
LMO	*LIM domain only*
MAPK	*mitogen-activated protein kinase*
MFI	medián intenzity fluorescence
MRD	minimální zbytková nemoc
MYC	*myelocytomatosis viral oncogene homolog*
NR3C1	*glucocorticoid receptor*
NTAL	n*on T-cell activation linker*
PAG	p*hosphorpotein associated with glycosfingolipid enriched microdomains*
PAX5	*paired box 5*
PDGFRB	*platelet-derived growth factor receptor, beta polypeptide*
PGR	*prednison good responder*
PI3K	*phosphoinositide-3-kinase*
PPR	*prednison poor responders*
PTCRA	*pre T-cell antigen receptor alpha*
PTEN	*phosphatase and tensin homolog*
qRT-PCR	kvantitativní reverzně –transkriptázpvá polymerázová řetězová rekace
RB1	*retinoblastoma 1*
STAT	*signal transducer and activator of transcription*
T-ALL	T-buněčná akutní lymfoblastická leukémie
TAL	*T-cell acute lymphoblastic leukemia*
TBL1XR1	*transducin (beta)-like 1 X-linked receptor 1*
TCR	T-lymfocytární receptor *(T-cell receptor)*
TLX	*T-cell leukemia homeobox*
TOX	*thymocyte selection-associated high mobility group box*
TRAPs	transmembránové adaptorové proteiny

7. Seznam autorských publikací a prezentací

7.1. Seznam publikací vztahujících se k tématu dizertační práce

Adaptors Molecules Expression in Normal Lymphopoiesis and in Childhood Leukemia

Karel Švojgr, Tatiana Burjanivová, Martina Vášková, Tomáš Kalina, Jan Starý, Jan Trka, Jan Zuna

Immunology Letters 2009 122(2):185-192   IF: 2,858

Adaptorové molekuly PAG, NTAL a LAT ve fyziologických lymfocytárních prekurzorech a u dětských leukémií.

Karel Švojgr, Tatiana Burjanivová, Martina Vášková, Tomáš Kalina, Tomáš Brdička, Tereza Kačerová, Jan Starý, Jan Trka, Jan Zuna

Transfuze a hematologie dnes, 15, 2009, No. 2, p. 107-113

Regulation of Src family kinases involved in T cell receptor signaling by protein-tyrosine phosphatase CD148

Ondřej Štěpánek, Tomáš Kalina, Pavel Dráber, Tereza Skopcová, Karel Švojgr, Pavla Angelisová, Václav Hořejší, Arthur Weiss, Tomáš Brdička

The Journal of Biological Chemistry 2011;24;288(25):22101-22112

IF: 5,838

The adaptor protein NTAL enhances proximal signaling and potentiates corticosteroid-induced apoptosis in T-ALL

Karel Švojgr, Tomáš Kalina, Veronika Kanderová, Tereza Skopcová, Tomáš Brdička, Jan Zuna.
Experimental Hematology 2012;40(5):379-85   IF: 3,198

7.2. Seznam prezentací vztahujících se k tématu dizertační práce

Prezentace na zahraničních konferencích:

Svojgr K, Burjanivova T, Vaskova M, Kalina T, Stary J, Trka J, Zuna J: Expression of Transmembrane Adaptors is Specific in Distinct Childhood Acute Lymphoblastic Leukaemia Subgroups and Indicates Early Treatment Response in T-ALL: 49. kongres Americké hematologické společnosti, San Francisco, USA, 2007

Svojgr K, Kalina T, Brdicka T, Kacerova T, Stary J, Zuna J: Adaptor protein NTAL enhances proximal signalling and potentiates corticosteroid induced apoptosis in T-ALL: 7. Bi-Annual Childhood Leukemia Symposim, Antalya, Turecko 2010

Prezentace na českých a slovenských konferencích:

Švojgr K, Burjanivová T, Vášková M, Kalina T, Starý J, Trka J, Zuna J: Exprese transmembránových adaptorových molekul je specifická v různých subtypech ALL a indikuje časnou odpověď na léčbu u T-ALL. 17. konference dětských hematologů a onkologů, Špindlerův mlýn, 2007

Švojgr K, Burjanivová T, Vášková M, Kalina T, Brdička T, Starý J, Trka J, Zuna J: Funkce adaptorových proteinů v procesu leukemogenezy, Vědecká konference 2.LF UK, 2009

Svojgr K, Kalina T, Brdicka T, Kacerova T, Stary J, Zuna J: Adaptor protein NTAL enhances proximal signalling and potentiates corticosteroid induced apoptosis in T-ALL: Olomoucké hematologické dny, 2010

7.3. Seznam publikací bez vztahu k tématu dizertační práce

Ikaros *(IKZF1)* alterations and minimal residual disease at day 15 assessed by flow cytometry predict prognosis of childhood *BCR/ABL*-negative acute lymphoblastic leukemia
Jana Volejníková, Ester Mejstříková, Petra Dörge, Barbara Meissner, Karel Švojgr, Martin Stanulla, Gunnar Cario, MartinSchrappe, Jan Starý, Ondřej Hrušák, Jan Trka, Eva Froňková
Odesláno k revizi do Pediatric Blood and Cancer   IF: 2,13

7.4. Seznam prezentací bez vztahu k tématu dizertační práce

Prezentace na zahraničních konferencích:

Volejnikova J, Mejstrikova E, Svojgr K, Stary J, Trka J, Fronkova E: Prognostic Impact of Ikaros (IKZF1) Gene Alterations In Childhood ALL Treated with ALL IC-BFM 2002 Protocol: A Comparison of Gene Expression and Genomic-Based Methods, 53. kongres Americké hematologické společnosti, Orlando, USA, 2010

8. Reference

[1]   Orkin SH, Nathan DG, Ginsburg D, Look AT, Fisher DE, Lux SE. Nathan and Oski's Hematology of Infancy and Childhood. Sanders,2008.

[2]   Pui CH, Evans WE. Treatment of acute lymphoblastic leukemia. N Engl J Med 2006;354:166-178.

[3]   Pui CH, Crist WM, Look AT. Biology and clinical significance of cytogenetic abnormalities in childhood acute lymphoblastic leukemia. Blood 1990;76:1449-1463.

[4]   Mayer J, Stary J. Leukémie. Avicenum, Grada Publishing: Praha,2002.

[5]   Stary J, Jabali Y, Trka J, Hrusak O, Gajdos P, Hrstkova H, Sterba J, Blazek B, Hak J, Prochazkova D, Cerna Z, Smisek P, Sedlacek P, Vavra V, Mihal V, Hrodek O. Long-term results of treatment of childhood acute lymphoblastic leukemia in the Czech Republic. Leukemia 2010;24:425-428.

[6]   Hrusak O, Trka J, Zuna J, Polouckova A, Kalina T, Stary J. Acute lymphoblastic leukemia incidence during socioeconomic transition: selective increase in children from 1 to 4 years. Leukemia 2002;16:720-725.

[7]   Simone JV. Childhood leukemia--successes and challenges for survivors. N Engl J Med 2003;349:627-628.

[8]   Frei E, 3rd, Karon M, Levin RH, Freireich EJ, Taylor RJ, Hananian J, Selawry O, Holland JF, Hoogstraten B, Wolman IJ, Abir E, Sawitsky A, Lee S, Mills SD, Burgert EO, Jr., Spurr CL, Patterson RB, Ebaugh FG, James GW, 3rd, Moon JH. The effectiveness of combinations of antileukemic agents in inducing and maintaining remission in children with acute leukemia. Blood 1965;26:642-656.

[9]   Pui CH, Relling MV, Downing JR. Acute lymphoblastic leukemia. N Engl J Med 2004;350:1535-1548.

[10]   Dordelmann M, Schrappe M, Reiter A, Zimmermann M, Graf N, Schott G, Lampert F, Harbott J, Niemeyer C, Ritter J, Dorffel W, Nessler G, Kuhl J, Riehm H. Down's syndrome in childhood acute lymphoblastic leukemia: clinical characteristics and treatment outcome in four consecutive BFM trials. Berlin-Frankfurt-Munster Group. Leukemia 1998;12:645-651.

[11]   Pizzo PA, Poplack DG. Principles and Practice of Pediatric Oncology Lippincott Williams & Wilkins,2010.

[12]   Preston DL, Kusumi S, Tomonaga M, Izumi S, Ron E, Kuramoto A, Kamada N, Dohy H, Matsuo T, Matsui T, et al. Cancer incidence in atomic bomb survivors. Part III. Leukemia, lymphoma and multiple myeloma, 1950-1987. Radiat Res 1994;137:S68-97.

[13]   Greaves M. Infection, immune responses and the aetiology of childhood leukaemia. Nat Rev Cancer 2006;6:193-203.

[14]   Burjanivova T, Madzo J, Muzikova K, Meyer C, Schneider B, Votava F, Marschalek R, Stary J, Trka J, Zuna J. Prenatal origin of childhood AML occurs less frequently than in childhood ALL. BMC Cancer 2006;6:100.

[15]   Gale KB, Ford AM, Repp R, Borkhardt A, Keller C, Eden OB, Greaves MF. Backtracking leukemia to birth: identification of clonotypic gene fusion sequences in neonatal blood spots. Proc Natl Acad Sci U S A 1997;94:13950-13954.

[16]   Mori H, Colman SM, Xiao Z, Ford AM, Healy LE, Donaldson C, Hows JM, Navarrete C, Greaves M. Chromosome translocations and covert leukemic clones are generated during normal fetal development. Proc Natl Acad Sci U S A 2002;99:8242-8247.

[17]   Zuna J, Madzo J, Krejci O, Zemanova Z, Kalinova M, Muzikova K, Zapotocky M, Starkova J, Hrusak O, Horak J, Trka J. ETV6/RUNX1 (TEL/AML1) is a frequent prenatal first hit in childhood leukemia. Blood 2011;117:368-369; author reply 370-361.

[18]   Greaves MF. Speculations on the cause of childhood acute lymphoblastic leukemia. Leukemia 1988;2:120-125.

[19]   Pui CH. Childhood leukemias. N Engl J Med 1995;332:1618-1630.

[20]   Kalina T, Mejsříková E, Vášková M, Hrušák O. Imunofenotypizace dětských leukémií. Transfuze a Hematologie dnes 2006;12:25-26.

[21]   Kalina T, Vaskova M, Mejstrikova E, Madzo J, Trka J, Stary J, Hrusak O. Myeloid antigens in childhood lymphoblastic leukemia: clinical data point to regulation of CD66c distinct from other myeloid antigens. BMC Cancer 2005;5:38.

[22]   Campana D, Coustan-Smith E. Minimal residual disease studies by flow cytometry in acute leukemia. Acta Haematol 2004;112:8-15.

[23]   Coustan-Smith E, Song G, Clark C, Key L, Liu P, Mehrpooya M, Stow P, Su X, Shurtleff S, Pui CH, Downing JR, Campana D. New markers for minimal residual disease detection in acute lymphoblastic leukemia. Blood 2011;117:6267-6276.

[24]   Mejstrikova E, Fronkova E, Kalina T, Omelka M, Batinic D, Dubravcic K, Pospisilova K, Vaskova M, Luria D, Cheng SH, Ng M, Leung Y, Kappelmayer J, Kiss F, Izraeli S, Stark B, Schrappe M, Trka J, Stary J, Hrusak O. Detection of residual B precursor lymphoblastic leukemia by uniform gating flow cytometry. Pediatr Blood Cancer 2008;54:62-70.

[25]   Bene MC. Immunophenotyping of acute leukaemias. Immunol Lett 2005;98:9-21.

[26]   Bene MC, Castoldi G, Knapp W, Ludwig WD, Matutes E, Orfao A, van't Veer MB. Proposals for the immunological classification of acute leukemias. European Group for the Immunological Characterization of Leukemias (EGIL). Leukemia 1995;9:1783-1786.

[27]   Coustan-Smith E, Mullighan CG, Onciu M, Behm FG, Raimondi SC, Pei D, Cheng C, Su X, Rubnitz JE, Basso G, Biondi A, Pui CH, Downing JR, Campana D. Early T-cell precursor leukaemia: a subtype of very high-risk acute lymphoblastic leukaemia. Lancet Oncol 2009;10:147-156.

[28]   Pui CH, Carroll WL, Meshinchi S, Arceci RJ. Biology, risk stratification, and therapy of pediatric acute leukemias: an update. J Clin Oncol 2011;29:551-565.

[29]   Nachman JB, Heerema NA, Sather H, Camitta B, Forestier E, Harrison CJ, Dastugue N, Schrappe M, Pui CH, Basso G, Silverman LB, Janka-Schaub GE. Outcome of treatment in children with hypodiploid acute lymphoblastic leukemia. Blood 2007;110:1112-1115.

[30]   Shurtleff SA, Buijs A, Behm FG, Rubnitz JE, Raimondi SC, Hancock ML, Chan GC, Pui CH, Grosveld G, Downing JR. TEL/AML1 fusion resulting from a cryptic t(12;21) is the most common genetic lesion in pediatric ALL and defines a subgroup of patients with an excellent prognosis. Leukemia 1995;9:1985-1989.

[31]   Zuna J, Hrusak O, Kalinova M, Muzikova K, Stary J, Trka J. Significantly lower relapse rate for TEL/AML1-positive ALL. Leukemia 1999;13:1633.

[32]   Lugo TG, Pendergast AM, Muller AJ, Witte ON. Tyrosine kinase activity and transformation potency of bcr-abl oncogene products. Science 1990;247:1079-1082.

[33]   Barr RD. Imatinib mesylate in children and adolescents with cancer. Pediatr Blood Cancer 2010;55:18-25.

[34]   Talpaz M, Shah NP, Kantarjian H, Donato N, Nicoll J, Paquette R, Cortes J, O'Brien S, Nicaise C, Bleickardt E, Blackwood-Chirchir MA, Iyer V, Chen TT, Huang F, Decillis

AP, Sawyers CL. Dasatinib in imatinib-resistant Philadelphia chromosome-positive leukemias. N Engl J Med 2006;354:2531-2541.

[35] Stam RW, Schneider P, Hagelstein JA, van der Linden MH, Stumpel DJ, de Menezes RX, de Lorenzo P, Valsecchi MG, Pieters R. Gene expression profiling-based dissection of MLL translocated and MLL germline acute lymphoblastic leukemia in infants. Blood 2010;115:2835-2844.

[36] Aifantis I, Raetz E, Buonamici S. Molecular pathogenesis of T-cell leukaemia and lymphoma. Nat Rev Immunol 2008;8:380-390.

[37] Meijerink JP. Genetic rearrangements in relation to immunophenotype and outcome in T-cell acute lymphoblastic leukaemia. Best Pract Res Clin Haematol 2010;23:307-318.

[38] van Grotel M, Meijerink JP, Beverloo HB, Langerak AW, Buys-Gladdines JG, Schneider P, Poulsen TS, den Boer ML, Horstmann M, Kamps WA, Veerman AJ, van Wering ER, van Noesel MM, Pieters R. The outcome of molecular-cytogenetic subgroups in pediatric T-cell acute lymphoblastic leukemia: a retrospective study of patients treated according to DCOG or COALL protocols. Haematologica 2006;91:1212-1221.

[39] van Grotel M, Meijerink JP, van Wering ER, Langerak AW, Beverloo HB, Buijs-Gladdines JG, Burger NB, Passier M, van Lieshout EM, Kamps WA, Veerman AJ, van Noesel MM, Pieters R. Prognostic significance of molecular-cytogenetic abnormalities in pediatric T-ALL is not explained by immunophenotypic differences. Leukemia 2008;22:124-131.

[40] Soulier J, Clappier E, Cayuela JM, Regnault A, Garcia-Peydro M, Dombret H, Baruchel A, Toribio ML, Sigaux F. HOXA genes are included in genetic and biologic networks defining human acute T-cell leukemia (T-ALL). Blood 2005;106:274-286.

[41] Van Vlierberghe P, Pieters R, Beverloo HB, Meijerink JP. Molecular-genetic insights in paediatric T-cell acute lymphoblastic leukaemia. Br J Haematol 2008;143:153-168.

[42] Mullighan CG. Genomic profiling of B-progenitor acute lymphoblastic leukemia. Best Pract Res Clin Haematol 2011;24:489-503.

[43] Iacobucci I, Lonetti A, Messa F, Cilloni D, Arruga F, Ottaviani E, Paolini S, Papayannidis C, Piccaluga PP, Giannoulia P, Soverini S, Amabile M, Poerio A, Saglio G, Pane F, Berton G, Baruzzi A, Vitale A, Chiaretti S, Perini G, Foa R, Baccarani M, Martinelli G. Expression of spliced oncogenic Ikaros isoforms in Philadelphia-positive acute lymphoblastic leukemia patients treated with tyrosine kinase inhibitors: implications for a new mechanism of resistance. Blood 2008;112:3847-3855.

[44] Mullighan CG, Goorha S, Radtke I, Miller CB, Coustan-Smith E, Dalton JD, Girtman K, Mathew S, Ma J, Pounds SB, Su X, Pui CH, Relling MV, Evans WE, Shurtleff SA, Downing JR. Genome-wide analysis of genetic alterations in acute lymphoblastic leukaemia. Nature 2007;446:758-764.

[45] Mullighan CG, Miller CB, Radtke I, Phillips LA, Dalton J, Ma J, White D, Hughes TP, Le Beau MM, Pui CH, Relling MV, Shurtleff SA, Downing JR. BCR-ABL1 lymphoblastic leukaemia is characterized by the deletion of Ikaros. Nature 2008;453:110-114.

[46] Kuiper RP, Waanders E, van der Velden VH, van Reijmersdal SV, Venkatachalam R, Scheijen B, Sonneveld E, van Dongen JJ, Veerman AJ, van Leeuwen FN, van Kessel AG, Hoogerbrugge PM. IKZF1 deletions predict relapse in uniformly treated pediatric precursor B-ALL. Leukemia;24:1258-1264.

[47] Medvedovic J, Ebert A, Tagoh H, Busslinger M. Pax5: a master regulator of B cell development and leukemogenesis. Adv Immunol;111:179-206.

[48]   John LB, Ward AC. The Ikaros gene family: transcriptional regulators of hematopoiesis and immunity. Mol Immunol;48:1272-1278.

[49]   Heltemes-Harris LM, Willette MJ, Ramsey LB, Qiu YH, Neeley ES, Zhang N, Thomas DA, Koeuth T, Baechler EC, Kornblau SM, Farrar MA. Ebf1 or Pax5 haploinsufficiency synergizes with STAT5 activation to initiate acute lymphoblastic leukemia. J Exp Med;208:1135-1149.

[50]   Virely C, Moulin S, Cobaleda C, Lasgi C, Alberdi A, Soulier J, Sigaux F, Chan S, Kastner P, Ghysdael J. Haploinsufficiency of the IKZF1 (IKAROS) tumor suppressor gene cooperates with BCR-ABL in a transgenic model of acute lymphoblastic leukemia. Leukemia;24:1200-1204.

[51]   Trageser D, Iacobucci I, Nahar R, Duy C, von Levetzow G, Klemm L, Park E, Schuh W, Gruber T, Herzog S, Kim YM, Hofmann WK, Li A, Storlazzi CT, Jack HM, Groffen J, Martinelli G, Heisterkamp N, Jumaa H, Muschen M. Pre-B cell receptor-mediated cell cycle arrest in Philadelphia chromosome-positive acute lymphoblastic leukemia requires IKAROS function. J Exp Med 2009;206:1739-1753.

[52]   Den Boer ML, van Slegtenhorst M, De Menezes RX, Cheok MH, Buijs-Gladdines JG, Peters ST, Van Zutven LJ, Beverloo HB, Van der Spek PJ, Escherich G, Horstmann MA, Janka-Schaub GE, Kamps WA, Evans WE, Pieters R. A subtype of childhood acute lymphoblastic leukaemia with poor treatment outcome: a genome-wide classification study. Lancet Oncol 2009;10:125-134.

[53]   Cario G, Zimmermann M, Romey R, Gesk S, Vater I, Harbott J, Schrauder A, Moericke A, Izraeli S, Akasaka T, Dyer MJ, Siebert R, Schrappe M, Stanulla M. Presence of the P2RY8-CRLF2 rearrangement is associated with a poor prognosis in non-high-risk precursor B-cell acute lymphoblastic leukemia in children treated according to the ALL-BFM 2000 protocol. Blood;115:5393-5397.

[54]   Russell LJ, Capasso M, Vater I, Akasaka T, Bernard OA, Calasanz MJ, Chandrasekaran T, Chapiro E, Gesk S, Griffiths M, Guttery DS, Haferlach C, Harder L, Heidenreich O, Irving J, Kearney L, Nguyen-Khac F, Machado L, Minto L, Majid A, Moorman AV, Morrison H, Rand V, Strefford JC, Schwab C, Tonnies H, Dyer MJ, Siebert R, Harrison CJ. Deregulated expression of cytokine receptor gene, CRLF2, is involved in lymphoid transformation in B-cell precursor acute lymphoblastic leukemia. Blood 2009;114:2688-2698.

[55]   Harvey RC, Mullighan CG, Wang X, Dobbin KK, Davidson GS, Bedrick EJ, Chen IM, Atlas SR, Kang H, Ar K, Wilson CS, Wharton W, Murphy M, Devidas M, Carroll AJ, Borowitz MJ, Bowman WP, Downing JR, Relling M, Yang J, Bhojwani D, Carroll WL, Camitta B, Reaman GH, Smith M, Hunger SP, Willman CL. Identification of novel cluster groups in pediatric high-risk B-precursor acute lymphoblastic leukemia with gene expression profiling: correlation with genome-wide DNA copy number alterations, clinical characteristics, and outcome. Blood 2010;116:4874-4884.

[56]   Mullighan CG, Collins-Underwood JR, Phillips LA, Loudin MG, Liu W, Zhang J, Ma J, Coustan-Smith E, Harvey RC, Willman CL, Mikhail FM, Meyer J, Carroll AJ, Williams RT, Cheng J, Heerema NA, Basso G, Pession A, Pui CH, Raimondi SC, Hunger SP, Downing JR, Carroll WL, Rabin KR. Rearrangement of CRLF2 in B-progenitor- and Down syndrome-associated acute lymphoblastic leukemia. Nat Genet 2009;41:1243-1246.

[57]   Soulier J, Trakhtenbrot L, Najfeld V, Lipton JM, Mathew S, Avet-Loiseau H, De Braekeleer M, Salem S, Baruchel A, Raimondi SC, Raynaud SD. Amplification of band q22 of chromosome 21, including AML1, in older children with acute lymphoblastic leukemia: an emerging molecular cytogenetic subgroup. Leukemia 2003;17:1679-1682.

[58]   Mullighan CG, Zhang J, Kasper LH, Lerach S, Payne-Turner D, Phillips LA, Heatley SL, Holmfeldt L, Collins-Underwood JR, Ma J, Buetow KH, Pui CH, Baker SD, Brindle PK, Downing JR. CREBBP mutations in relapsed acute lymphoblastic leukaemia. Nature 2011;471:235-239.

[59]   Breit S, Stanulla M, Flohr T, Schrappe M, Ludwig WD, Tolle G, Happich M, Muckenthaler MU, Kulozik AE. Activating NOTCH1 mutations predict favorable early treatment response and long-term outcome in childhood precursor T-cell lymphoblastic leukemia. Blood 2006;108:1151-1157.

[60]   Weng AP, Ferrando AA, Lee W, Morris JPt, Silverman LB, Sanchez-Irizarry C, Blacklow SC, Look AT, Aster JC. Activating mutations of NOTCH1 in human T cell acute lymphoblastic leukemia. Science 2004;306:269-271.

[61]   Ellisen LW, Bird J, West DC, Soreng AL, Reynolds TC, Smith SD, Sklar J. TAN-1, the human homolog of the Drosophila notch gene, is broken by chromosomal translocations in T lymphoblastic neoplasms. Cell 1991;66:649-661.

[62]   Paganin M, Ferrando A. Molecular pathogenesis and targeted therapies for NOTCH1-induced T-cell acute lymphoblastic leukemia. Blood Rev 2011;25:83-90.

[63]   Thompson BJ, Jankovic V, Gao J, Buonamici S, Vest A, Lee JM, Zavadil J, Nimer SD, Aifantis I. Control of hematopoietic stem cell quiescence by the E3 ubiquitin ligase Fbw7. J Exp Med 2008;205:1395-1408.

[64]   Grabher C, von Boehmer H, Look AT. Notch 1 activation in the molecular pathogenesis of T-cell acute lymphoblastic leukaemia. Nat Rev Cancer 2006;6:347-359.

[65]   Bellavia D, Campese AF, Checquolo S, Balestri A, Biondi A, Cazzaniga G, Lendahl U, Fehling HJ, Hayday AC, Frati L, von Boehmer H, Gulino A, Screpanti I. Combined expression of pTalpha and Notch3 in T cell leukemia identifies the requirement of preTCR for leukemogenesis. Proc Natl Acad Sci U S A 2002;99:3788-3793.

[66]   Talora C, Campese AF, Bellavia D, Pascucci M, Checquolo S, Groppioni M, Frati L, von Boehmer H, Gulino A, Screpanti I. Pre-TCR-triggered ERK signalling-dependent downregulation of E2A activity in Notch3-induced T-cell lymphoma. EMBO Rep 2003;4:1067-1072.

[67]   von Lintig FC, Huvar I, Law P, Diccianni MB, Yu AL, Boss GR. Ras activation in normal white blood cells and childhood acute lymphoblastic leukemia. Clin Cancer Res 2000;6:1804-1810.

[68]   Palomero T, Sulis ML, Cortina M, Real PJ, Barnes K, Ciofani M, Caparros E, Buteau J, Brown K, Perkins SL, Bhagat G, Agarwal AM, Basso G, Castillo M, Nagase S, Cordon-Cardo C, Parsons R, Zuniga-Pflucker JC, Dominguez M, Ferrando AA. Mutational loss of PTEN induces resistance to NOTCH1 inhibition in T-cell leukemia. Nat Med 2007;13:1203-1210.

[69]   Graux C, Cools J, Melotte C, Quentmeier H, Ferrando A, Levine R, Vermeesch JR, Stul M, Dutta B, Boeckx N, Bosly A, Heimann P, Uyttebroeck A, Mentens N, Somers R, MacLeod RA, Drexler HG, Look AT, Gilliland DG, Michaux L, Vandenberghe P, Wlodarska I, Marynen P, Hagemeijer A. Fusion of NUP214 to ABL1 on amplified episomes in T-cell acute lymphoblastic leukemia. Nat Genet 2004;36:1084-1089.

[70]   Lacronique V, Boureux A, Valle VD, Poirel H, Quang CT, Mauchauffe M, Berthou C, Lessard M, Berger R, Ghysdael J, Bernard OA. A TEL-JAK2 fusion protein with constitutive kinase activity in human leukemia. Science 1997;278:1309-1312.

[71]   Riehm H, Reiter A, Schrappe M, Berthold F, Dopfer R, Gerein V, Ludwig R, Ritter J, Stollmann B, Henze G. [Corticosteroid-dependent reduction of leukocyte count in blood as a prognostic factor in acute lymphoblastic leukemia in childhood (therapy study ALL-BFM 83)]. Klin Padiatr 1987;199:151-160.

[72]   Bruggemann M, Schrauder A, Raff T, Pfeifer H, Dworzak M, Ottmann OG, Asnafi V, Baruchel A, Bassan R, Benoit Y, Biondi A, Cave H, Dombret H, Fielding AK, Foa R, Gokbuget N, Goldstone AH, Goulden N, Henze G, Hoelzer D, Janka-Schaub GE, Macintyre EA, Pieters R, Rambaldi A, Ribera JM, Schmiegelow K, Spinelli O, Stary J, von Stackelberg A, Kneba M, Schrappe M, van Dongen JJ. Standardized MRD quantification in European ALL trials: proceedings of the Second International Symposium on MRD assessment in Kiel, Germany, 18-20 September 2008. Leukemia 2010;24:521-535.

[73]   Cave H, van der Werff ten Bosch J, Suciu S, Guidal C, Waterkeyn C, Otten J, Bakkus M, Thielemans K, Grandchamp B, Vilmer E. Clinical significance of minimal residual disease in childhood acute lymphoblastic leukemia. European Organization for Research and Treatment of Cancer--Childhood Leukemia Cooperative Group. N Engl J Med 1998;339:591-598.

[74]   Fronkova E, Mejstrikova E, Avigad S, Chik KW, Castillo L, Manor S, Reznickova L, Valova T, Zdrahalova K, Hrusak O, Jabali Y, Schrappe M, Conter V, Izraeli S, Li CK, Stark B, Stary J, Trka J. Minimal residual disease (MRD) analysis in the non-MRD-based ALL IC-BFM 2002 protocol for childhood ALL: is it possible to avoid MRD testing? Leukemia 2008;22:989-997.

[75]   van Dongen JJ, Seriu T, Panzer-Grumayer ER, Biondi A, Pongers-Willemse MJ, Corral L, Stolz F, Schrappe M, Masera G, Kamps WA, Gadner H, van Wering ER, Ludwig WD, Basso G, de Bruijn MA, Cazzaniga G, Hettinger K, van der Does-van den Berg A, Hop WC, Riehm H, Bartram CR. Prognostic value of minimal residual disease in acute lymphoblastic leukaemia in childhood. Lancet 1998;352:1731-1738.

[76]   Ostman A, Hellberg C, Bohmer FD. Protein-tyrosine phosphatases and cancer. Nat Rev Cancer 2006;6:307-320.

[77]   Horejsi V. Transmembrane adaptor proteins in membrane microdomains: important regulators of immunoreceptor signaling. Immunol Lett 2004;92:43-49.

[78]   Horejsi V, Zhang W, Schraven B. Transmembrane adaptor proteins: organizers of immunoreceptor signalling. Nat Rev Immunol 2004;4:603-616.

[79]   Otahal P, Angelisova P, Hrdinka M, Brdicka T, Novak P, Drbal K, Horejsi V. A new type of membrane raft-like microdomains and their possible involvement in TCR signaling. J Immunol 2010;184:3689-3696.

[80]   Otahal P, Pata S, Angelisova P, Horejsi V, Brdicka T. The effects of membrane compartmentalization of csk on TCR signaling. Biochim Biophys Acta 2011;1813:367-376.

[81]   Brdicka T, Pavlistova D, Leo A, Bruyns E, Korinek V, Angelisova P, Scherer J, Shevchenko A, Hilgert I, Cerny J, Drbal K, Kuramitsu Y, Kornacker B, Horejsi V, Schraven B. Phosphoprotein associated with glycosphingolipid-enriched microdomains (PAG), a novel ubiquitously expressed transmembrane adaptor protein, binds the protein tyrosine kinase csk and is involved in regulation of T cell activation. J Exp Med 2000;191:1591-1604.

[82]   Posevitz-Fejfar A, Smida M, Kliche S, Hartig R, Schraven B, Lindquist JA. A displaced PAG enhances proximal signaling and SDF-1-induced T cell migration. Eur J Immunol 2008;38:250-259.

[83]   Kurosaki T. Regulation of B cell fates by BCR signaling components. Curr Opin Immunol 2002;14:341-347.

[84]   Svec A, Velenska Z, Horejsi V. Expression pattern of adaptor protein PAG: correlation between secondary lymphatic follicle and histogenetically related malignant lymphomas. Immunol Lett 2005;100:94-97.

[85]   Baumgartner M, Angelisova P, Setterblad N, Mooney N, Werling D, Horejsi V, Langsley G. Constitutive exclusion of Csk from Hck-positive membrane microdomains permits Src kinase-dependent proliferation of Theileria-transformed B lymphocytes. Blood 2003;101:1874-1881.

[86]   Zhang W, Sommers CL, Burshtyn DN, Stebbins CC, DeJarnette JB, Trible RP, Grinberg A, Tsay HC, Jacobs HM, Kessler CM, Long EO, Love PE, Samelson LE. Essential role of LAT in T cell development. Immunity 1999;10:323-332.

[87]   Su YW, Jumaa H. LAT links the pre-BCR to calcium signaling. Immunity 2003;19:295-305.

[88]   Su YW, Herzog S, Lotz M, Feldhahn N, Muschen M, Jumaa H. The molecular requirements for LAT-mediated differentiation and the role of LAT in limiting pre-B cell expansion. Eur J Immunol 2004;34:3614-3622.

[89]   Brdicka T, Imrich M, Angelisova P, Brdickova N, Horvath O, Spicka J, Hilgert I, Luskova P, Draber P, Novak P, Engels N, Wienands J, Simeoni L, Osterreicher J, Aguado E, Malissen M, Schraven B, Horejsi V. Non-T cell activation linker (NTAL): a transmembrane adaptor protein involved in immunoreceptor signaling. J Exp Med 2002;196:1617-1626.

[90]   Wang Y, Horvath O, Hamm-Baarke A, Richelme M, Gregoire C, Guinamard R, Horejsi V, Angelisova P, Spicka J, Schraven B, Malissen B, Malissen M. Single and combined deletions of the NTAL/LAB and LAT adaptors minimally affect B-cell development and function. Mol Cell Biol 2005;25:4455-4465.

[91]   Stork B, Engelke M, Frey J, Horejsi V, Hamm-Baarke A, Schraven B, Kurosaki T, Wienands J. Grb2 and the non-T cell activation linker NTAL constitute a Ca(2+)-regulating signal circuit in B lymphocytes. Immunity 2004;21:681-691.

[92]   Zhu M, Koonpaew S, Liu Y, Shen S, Denning T, Dzhagalov I, Rhee I, Zhang W. Negative regulation of T cell activation and autoimmunity by the transmembrane adaptor protein LAB. Immunity 2006;25:757-768.

[93]   Chambard JC, Lefloch R, Pouyssegur J, Lenormand P. ERK implication in cell cycle regulation. Biochim Biophys Acta 2007;1773:1299-1310.

[94]   Teixeiro E, Daniels MA. ERK and cell death: ERK location and T cell selection. Febs J 2010;277:30-38.

[95]   Daniels MA, Teixeiro E, Gill J, Hausmann B, Roubaty D, Holmberg K, Werlen G, Hollander GA, Gascoigne NR, Palmer E. Thymic selection threshold defined by compartmentalization of Ras/MAPK signalling. Nature 2006;444:724-729.

[96]   Zuna J, Krejci O, Madzo J, Fronkova E, Sramkova L, Hrusak O, Kalina T, Vaskova M, Stary J, Trka J. TEL/AML1 and immunoreceptor gene rearrangements-which comes first? Leuk Res 2005;29:633-639.

[97]   Tedoldi S, Paterson JC, Hansmann ML, Natkunam Y, Rudiger T, Angelisova P, Du MQ, Roberton H, Roncador G, Sanchez L, Pozzobon M, Masir N, Barry R, Pileri S, Mason DY, Marafioti T, Horejsi V. Transmembrane adaptor molecules: a new category of lymphoid-cell markers. Blood 2006;107:213-221.

[98]   Vaskova M, Fronkova E, Starkova J, Kalina T, Mejstrikova E, Hrusak O. CD44 and CD27 delineate B-precursor stages with different recombination status and with an uneven distribution in nonmalignant and malignant hematopoiesis. Tissue Antigens 2008;71:57-66.

[99]   Finco TS, Kadlecek T, Zhang W, Samelson LE, Weiss A. LAT is required for TCR-mediated activation of PLCgamma1 and the Ras pathway. Immunity 1998;9:617-626.

[100] Honda H, Inazawa J, Nishida J, Yazaki Y, Hirai H. Molecular cloning, characterization, and chromosomal localization of a novel protein-tyrosine phosphatase, HPTP eta. Blood 1994;84:4186-4194.

[101] Hermiston ML, Zikherman J, Zhu JW. CD45, CD148, and Lyp/Pep: critical phosphatases regulating Src family kinase signaling networks in immune cells. Immunol Rev 2009;228:288-311.

[102] Lin J, Zhu JW, Baker JE, Weiss A. Regulated expression of the receptor-like tyrosine phosphatase CD148 on hemopoietic cells. J Immunol 2004;173:2324-2330.

[103] Autschbach F, Palou E, Mechtersheimer G, Rohr C, Pirotto F, Gassler N, Otto HF, Schraven B, Gaya A. Expression of the membrane protein tyrosine phosphatase CD148 in human tissues. Tissue Antigens 1999;54:485-498.

[104] Singer A, Adoro S, Park JH. Lineage fate and intense debate: myths, models and mechanisms of CD4- versus CD8-lineage choice. Nat Rev Immunol 2008;8:788-801.

Adaptor molecules expression in normal lymphopoiesis and in childhood leukemia

Karel Svojgr [a,b,*,1], Tatiana Burjanivova [a,b,1], Martina Vaskova [a,b], Tomas Kalina [a,b], Jan Stary [b], Jan Trka [a,b], Jan Zuna [a,b]

[a] *CLIP – Childhood Leukemia Investigation Prague, Czech Republic*
[b] *Department of Pediatric Hematology and Oncology, Charles University Prague, 2nd Faculty of Medicine, Czech Republic*

ARTICLE INFO

ABSTRACT

Transmembrane adaptor proteins are key mediators of antigen receptor signaling in lymphocytes. By influencing proliferation and differentiation, these molecules might play a role in ethiopathogenesis of acute lymphoblastic leukemia (ALL). The aim of this study was to characterize expression of PAG, LAT, NTAL and LIME adaptors at the mRNA and protein levels in normal B- and T-precursors. Moreover, diagnostic samples of childhood ALL cases were analyzed.

During normal lymphocyte development, some adaptors show significant dynamics (gradual decrease of NTAL and increase of LAT and LIME during the T-cell maturation, decrease of PAG in B-precursors, high levels of LIME in peripheral B-lymphocytes). Analysis of childhood ALL samples revealed that in B-cell precursor ALL, the TEL/AML1 subgroup have unique adaptor profile compared to other leukemias. More-over, NTAL expression separates T lineage leukemias into two subgroups with good and poor response to initial prednisone therapy showing prognostic impact of this molecule in T-ALL.

© 2009 Elsevier B.V. All rights reserved.

1. Introduction

Acute lymphoblastic leukemia (ALL) is the most common childhood malignancy. Majority of cases are associated with known genetic aberrations of the lymphoid precursor. Most of the childhood ALLs arise from a B-cell precursor (BCP) (∼85%), the remaining ∼15% of cases are T-ALLs. The most frequent genetic abnormalities in pediatric ALL with prognostic impact are hyperdiploidy and translocations t(12;21), t(4;11) and t(9;22) with TEL/AML1, MLL/AF4 and BCR/ABL fusion genes, respectively. All these aberration are found almost exclusively in BCP leukemias and the genetic aberrations usually closely correlate with a corresponding immunophenotype. Thus leukemias with MLL/AF4 fusion (typical for infant age) are mostly formed by very immature B-cell precursors (CD19+, CD10−) while hyperdiploid and TEL/AML1 positive cases (comprising together about 45% of all childhood ALLs) show mature immunophenotype with CD10 positivity. Importantly, even in the cases with known genetic background the mechanisms of leukemogenesis are not fully understood.

Children with acute lymphoblastic leukemia (ALL) are usually treated according to risk groups defined by both clinical and laboratory features. Prognosis and thus also the intensity of treatment varies substantially among subsets of ALL. Treatment stratification in BFM protocols is partially based on genotype of the leukemic cells and also on early response to the 7-day prednisone treatment. Patients with a reduction in peripheral blast count to less than $1000/\mu l$ after a 7-day induction phase with prednisone and one dose of intrathecal methotrexate (a good prednisone response) have a more favorable prognosis than do patients whose peripheral blast counts remain above $1000/\mu l$ (a poor prednisone response).

PAG, LAT, NTAL and LIME proteins belong to the category of transmembrane adaptor proteins (TRAPs). TRAPs might play an important role in the ethiopathogenesis of ALL. At least some of these molecules are key mediators of antigen receptor signaling in lymphocytes and their abnormal function influences proliferation and differentiation of the cells. So far, seven TRAPs have been identified in detail where four of them (PAG, LAT, NTAL and LIME) are associated with glycosphingolipid-enriched microdomains (GEMs) called also membrane rafts [1]. Membrane rafts are submicroscopic regions enriched in glycosphingolipids and cholesterol. They possess an important role in signaling via immunoreceptors [2].

PAG ("phosphoprotein associated with glycosphingolipid-enriched microdomains"), also known as Csk-binding protein (Cbp), binds a tyrosine kinase Csk and thus enables its role of the major negative regulator of Src-family kinases [3]. Relatively high

* Corresponding author at: CLIP – Childhood Leukemia Investigation Prague, Department of Pediatric Hematology and Oncology Charles University Prague, 2nd Medical School, V Uvalu 84, 150 06 Prague 5, Czech Republic. Tel.: +420 224 436 580; fax: +420 224 436 521.
E-mail address: karel.svojgr@lfmotol.cuni.cz (K. Svojgr).
[1] These authors contributed equally to this research.

levels of PAG leading to the suppression of some Src-kinases (Lck and Fyn) activity were described in resting peripheral blood T-lymphocytes. T-cell receptor (TCR)-triggered activation causes reduction of PAG–Csk association resulting in elimination of the Csk-mediated inhibition of Lck and Fyn during the initial phase of T-cell activation [4]. Current study shows that for a proper inhibitory function of PAG in T-lymphocytes, PAG has to be localized in lipid rafts whereas its displacement from raft leads to increased chemotaxis of lymphocytes [5]. Moreover, Smida et al. [6] propose that in anergy T-cells, PAG recruits RasGAP to membrane enabling its fast degradation independently of Csk and thereby augments inhibition of signaling. In contrast, cross-linking of B-cell receptor (BCR) in B-cells induces an increase in PAG phosphorylation. This probably reflects the fact that Src-kinases in B-cells are more involved in negative regulation of the antigen receptor signaling. Suppression of the Src-kinases by the PAG/Csk complex may temporarily block the negative regulatory signals based on immunoreceptor tyrosine-based inhibitory motifs (ITIM) phosphorylation [1]. This theory is supported also by the data showing a high expression of PAG in proliferating cells of germinal centers and in follicular lymphomas [7]. Baumgartner et al. indicated a possible connection between PAG gene and leukemia. Protozoan parasite *Theileria parva* induce "leukemic" phenotype of cattle lymphocytes was associated with decreasing expression of PAG. The transformed phenotype reverts on drug-induced parasite death, and the PAG expression in cured lymphocytes return to normal [8].

LAT ("linker for activation of T-cells") is essential for the development of T-cells [9].

Following TCR ligation, LAT is a crucial molecule transferring the signal downstream into the cell. LAT−/− mice lack mature peripheral T-cells as their thymocytes fail to develop beyond the double-negative (DN) stage [9]. LAT is expressed also in pre-B-cells being connected to a pre-B-cell signaling and maturation of the pre-B-cell towards the immature B-lymphocyte. B-lymphocytes in LAT −/− mice are partially blocked at pre-B-cell stage, and the hematopoiesis shows increased numbers of pre-B-lymphocytes [10]. LAT can act in B-cells as a putative tumor suppressor inducing physiological B-cell differentiation [11].

NTAL ("linker for activation of T-cells 2"), also called LAT2, LAB or WBSCR5, was originally identified as a potential homologue of LAT in non-T-cell lymphocytes [12]. NTAL is physiologically present in B-cells, NK cells and myeloid cells. After cross-link of BCR receptor NTAL becomes phosphorylated by Syk and associates with Grb2, Sos1, Gap1 and c-Cbl, but not with PLCgamma [12]—thus the NTAL adaptor is not involved in early Ca intake signaling pathway. Using NTAL deficient mouse, Wang et al. [13] demonstrated increase of Ca influx and better proliferation in B-cells after antigen stimulation. Being engaged in a prolonged rather than early Ca intake [14], NTAL is not an equivalent of LAT in B-cells. Zhu et al. [15] suggested that in activated T-lymphocytes NTAL acts as an inhibitor of TCR signaling by competition with LAT in palmitoylation and localization to lipid raft. Herzog and Jumaa [16] demonstrated that in pre-B-cells this inhibitory effect of NTAL depends on N-terminal part of NTAL protein that localizes NTAL to different part of plasma membrane than LAT. Mutch et al. [17] showed that NTAL is involved in internalization of BCR after antigen stimulation. Thus, NTAL probably acts as a negative regulator of lymphocyte signaling.

LIME ("lck interacting molecule") is present in T-lymphocytes and is associated with CD4 and CD8 coreceptors. After phosphorylation, LIME associates with Src-kinases Lck and Fyn and their major inhibitor Csk [18]. This association paradoxically leads to increased TCR signaling, Ca flux, phosphorylation of Erk and increased activity of IL-2 promoter [18,19]. Taken together, LIME is probably involved in inhibitory signals mediated by CD4 and CD8 coreceptors after their cross-link without TCR engagement. Recent study indicates that LIME is important for B-cell signaling in mice. After cross-link

of BCR, LIME is phosphorylated by Lyn and associates with Lyn, Grb2 and PLCgamma. It leads to MAPK activation, Ca influx, PI3K and subsequently NFkappaB and NF-AT activation [20]. However, lymphocytes in LIME knock-out mice have normal morphology.

The dynamics of PAG, LAT, NTAL and LIME expression at the mRNA and protein levels during the human B and T-cell maturation was not thoroughly described yet. The recently published studies suggest that transmembrane adaptor molecules can be useful immunophenotypic markers relevant for the diagnosis and prognosis of lymphomas [7,21].

The objective of this study was to characterize the expression of transmembrane adaptors PAG, LAT, NTAL and LIME at the mRNA level by real-time quantitative reverse-transcriptase polymerase chain reaction (qRT-PCR) and (with the exception of LIME) also at the protein level by flow cytometry in normal B- and T-precursors and to investigate their role in childhood leukemia. Our results demonstrate significant changes in the expression between leukemic cells and their physiological counterparts (in particular in TEL/AML1 subgroup of childhood ALL). Moreover, we show that variable expression of NTAL adaptor has a prognostic impact in T-ALL.

2. Materials and methods

2.1. Normal hematopoietic tissue and leukemic samples

For the analysis of mature primary lymphocytes peripheral blood from healthy volunteer donors were used. For the investigation of B-cell development, bone marrow populations from children without any evidence of malignant disease (patients one or more years after the end of the ALL therapy and patients investigated to exclude hematological malignancy) were analyzed as non-malignant counterparts of leukemic cells.

For the primary T-cell precursors thymic T-cells from children undergoing heart surgery were used.

For the analysis of malignant lymphoid precursors we used diagnostic samples of 75 childhood ALL-patients treated according to the BFM (Berlin–Frankfurt–Münster) protocols. Of those, 36 cases were B-cell precursor (BCP) leukemias (15 TEL/AML1 positive, 5 infants MLL/AF4 positive, 8 hyperdiploid BCP-ALLs and 8 TEL/AML1 negative, MLL/AF4 negative and non-hyperdiploid BCP-ALLs) and 39 T-ALLs (7 pre T-ALLs, 13 intermediate T-ALLs, 19 mature T-ALLs).

All experiments were conducted according to the principles expressed in the Declaration of Helsinki. Ethical committee and Institutional review board approved the project and all samples were analyzed with written informed consent of all subjects or their guardians.

2.2. Cell sorting

Non-malignant samples were FACS sorted (FACS Aria, BD, San Jose) into fractions corresponding to ALLs with different maturation status according to immunophenotype.

The expression of PAG, LAT, NTAL and LIME proteins during B-cell development was analyzed in successive bone marrow stages defined as (1) CD34+CD19− cells which represent uncommitted progenitors of lymphoid as well as myeloid lineage (n = 8), (2) CD19+CD10+CD34+ subpopulation corresponding to B-precursors completing rearrangement of immunoglobulin heavy chain gene (n = 8), (3) CD19+CD10+CD34− immunoglobulin light chain gene rearranging cells (n = 8), and (4) CD19+CD20+CD10− which represent the most mature B-cells in the bone marrow (n = 8). By qRT-PCR only the mRNA expression in CD10+CD20+/− and CD10−CD20+ populations, corresponding to above mentioned stage (2 + 3) and

(4), respectively, were analyzed. Furthermore, the expression of PAG, LAT, NTAL and LIME in peripheral blood CD19+ B-cells was analyzed as stage (5) by both techniques.

For the investigation of mRNA expression during the T-cell development we fitted maturation stages to the classification of T-ALL proposed by EGIL [22], where the "intermediate T-cell group" was split into CD3− "early intermediate T-cell" and CD3+ "late intermediate T-cell", TCR alpha/beta and TCR gamma/delta were merged into "mature T-cells". Stages 1–4 were FACS sorted from thymus: (1st stage "pro/pre T-cell" CD7+CD3−CD1a−CD8−; 2nd stage "early intermediate T-cell" CD7+CD3−CD1a+CD8+/−; 3rd stage "late intermediate T-cell" CD7+CD3+CD1a+; 4th stage "mature T-cell" CD7+CD3+CD1a−). Stage 5 was FACS sorted as CD3+ T-cells from peripheral blood. Sorting purity was 87–97.9%.

These stages overlap with classical thymic developmental stages [23] as follows: 1st stage "pro/pre T-cell" (pro T + pre/pro T), 2nd stage "early intermediate T-cell" (pre T), 3rd stage "late intermediate T-cell" (immature single positive), 4th stage "mature T-cell" (double-positive + single-positive).

Thymic development stage definition for flow cytometry was the same as for qRT-PCR sorting but further supported by CD34 positivity in stages 1 and 2 and stage 4 was divided into double-positive (CD4+CD8+) and single-positive (CD4+CD8− or CD4−CD8+).

2.3. RNA preparation and qRT-PCR

RNA from patients' cells was extracted using a modified method described by Chomczynski and Sacchi [24]. RNA from sorted cells was isolated using RNeasy Micro Kit and RNeasy Mini Kit (Qiagen GmbH, Hilden, Germany) depending on the size of the sorted population. The RNA was reverse-transcribed into cDNA using MoMLV Reverse Transcriptase (Gibco BRL, Carlsbad, TX, USA) according to the manufacturer's protocol.

All qRT-PCR analyses were performed using an iCycler iQ system (Bio-Rad, Hercules, CA, USA) or ABI 7700 (Applied Biosystems, Foster City, CA, USA). For the housekeeping gene ABL the qRT-PCR was utilized to evaluate the amount and quality of cDNA as described previously [25]. ABL is a commonly used housekeeping gene in hematopoietic system as its expression was shown to be very stable in different stages of lymphoid differentiation [26]. The only caveat regards BCR/ABL-positive leukemias (no ALL of this subtype was analyzed in our cohort). To avoid a genomic DNA contamination, we used also an alternative forward primer overlapping an interface between Exon 2 and Exon 3. The new forward primer sequence was 5′-CTC TAA GCA TAA CTA AAG GTG AAA AGC-3′. Primers and probes for LAT, NTAL, LIME and PAG genes were designed using the Primer Express 2.0 Software (Applied Biosystems, Foster City, CA) and Vector NTI Software (Invitrogen Corporation, Carlsbad, CA, USA). For LAT, primer and probe sequences were as follows: forward primer, 5′-GAG AGC GCA GAA GCG TCT CT-3′; reverse primer, 5′-CAG TCT TAG CCG CTC CAG GAT-3′; probe, 5′-(FAM) ATG GCA GCC GGG AGT ATG TGA ATG TG. For the amplification of PAG: forward primer, 5′-AAG CCG CGA CAG CAT AGT G; reverse primer, 5′-TGA ACG GCT GAA CAT CTC CTT-3′; probe, 5′-(FAM) ACC ATG AGA ACC TGA TGA ACG TGC CTT C-3′. NTAL cDNA was amplified using forward primer, 5′-GGA CAT GGC ACC CAC AAG GA-3′; reverse primer, 5′-GGA ATT GGC ATC ATC ATC TTC TGG-3′; probe, 5′-(FAM) CTA TGT AGG CTT CCT CCG ACC CGT GTC TGC T-3′. LIME forward primer, 5′-GCG GAA GCG TCC CTA CTG AG-3′; LIME reverse primer, 5′-GAC ACC TCC AGC CAG TGT GG-3′; LIME probe, 5′-(FAM) CCT CTG CTC CCT CAG CAA GTC GGA-3′. Detection of PAG, LAT, NTAL, LIME and ABL was carried out in duplicate reactions.

PCR reactions for PAG, LAT, NTAL, LIME and ABL targets were performed in the final volume of 25 μl containing $MgCl_2$ (from 1.5 mM to 4 mM depending on the target gene), 1 U of polymerase, 200 nM of each dNTP, primers (from 300 nM to 1000 nM), 200 nM of probe

and 1 μl of template cDNA. ROX-6 was used as a reference color at TaqMan systems (1000 nM). Cycling conditions were 5 min at 94 °C for initial denaturation followed by 50 cycles of 94 °C/15 s and 60 °C/1 min for PAG, LAT and ABL. For NTAL and LIME the annealing temperature was 63 °C/30 s. Standard curves for the quantification of the ABL, LAT, and PAG genes were prepared by serial dilution of healthy volunteer donor's total cDNA into water, for NTAL and LIME cDNA from cell lines REH (NTAL) and MV4;11 (LIME) were used. Normalized PAG (LAT, NTAL, LIME) expression used for all analyses was determined in each individual sample as a ratio between the expression of PAG (LAT, NTAL, LIME) and ABL assessed by the qRT-PCR.

2.4. Flow cytometry

Whole bone marrow (BM) samples, peripheral blood (PB) samples or cryopreseved thymocytes were stained with following monoclonal antibodies (mAbs): anti-CD1a PE or anti-CD1a PC5, anti-CD3 FITC, anti-CD4 ECD, anti-CD7 FITC, anti-CD7 PE, anti-CD5 PC7, anti-CD10 ECD, anti-CD19 PC7, anti-CD34 FITC, anti-CD34 PC7 (Immunotech, Marseille, France), anti-CD8 Pacific Blue (Dako), anti-CD20 Alexa405 (Serotec, Kidlington, Oxford, UK) or anti-CD20 Pacific Blue (eBioscience, San Diego, CA, USA), anti-CD3 Alexa Fluor 700 anti-CD7 Pacific Blue (Exbio Praha, a.s., Czech Republic), antibodies to adaptor molecules were previously characterized [3,12,21,27] and available as direct conjugates from Exbio Praha: anti-Cbp/PAG (MEM-255) Dyomics647, anti-LAT (LAT-01) Dyomics647, anti-NTAL (NAP-07) PE. To control for non-specific staining we used control reagents at equal concentration Mouse IgG2a Isotype Control Dyomics647 and Mouse IgG1 Isotype Control Dyomics647 (Exbio). Cells were stained with antibodies, red blood cells were lysed with ammonium chloride lysing solution (containing NH_4Cl 0.16 M, $NaHCO_3$ 12 mM, EDTA 0.13 mM, NaN_3 0.02%, pH adjusted to 7.2–7.4), washed and resuspended in PBS. FIX&PERM cell permeabilization kit (An der Grub, Kaumbach, Austria) was used for intracellular staining of adaptor proteins according to the manufacturer's instructions. Samples were analyzed in FACS Aria flow cytometer (BD, San Jose, CA), CyAn ADP (Dako, Glostrup, Denmark) or BD LSRII (BD). All instruments are equipped with the same configuration 405 nm, 488 nm, 633–635 nm laser and 9-color detection. For polychromatic flow cytometry experiments, PMT voltage was set above electronic noise threshold and automated compensation matrix calculation was performed using single color stained tubes (DiVa 4.1.2 or Summit 4.3). Gating strategy of compensated data was determined using Fluorescence Minus One controls [28]. Analysis was performed using FlowJo 8.1.1 software (Treestar, Ashland, OR, USA). BCP-ALL samples were stained with following combinations of mAbs: anti-CD3 FITC, anti-CD10 ECD, anti-CD19 PC7, anti-CD20 Alexa405 and anti-Cbp/PAG Dyomics 647 or anti-LAT Dyomics 647. T-ALL specimens were stained with anti-CD3 FITC, anti-CD7 PE, anti-CD5 PC7, anti-CD20 Alexa405 and anti-Cbp/PAG Dyomics 647 or anti-LAT Dyomics 647. Non-malignant bone marrow cells were stained with anti-CD34 FITC, anti-CD10 ECD, anti-CD19 PC7, anti-CD20 Alexa405 and anti-Cbp/PAG Dyomics 647 or anti-LAT Dyomics 647. Thymocytes were stained with anti-CD8 Pacific Blue, anti-CD7 FITC, anti-CD1a PE, anti-CD4 ECD, anti-CD34 PC7, anti-CD3 Alexa Fluor 680 and anti-Cbp/PAG Dyomics 647 or anti-LAT Dyomics 647. For NTAL determination in thymocytes we used anti-CD7 Pacific Blue, anti-CD8 Pacific Blue, anti-CD8 FITC, anti-NTAL PE, anti-CD4 ECD, anti-CD1a PC5, anti-CD34 PC7 and anti-CD3 Alexa Fluor 700.

LAT, PAG and NTAL expression in gated subsets is shown as a ratio of their mean fluorescence intensity (MFI) to isotype control MFI in respective gate. This type of representation is used to normalize the MFI values, which differ between flow cytometers.

Table 1
The overall expression data of adaptor molecules PAG, LAT, NTAL and LIME.

		PAG (mRNA)		PAG (protein)		LAT (mRNA)		LAT (protein)	
		Mean	S.D.	Mean	S.D.	Mean	S.D.	Mean	S.D.
Normal B lineage	BCP 0	n.a.	n.a.	3.300	0.890	n.a.	n.a.	n.a.	n.a.
	BCP 1	n.a.	n.a.	6.775	1.263	n.a.	n.a.	n.a.	n.a.
	BCP 2	0.765	0.124	4.363	1.054	0.203	0.072	n.a.	n.a.
	BCP 3	1.030	0.110	3.400	1.167	0.116	0.045	n.a.	n.a.
	PB	0.464	0.177	2.353	0.448	0.200	0.086	n.a.	n.a.
BCP-ALL	MLL/AF4	0.345	0.137	n.a.	n.a.	0.251	0.224	n.a.	n.a.
	HD	1.111	0.384	5.978	1.792	0.126	0.160	n.a.	n.a.
	TEL/AML1	3.790	1.977	13.502	4.969	0.219	0.209	n.a.	n.a.
	Other	1.475	0.557	6.050	3.583	0.050	0.039	n.a.	n.a.
Normal T lineage	TCP 1	0.120	0.050	3.282	1.384	0.201	0.066	2.302	0.691
	TCP 2	0.003	0.000	2.712	1.354	0.183	0.075	1.786	0.831
	TCP 3	0.104	0.105	3.000	1.088	0.299	0.055	3.857	0.896
	TCP 4	0.091	0.032	n.a.	n.a.	0.323	0.146	n.a.	n.a.
	TCP 4a	n.a.	n.a.	3.184	1.191	n.a.	n.a.	5.002	2.079
	TCP 4b	n.a.	n.a.	3.349	1.276	n.a.	n.a.	8.311	2.641
	PB	1.215	0.079	3.850	1.582	3.601	0.286	19.672	5.981
T-ALL	Pre	0.446	0.059	2.100	n.a.	1.541	1.469	1.180	n.a.
	IM	0.261	0.240	2.300	n.a.	2.190	2.021	8.500	n.a.
	Mature	0.182	0.087	2.668	0.881	2.643	2.809	13.100	1.980
		NTAL (mRNA)		NTAL (protein)		LIME (mRNA)		LIME (protein)	
		Mean	S.D.	Mean	S.D.	Mean	S.D.	Mean	S.D.
Normal B lineage	BCP 0	n.a.	n.a.	182.230	304.240	n.a.	n.a.	n.a.	n.a.
	BCP 1	n.a.	n.a.	5.104	1.896	n.a.	n.a.	n.a.	n.a.
	BCP 2	22.617	8.707	4.477	1.301	45.320	24.089	n.a.	n.a.
	BCP 3	23.170	9.546	4.275	1.080	15.495	4.878	n.a.	n.a.
	PB	29.638	n.a.	4.879	1.341	428.959	n.a.	n.a.	n.a.
BCP-ALL	MLL/AF4	82.079	32.661	n.a.	n.a.	8.210	2.911	n.a.	n.a.
	HD	86.076	75.267	n.a.	n.a.	4.714	2.674	n.a.	n.a.
	TEL/AML1	25.889	14.332	n.a.	n.a.	21.499	26.626	n.a.	n.a.
	Other	49.592	21.394	n.a.	n.a.	13.921	8.545	n.a.	n.a.
Normal T lineage	TCP 1	11.531	2.493	38.451	60.278	137.949	44.974	n.a.	n.a.
	TCP 2	3.812	1.271	4.672	1.143	164.098	61.968	n.a.	n.a.
	TCP 3	3.589	1.351	3.101	0.635	373.590	113.701	n.a.	n.a.
	TCP 4	1.379	0.784	n.a.	n.a.	384.059	321.945	n.a.	n.a.
	TCP 4a	n.a.	n.a.	3.880	0.688	n.a.	n.a.	n.a.	n.a.
	TCP 4b	n.a.	n.a.	3.030	0.351	n.a.	n.a.	n.a.	n.a.
	PB	0.337	n.a.	3.276	0.614	n.a.	n.a.	n.a.	n.a.
T-ALL	Pre	9.024	7.821	n.a.	n.a.	77.596	40.242	n.a.	n.a.
	IM	4.922	5.042	n.a.	n.a.	66.407	43.594	n.a.	n.a.
	Mature	5.697	4.176	n.a.	n.a.	103.679	57.850	n.a.	n.a.

The mean of the PAG and LAT mRNA expression is set to the amount of PAG and LAT in normal peripheral blood lymphocytes (buffy coat). NTAL is normalized to the REH cell line and LIME to the MV4;11 cell line expression. For protein analysis, the mean of the levels of LAT, PAG and NTAL expression is shown as a ratio of their mean fluorescence intensity to isotype control. For the assignment of B and T lineage maturation stages, see Section 2. S.D., standard deviation; n.a., not available.

2.5. Statistical analysis

Mann–Whitney test was applied for statistical analyses performed using StatView software (SAS Institute, Cary, NC, USA).

3. Results

The overall data are summarized in Table 1.

3.1. PAG expression in normal and leukemic B lineage

The graph showing PAG expression in B lineage is shown in Fig. 1.

In the non-malignant tissue, the most immature CD19−CD34+ lineage uncommitted cells have a very low expression of PAG protein. With acquisition of CD19 positivity the PAG expression raises promptly and subsequently the levels of both PAG protein and mRNA gradually decrease with B-cell development towards mature peripheral B-lymphocytes as demonstrated by flow cytometry and qRT-PCR data, respectively.

PAG expression was analyzed in the following subgroups of childhood BCP-ALL: TEL/AML1 positive, MLL/AF4 positive (infants), hyperdiploid and others.

The dynamics of PAG protein and mRNA expression levels correspond very well. The levels of PAG in the group of "other" BCP-ALLs (non-hyperdiploid with TEL/AML1 negativity and MLL/AF4 negativity) as well as the hyperdiploid cases match the expression in the non-malignant counterparts (stages (2) and (3) formed by CD10+ progenitors). Also the low levels of PAG mRNA in MLL/AF4 positive cases of infant ALL seem to fit into the picture as these leukemias are formed by very early CD10− progenitors and the stage (1) CD34+CD19− cells are the closest non-malignant controls for these cases.

Interestingly, TEL/AML1 positive patients expressed higher PAG levels in comparison with the other CD10+ ALL subgroups (i.e. hyperdiploid and "other" ALLs; $p = 0.0035$ for protein and $p < 0.0001$ for mRNA) and with the non-malignant counterparts (CD19+CD10+CD34+ for protein expression, $p = 0.0045$; CD20+/−CD10+ for mRNA expression, $p = 0.0526$) (Fig. 2).

3.2. LAT expression in normal and leukemic B lineage

The total amounts of LAT mRNA in B-cell precursors are generally low. Levels of LAT do not differ significantly at the different stages of B-cell development.

LAT expression in analyzed subgroups of childhood BCP-ALL corresponds to their non-malignant counterparts with the exception of the non-hyperdiploid, fusion gene negative BCP-ALL showing lower LAT levels. The difference between this subgroup and normal B-cell precursors reaches a statistical significance $p = 0.0247$). Variable expression of LAT mRNA in different BCP-ALL subgroups was detected with TEL/AML1 and MLL/AF4 positive samples having higher mRNA levels. We were not able to detect any significant expression of the LAT protein by flow cytometry neither in normal B-precursors nor in BCP-ALL samples.
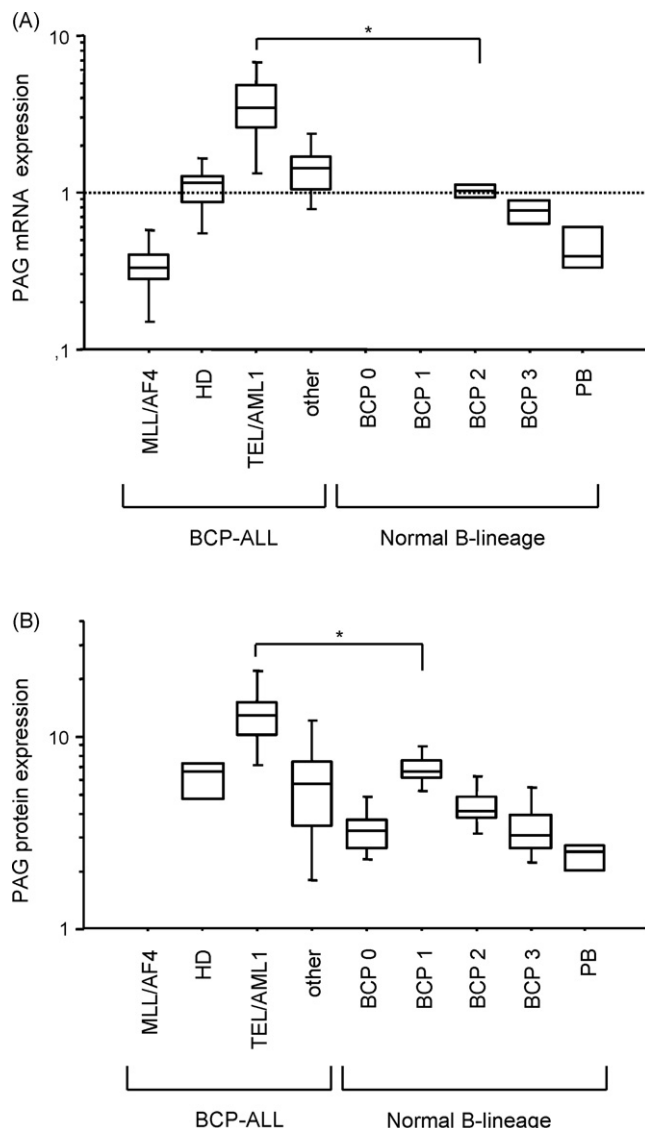
Fig. 1. Expression of PAG mRNA (A) and protein (B) during B-cell development and in childhood BCP-ALL samples. BCP-ALL, B-cell precursor leukemias; HD, hyperdiploid; other, non-hyperdiploid, fusion gene negative B-cell precursor leukemias; normal BCP 0, CD34+CD19− cells; normal BCP 1, CD19+CD10+CD34+; normal BCP 2, CD19+CD10+CD34− in protein analysis and CD10+CD20+/− in mRNA analysis; normal BCP 3, CD19+CD20+CD10− in protein analysis and CD20+CD10− in mRNA analysis; PB, normal peripheral blood B-lymphocytes, CD19+.
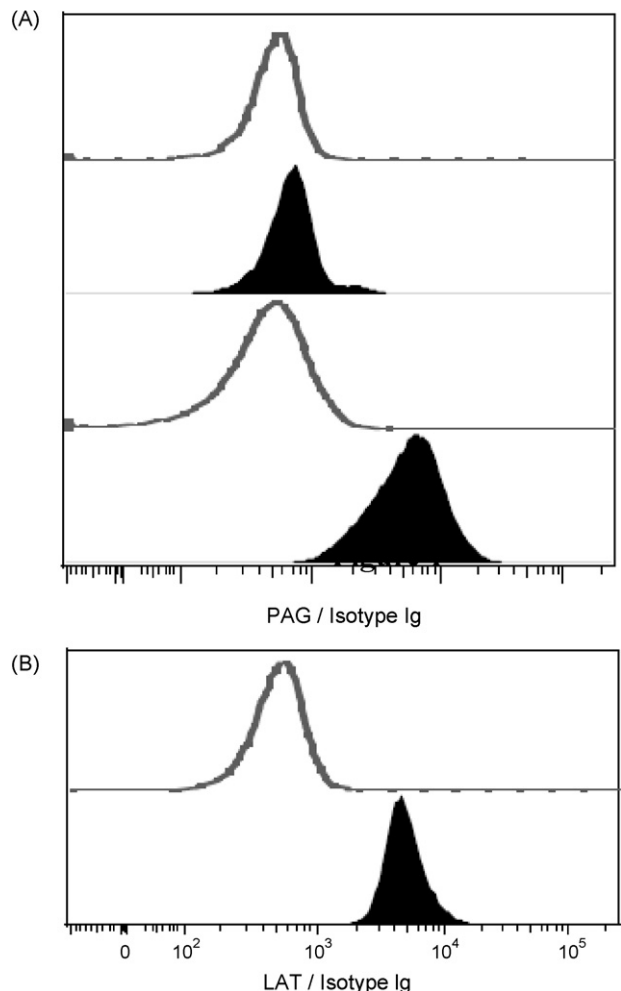
Fig. 2. Example of FACS analysis. (A) PAG protein expression in BCP-ALL case without any fusion gene (upper histograms) or with TEL/AML1 fusion gene (lower histograms). Gated on blast cells (CD19+ and CD10+). (B) LAT protein expression in T-ALL case. Gated on blast cells (CD3+). Isotype controls are depicted by open histograms, filled histograms depict PAG (in figure A) and LAT (in figure B).

3.3. NTAL expression in normal and leukemic B lineage

The amount of NTAL mRNA in B-lymphocyte precursors is comparable in the CD10+CD20+/− and CD10−CD20+ subpopulations and insignificantly higher in the mature peripheral B-cells. The same results are shown by the protein analysis, however, the most immature B-cells (analyzed only for protein expression) show the highest NTAL positivity among all other subsets (data not shown). We do not see any significant difference in NTAL expression among hyperdiploid, MLL/AF4 and non-hyperdiploid, fusion gene negative BCP-ALLs ($p = 0.42$). All these subtypes show higher NTAL expression compared to normal B-cell precursors. NTAL expression in the TEL/AML1 positive patients is significantly lower compared to the other BCP-leukemia subtypes and is comparable to the expression in normal B-precursors. The difference between NTAL mRNA level in TEL/AML1 and hyperdiploid BCP-ALL is statistically highly significant ($p = 0.004$).

3.4. LIME expression in normal and leukemic B lineage

We detected LIME mRNA in B-cell precursors, CD19+, CD10+ cells showing higher levels of LIME mRNA than CD19+, CD20+ precursors. However, the difference did not reach statistical significance, probably due to the low number of available samples ($p = 0.14$).

Peripheral B-lymphocytes express higher levels of LIME compared to B-cell precursors.

All BCP-ALL subgroups demonstrate significantly lower levels of LIME mRNA compared to the corresponding normal B-cell precursors. TEL/AML1, MLL/AF4+ and non-hyperdiploid, fusion gene negative BCP-ALLs have comparable amount of LIME mRNA, hyperdiploid leukemias display lower LIME levels ($p = 0.0074$).

3.5. PAG expression in normal and leukemic T lineage

We found only a weak expression of PAG in the T lineage.

The levels of PAG mRNA are constant in normal thymocytes with the exception of the "early intermediate T-cell" stage (CD7+CD3−CD1a+CD8+/−) showing tendency to lower PAG expression ($p = 0.0495$). The mature peripheral blood T-cells have significantly higher expression of PAG mRNA compared to the levels in thymocytes ($p = 0.0339$).

In the T-ALL samples there is a tendency to decrease the PAG expression with more mature phenotype of malignant population (pre T-ALL vs. mature T-ALL, $p = 0.0367$), however, there is no significant difference between malignant T-cells and thymocytes.

At the protein level the PAG expression is constantly low with no differences between various maturation stages of normal T-cells including both thymocytes and peripheral T-lymphocytes. Also the levels in malignant blasts of T-ALL are constant and do not differ from the normal T-cells.

3.6. LAT expression in normal and leukemic T lineage

The expression of LAT increases during the normal T-cell maturation as shown in Fig. 3. While at the mRNA level the increase is significant only between thymocytes and peripheral T-cells ($p = 0.0036$), the differences at the protein level are detectable already during the thymic period (CD7+CD3−CD1a+CD8+/− "early intermediate T-cells" vs. CD7+CD3+CD1a+ "late intermediate T-cells", $p = 0.0163$; mature double-positive vs. mature single-positive T-cells, $p = 0.0373$; thymocytes vs. CD3+ peripheral T-lymphocytes, $p = 0.0143$).

The LAT levels show also a tendency to rise with more mature immunophenotype of T-ALL but due to a low number of samples with the particular T-ALL subgroups (pre T-, intermediate T-, mature T-ALL) the differences do not reach a statistical significance. The pre T-ALLs and intermediate T-ALLs show higher LAT levels than the normal pre T and intermediate T-cells, respectively. The mature T-ALLs have a higher expression of LAT compared to normal mature thymocytes, although the statistically significant difference can be seen only at the protein level ($p = 0.0079$ to "single positive" thymocytes and $p = 0.0062$ to "double-positive" thymocytes). However, the LAT expression in mature T-ALLs does not reach the level detected in the normal peripheral T-cells ($p = 0.0887$ for mRNA and $p = 0.0428$ for protein expression) (Fig. 3).

3.7. NTAL expression in normal and leukemic T lineage

We were able to detect NTAL mRNA, albeit at low levels, in all sorted thymocyte populations. The NTAL mRNA expression decreases during normal T-lymphocyte differentiation and the same trend is visible in the protein analysis with pro/pre T-cells showing the highest NTAL levels.

T-ALL cases show various levels of NTAL and the patients can be divided into two distinct subgroups–those with low and with high NTAL expression. The threshold between the "high" and "low" expression was stated as twofold level of NTAL expression in the REH cell line (REH cell line was used for dilution series in NTAL experiments). The NTAL "high" and "low" assignment does not correlate with immunophenotype, age of the patients at diagnosis nor
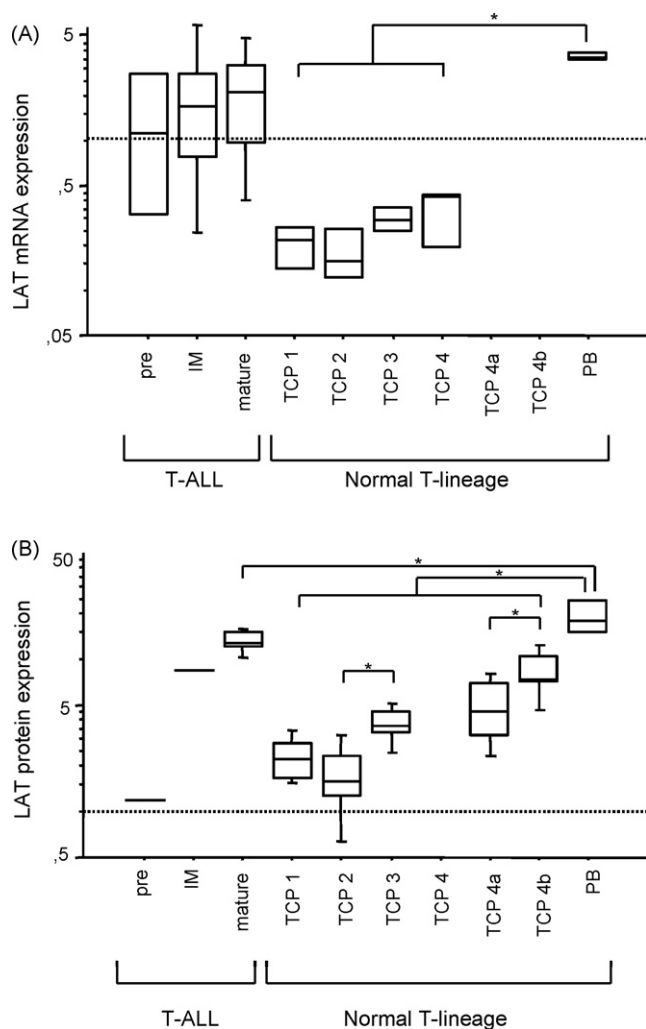
Fig. 3. Expression of LAT mRNA (A) and protein (B) during T-cell development and in childhood T-ALL samples. IM, intermediate T-ALL; TCP 1, CD34+CD7+CD3−CD1a−CD8− in protein analysis and CD7+CD3−CD1a−CD8− in mRNA analysis; TCP 2, CD34+CD7+CD3−CD1a+CD8+/− in protein analysis and CD7+CD3−CD1a+CD8+/− in mRNA analysis; TCP 3, CD7+CD3+CD1a+; TCP 4, CD7+CD3+CD1a−; TCP 4a, CD7+CD3+CD1a−CD4+CD8+; TCP 4b, CD7+CD3+CD1a−CD4+CD8− or CD7+CD3+CD1a−CD8+CD4−; PB, normal peripheral blood T-lymphocytes, CD3+.
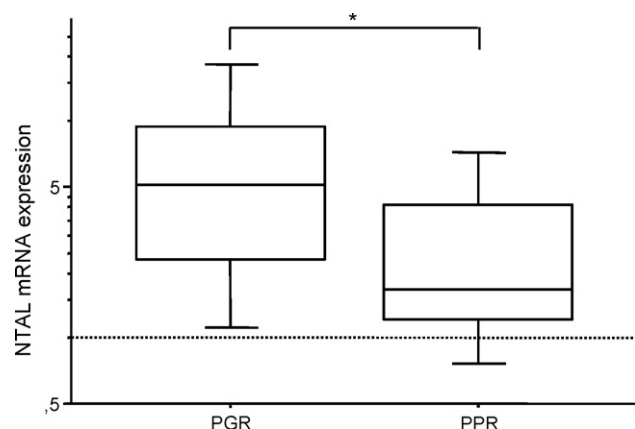
Fig. 4. Expression of NTAL mRNA in T-cell leukemia. PGR: prednisone good responders; PPR: prednisone poor responders.
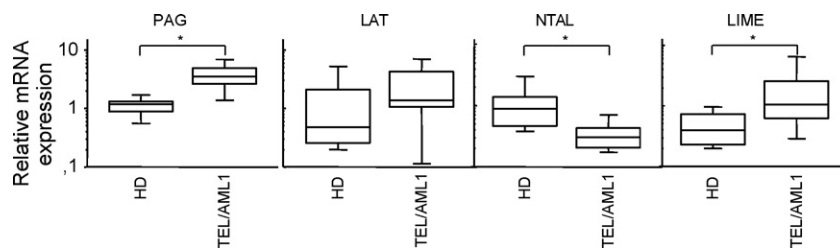
Fig. 5. Expression of PAG, LAT, NTAL and LIME mRNA in hyperdiploid (HD) and TEL/AML1 positive BCP-ALL.

with the initial white blood cell count. However, the two NTAL groups differ significantly in response to the initial therapy. While more than a half of the patients (6/11) with low NTAL expression responded poorly to the initial prednisone treatment (= prednisone poor responders), the vast majority (20/24) of the NTAL-high group showed good prednisone response ($p = 0.04$). The difference in the NTAL expression between the prednisone poor vs. good responders is statistically significant ($p = 0.0285$) (Fig. 4).

3.8. LIME expression in normal and leukemic T lineage

The level of LIME mRNA increases during maturation of T-lymphocyte precursors.

In leukemic samples, intermediate T-ALLs and pre T-ALLs display lower LIME mRNA levels compared to mature T-ALL ($p = 0.04$). The overall expression of LIME is significantly higher in T-ALL compared to BCP-ALL ($p < 0.0001$); however, it does not reach the level found in physiologic T-lymphocyte precursors.

4. Discussion

Using qRT-PCR and flow cytometry we analyzed expression status of four transmembrane adaptors – PAG, LAT, NTAL and LIME – at the mRNA and – with the exception of LIME – also at protein levels. In general, the mRNA and protein levels and dynamics correspond very well. We defined changes of adaptor expression during normal lymphocyte development in human and, moreover, we correlated the physiological expression with mRNA and protein levels found in principal subtypes of childhood ALL. We found significant differences in the expression in ALLs with different genetic background and we show prognostic impact of the different expression levels. Our primary data can be used for subsequent functional analysis of these molecules that is needed to fully elucidate its role in B- and T-cell development and in leukemia.

Protein and mRNA expression analysis show that while some of the adaptor molecules are present at relatively constant levels (e.g. PAG in T lineage) during normal B- or T-lymphocyte development, others show significant dynamics (decrease of NTAL and increase of LIME and LAT levels during T-cell maturation, decrease of PAG during B-cell development, high LIME levels in mature peripheral B-lymphocytes). Our findings suggest that different signaling pathways are activated and different adaptors are involved during physiologic lymphocyte maturation.

Studying malignant counterparts of normal lymphocyte precursors might be very useful for further understanding of function and pathology of these molecules. We analyzed leukemic cells of various childhood ALL subgroups, compared the expression of the adaptor proteins with normal precursors and subsequently elucidated prognostic impact of different expression levels.

The TEL/AML1-positive and hyperdiploid leukaemias compose together about one half of all childhood ALL cases. These two well-defined subgroups have a very similar characteristics in terms of incidence (each subgroup comprises 20–25% of all childhood ALLs), age at diagnosis (vast majority diagnosed in pre-school age 1–5

years), immunophenotype (CD34+19+10+), treatment response and overall prognosis (very good outcome). Interestingly, the expression of adaptor proteins differs markedly in these two subgroups (TEL/AML1 showing higher expression of PAG and LIME and lower levels of NTAL, $p = 0.001$, $p = 0.023$ and $p = 0.004$, respectively) (Fig. 5) and both the TEL/AML1 and hyperdiploid cases show significantly different expression not only compared to other, phenotypically comparable leukemias, but the expression also significantly differs from the levels found in corresponding normal B-precursors. This observation probably reflects a different biological background of these subgroups and implies that the adaptor molecules may play a role – direct or indirect – in the etiopathogenesis of the TEL/AML1 positive and/or hyperdiploid ALL.

The most prominent change in B-cell precursor leukemias is the high expression of PAG in TEL/AML1-positive cases. The high levels of PAG in this subgroup might mirror the origin of these leukemias in an early B-progenitor. This would correspond with our previous observation based on detailed immunophenotypic analysis of this group [29]. The higher PAG activity in TEL/AML1 positive samples could also explain another known phenomenon seen in these cells, the higher activity of VDJ recombination machinery resulting in significantly higher number of immunoglobulin and T-cell receptor rearrangements in TEL/AML1 positive compared to TEL/AML1 negative leukemias [30]. As suggested previously, the higher PAG activity in B-precursors leads to a higher recruitment of Csk and subsequent inhibition of Src-kinases activity. Resulting decrease of phosphorylation of inhibitory ITIM motifs then allows higher propagation of activation signals including the VDJ recombinase activity. Interestingly, the PAG levels correlate significantly with the expression of CD27 antigen. This molecule has been shown to be expressed on the B-cells with high activity of VDJ recombinase machinery—IgH rearranging early B-progenitors, germinal centre B-cells and also ALL cases with positivity of the TEL/AML1 fusion gene [7,21,31,32]. High expression of PAG protein was recently described also in the samples of follicular lymphoma [7].

In T-ALL cases, LAT increases significantly with the maturation of both malignant and non-malignant precursors. However, in mature T-ALL the expression of LAT exceeds the level found in mature thymocytes but it does not reach the level of peripheral blood T-cells. Since LAT is required for T-cell receptor activation [33], the marked increase of LAT expression in peripheral blood T-cells can reflect antigenic experience of these cells. The lower levels in leukemic samples probably reflect the fact that despite these malignant and non-malignant cells are phenotypically in the comparable maturation stage and both are present in peripheral circulation, the malignant T-cells are not capable of adequate response to antigen stimulation.

While the levels of other adaptors are relatively stable within particular genetic subgroups of ALL, expression of LAT (in both BCP and T-ALL) and NTAL (in T-ALL) varies markedly. Our results show that the variable expression of these adaptor molecules in the leukemic cells might have an impact on treatment response and prognosis. In particular, low expression of NTAL at the time of diagnosis of childhood T-ALL significantly correlates with poor response

to the initial one-week prednisone pre-phase ($p = 0.028$). As NTAL is a putative tumor suppressor gene acting probably through competitive inhibition of LAT and thus decreasing the phosphorylation level of Src-kinases, the differences in NTAL expression could explain the early treatment response variability. On the other hand, the high NTAL expression has rather unfavorable prognostic impact in the TEL/AML1 subgroup as the patients who suffer subsequent relapse have tendency to a higher NTAL expression. Despite the fact that this difference does not reach a statistical significance ($p = 0.071$), this phenomenon suggests different role of NTAL in malignant B- and T-precursors.

In conclusion, our data show that expression of membrane adaptor molecules on leukemic blasts is specific in some ALL subgroups—particularly in TEL/AML1-positive ALL. Moreover, we demonstrate that the variable expression may play an important role in early treatment response. In addition to the ALL data, we show for the first time a detailed analysis of adaptor molecules expression dynamics during normal human lymphocyte differentiation.

Acknowledgements

References

[1] Horejsi V, Zhang W, Schraven B. Transmembrane adaptor proteins: organizers of immunoreceptor signalling. Nat Rev Immunol 2004;4:603–16.

[2] Hancock JF. Lipid rafts: contentious only from simplistic standpoints. Nat Rev Mol Cell Biol 2006;7:456–62.

[3] Brdicka T, Pavlistova D, Leo A, Bruyns E, Korinek V, Angelisova P, et al. Phosphoprotein associated with glycosphingolipid-enriched microdomains (PAG), a novel ubiquitously expressed transmembrane adaptor protein, binds the protein tyrosine kinase Csk and is involved in regulation of T cell activation. J Exp Med 2000;191:1591–604.

[4] Horejsi V. Transmembrane adaptor proteins in membrane microdomains: important regulators of immunoreceptor signaling. Immunol Lett 2004;92:43–9.

[5] Posevitz-Fejfar A, Smida M, Kliche S, Hartig R, Schraven B, Lindquist JA. A displaced PAG enhances proximal signaling and SDF-1-induced T cell migration. Eur J Immunol 2008;38:250–9.

[6] Smida M, Posevitz-Fejfar A, Horejsi V, Schraven B, Lindquist JA. A novel negative regulatory function of the phosphoprotein associated with glycosphingolipid-enriched microdomains: blocking Ras activation. Blood 2007;110:596–615.

[7] Svec A, Velenska Z, Horejsi V. Expression pattern of adaptor protein PAG: correlation between secondary lymphatic follicle and histogenetically related malignant lymphomas. Immunol Lett 2005;100:94–7.

[8] Baumgartner M, Angelisova P, Setterblad N, Mooney N, Werling D, Horejsi V, et al. Constitutive exclusion of Csk from Hck-positive membrane microdomains permits Src kinase-dependent proliferation of Theileria-transformed B lymphocytes. Blood 2003;101:1874–81.

[9] Zhang W, Sommers CL, Burshtyn DN, Stebbins CC, DeJarnette JB, Trible RP, et al. Essential role of LAT in T cell development. Immunity 1999;10:323–32.

[10] Su YW, Jumaa H. LAT links the pre-BCR to calcium signaling. Immunity 2003;19:295–305.

[11] Su YW, Herzog S, Lotz M, Feldhahn N, Muschen M, Jumaa H. The molecular requirements for LAT-mediated differentiation and the role of LAT in limiting pre-B cell expansion. Eur J Immunol 2004;34:3614–22.

[12] Brdicka T, Imrich M, Angelisova P, Brdickova N, Horvath O, Spicka J, et al. Non-T cell activation linker (NTAL): a transmembrane adaptor protein involved in immunoreceptor signaling. J Exp Med 2002;196:1617–26.

[13] Wang Y, Horvath O, Hamm-Baarke A, Richelme M, Gregoire C, Guinamard R, et al. Single and combined deletions of the NTAL/LAB and LAT adaptors minimally affect B-cell development and function. Mol Cell Biol 2005;25:4455–65.

[14] Stork B, Engelke M, Frey J, Horejsi V, Hamm-Baarke A, Schraven B, et al. Grb2 and the non-T cell activation linker NTAL constitute a Ca(2+)-regulating signal circuit in B lymphocytes. Immunity 2004;21:681–91.

[15] Zhu M, Koonpaew S, Liu Y, Shen S, Denning T, Dzhagalov I, et al. Negative regulation of T cell activation and autoimmunity by the transmembrane adaptor protein LAB. Immunity 2006;25:757–68.

[16] Herzog S, Jumaa H. The N terminus of the non-T cell activation linker (NTAL) confers inhibitory effects on pre-B cell differentiation. J Immunol 2007;178:2336–43.

[17] Mutch CM, Sanyal R, Unruh TL, Grigoriou L, Zhu M, Zhang W, et al. Activation-induced endocytosis of the raft-associated transmembrane adaptor protein LAB/NTAL in B lymphocytes: evidence for a role in internalization of the B cell receptor. Int Immunol 2007;19:19–30.

[18] Brdickova N, Brdicka T, Angelisova P, Horvath O, Spicka J, Hilgert I, et al. LIME: a new membrane Raft-associated adaptor protein involved in CD4 and CD8 coreceptor signaling. J Exp Med 2003;198:1453–62.

[19] Hur EM, Son M, Lee OH, Choi YB, Park C, Lee H, et al. LIME, a novel transmembrane adaptor protein, associates with p56lck and mediates T cell activation. J Exp Med 2003;198:1463–73.

[20] Ahn E, Lee H, Yun Y. LIME acts as a transmembrane adapter mediating BCR-dependent B-cell activation. Blood 2006;107:1521–7.

[21] Tedoldi S, Paterson JC, Hansmann ML, Natkunam Y, Rudiger T, Angelisova P, et al. Transmembrane adaptor molecules: a new category of lymphoid-cell markers. Blood 2006;107:213–21.

[22] Bene MC, Castoldi G, Knapp W, Ludwig WD, Matutes E, Orfao A, et al. Proposals for the immunological classification of acute leukemias. European Group for the Immunological Characterization of Leukemias (EGIL). Leukemia 1995;9:1783–6.

[23] Staal FJ, Weerkamp F, Langerak AW, Hendriks RW, Clevers HC. Transcriptional control of T lymphocyte differentiation. Stem Cells 2001;19:165–79.

[24] Chomczynski P, Sacchi N. Single-step method of RNA isolation by acid guanidinium thiocyanate-phenol-chloroform extraction. Anal Biochem 1987;162:156–9.

[25] Boublikova L, Kalinova M, Ryan J, Quinn F, O'Marcaigh A, Smith O, et al. Wilms' tumor gene 1 (WT1) expression in childhood acute lymphoblastic leukemia: a wide range of WT1 expression levels, its impact on prognosis and minimal residual disease monitoring. Leukemia 2006;20:254–63.

[26] Beillard E, Pallisgaard N, van der Velden VH, Bi W, Dee R, van der Schoot E, et al. Evaluation of candidate control genes for diagnosis and residual disease detection in leukemic patients using 'real-time' quantitative reverse-transcriptase polymerase chain reaction (RQ-PCR)—a Europe against cancer program. Leukemia 2003;17:2474–86.

[27] Tkaczyk C, Horejsi V, Iwaki S, Draber P, Samelson LE, Satterthwaite AB, et al. NTAL phosphorylation is a pivotal link between the signaling cascades leading to human mast cell degranulation following Kit activation and Fc epsilon RI aggregation. Blood 2004;104:207–14.

[28] Roederer M. Spectral compensation for flow cytometry: visualization artifacts, limitations, and caveats. Cytometry 2001;45:194–205.

[29] Vaskova M, Mejstrikova E, Kalina T, Trka J, Stary J, Hrusak O. CD27 expression in malignant and normal human B precursors: a confirmed phenomenon. Reply to Nilsson and colleagues. Exp Hematol 2006;34:573–4.

[30] Zuna J, Krejci O, Madzo J, Fronkova E, Sramkova L, Hrusak O, et al. TEL/AML1 and immunoreceptor gene rearrangements-which comes first? Leuk Res 2005;29:633–9.

[31] Klein U, Tu Y, Stolovitzky GA, Keller JL, Haddad Jr J, Miljkovic V, et al. Gene expression dynamics during germinal center transit in B cells. Ann N Y Acad Sci 2003;987:166–72.

[32] Vaskova M, Fronkova E, Starkova J, Kalina T, Mejstrikova E, Hrusak O. CD44 and CD27 delineate B-precursor stages with different recombination status and with an uneven distribution in nonmalignant and malignant hematopoiesis. Tissue Antigens 2008;71:57–66.

[33] Finco TS, Kadlecek T, Zhang W, Samelson LE, Weiss A. LAT is required for TCR-mediated activation of PLCgamma1 and the Ras pathway. Immunity 1998;9:617–26.

Experimental Hematology

The adaptor protein NTAL enhances proximal signaling and potentiates corticosteroid-induced apoptosis in T-ALL

Karel Svojgr[a,b], Tomas Kalina[a,b], Veronika Kanderova[a,b], Tereza Skopcova[c], Tomas Brdicka[c], and Jan Zuna[a,b]

[a]CLIP-Childhood Leukemia Investigation Prague, Prague, Czech Republic; [b]Department of Pediatric Hematology and Oncology, 2nd Faculty of Medicine, Charles University Prague and University Hospital Motol, Prague, Czech Republic; [c]Institute of Molecular Genetics, Academy of Sciences, Prague, Czech Republic

The biology of T-cell acute lymphoblastic leukemia (ALL) is characterized by functional pre−T-cell receptor (TCR) signaling. Non−T-cell activation linker (NTAL) is a nonenzymatic transmembrane adaptor molecule that is involved in the proximal signaling of lymphocytes. In our previous work, we found an association between high NTAL expression in T-cell ALL blasts and a favorable response to initial glucocorticoid treatment. In the present study, we confirm our previous observation in an experimental model. In addition, the molecular mechanism of the contribution of NTAL to malignant T-cell ALL blast signaling and to methylprednisolone-induced cell death is analyzed. In the in vitro experiments, we used the T-cell ALL Jurkat cell line (Jurkat/wt) and derived Jurkat cell line with stable NTAL expression (Jurkat/NTAL+). Cell signaling and cell death after methylprednisolone treatment and after TCR stimulation were analyzed using flow cytometry, Western blot, and quantitative polymerase chain reaction. Jurkat/NTAL+ cells are significantly more sensitive to both methylprednisolone treatment and TCR-induced stimulation. In addition, after TCR stimulation, Jurkat/NTAL+ cells show a higher level of intracellular extracellular signal-regulated kinase 1/2 (ERK) phosphorylation and increased expression of the CD69 activation marker on the cell surface than the Jurkat/wt cells. The ERK inhibitor U0126 almost completely abrogates TCR-induced cell death and, importantly, reverses the sensitizing effect of the NTAL protein on methylprednisolone-induced cell death. In conclusion, NTAL acts as a tumor suppressor that enhances the proximal signaling of leukemic blasts. The key downstream molecule responsible for the biological effect of TCR signaling is ERK. Higher ERK phosphorylation leads to enhanced cell death after TCR stimulation and increases cell sensitivity to methylprednisolone-induced cell death.   © 2012 ISEH - Society for Hematology and Stem Cells.   Published by Elsevier Inc.

Acute lymphoblastic leukemia (ALL) is the most common malignancy in childhood. Approximately 15% of cases are T-cell ALLs that originate in immature thymocytes. Childhood leukemia is a highly curable disease in general [1]; however, 20% of patients relapse, and the prognosis for these patients is usually poor. According to the Berlin-Frankfurt-Münster group treatment protocols, only glucocorticoids and intrathecal methotrexate are administered during the first week of therapy. The reduction of malignant blasts to <1000 in 1 μL peripheral blood defines a favorable response to initial glucocorticoid treatment and is one of the most important prognostic factors in ALL [2]. In our previous work, we demonstrated that the level of non−T-cell activation linker (NTAL) messenger RNA (mRNA) affects the response to prednisone treatment in T-cell ALL; good responders have significantly higher levels of NTAL mRNA in leukemic blasts than poor responders [3]. In the present study, we aimed to investigate the role of the NTAL molecule in T-cell ALL in more detail.

For T-cell leukemogenesis, pre−T-cell receptor signaling [4] and subsequent extracellular signal-regulated kinase 1/2 (ERK) activation [5] is essential. NTAL and

Offprint requests to: Karel Svojgr, M.D., CLIP-Childhood Leukemia Investigation Prague, Department of Pediatric Hematology and Oncology, 2nd Faculty of Medicine, Charles University Prague and University Hospital Motol, V Uvalu 84, 150 06, Prague 5, Czech Republic; E-mail: karel.svojgr@lfmotol.cuni.cz
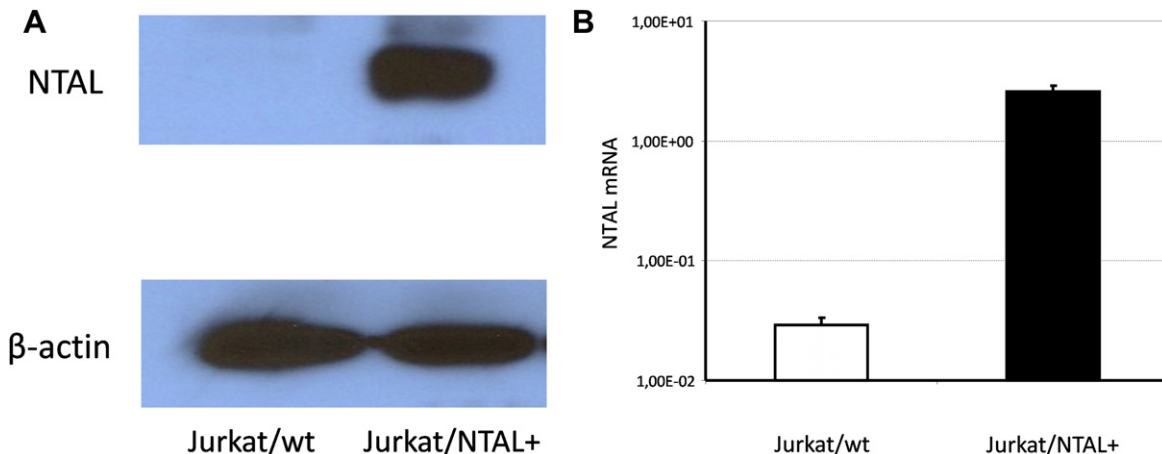
Figure 1. Expression of the NTAL molecule in Jurkat/wt and Jurkat/NTAL^{+} cells. Expression of the NTAL molecule in Jurkat/wt and Jurkat/NTAL^{+} cells assed by (**A**) Western blot and (**B**) quantitative reverse transcription PCR.

linker for activation of T-cell (LAT) are nonenzymatic signaling molecules that belong to a category of transmembrane adaptor proteins. NTAL and LAT are localized in glycol-sphingolipid–enriched microdomains (also called "lipid rafts") and provide docking sites for effector signaling molecules to enable signal transmission from immunoreceptors to the nucleus [6]. The crucial adaptor protein for signal transmission from the T-cell receptor (TCR) is LAT. After TCR engagement, LAT is phosphorylated by Syk kinase ζ-chain–associated protein kinase 70 and associates directly with growth factor receptor–bound protein 2 (GRB2), GRB2-related adaptor protein 2, and phospholipase C−γ [6]. This association leads to assembly of a signalosome in glycol-sphingolipid–enriched microdomains and efficient signal transmission to the nucleus. The NTAL molecule (also called LAB, LAT2, or WBSCR5) has a very similar structure to LAT (binds to GRB2 and c-cbl), but does not directly associate with phospholipase C−γ [7]. In B lymphocytes, the function of the NTAL molecule is relatively well described and a presumable activating role of NTAL has been shown; NTAL is involved in sustained calcium influx from the extracellular space after B-cell receptor stimulation [8]. However, in physiological T lymphocytes, NTAL has rather an inhibitory role in TCR-induced signaling. NTAL is not expressed in resting T lymphocytes [7], but its expression is heavily upregulated after TCR stimulation, leading to decreased T-cell activation [9]. Overexpression of NTAL in physiological T lymphocytes decreases the phosphorylation of ERK and Akt [9]. In T-cell development, NTAL can partially substitute for the absence of LAT [10], partly restoring calcium influx [11]. In addition, NTAL$^{-/-}$ mice develop an autoimmune syndrome characterized by activated T cells. In summary, NTAL probably acts both as an activator and inhibitor of lymphocyte signaling, depending on the cell type.

ERK is a serine/threonine kinase that is activated after TCR engagement by sequential phosphorylation in the RAS/RAF/MEK/ERK signaling cascade. ERK is involved in diverse and often opposite cellular functions, including cell cycle progression and cell cycle arrest [12], and in cell survival and cell death [13]. In physiological T-lymphocyte development, the magnitude, localization, and duration of ERK phosphorylation after TCR engagement determines whether the lymphocyte undergoes positive or negative selection. Strong TCR engagement (negative selectors) induces rapid and high ERK phosphorylation, and ERK is translocated to the plasma membrane. In contrast, positive selectors induce slower ERK phosphorylation, and ERK is localized to the Golgi complex [14].

In the current study, we examined the role of the NTAL molecule in glucocorticoid-induced cell death in a native and derivative Jurkat cell line. We also determined the influence of the NTAL protein on the response to TCR signaling.

Materials and methods

Jurkat wild-type and Jurkat/NTAL^{+} cell lines
The Jurkat cell line (Jurkat/wt), which was derived from a 14-year-old patient at the first relapse of T-cell ALL, was used in the in vitro experiments. Expression of the NTAL protein is not detectable in this cell line, and a very low amount of NTAL mRNA is expressed (Fig. 1). A Jurkat cell line with stable expression of the NTAL protein (Jurkat/NTAL^{+}) was used as a model for NTAL-positive T-cell ALL malignant blasts. To establish the Jurkat/NTAL^{+} cell line, we transfected Jurkat cells with a NTAL-pEFIRES-N construct by electroporation on a BioRad Gene Pulser, followed by selection using a limiting dilution in the presence of G418 (2 mg/mL) to select single cell clones. The presence of the NTAL construct was confirmed using quantitative reverse transcription polymerase chain reaction (PCR) and Western blot (Fig. 1).

Generation of NTAL-pEFIRES-N construct (entire coding sequence of human NTAL cloned into EcoRI site of pEFIRES-N vector [15]) has been described earlier [7]. Cells were maintained in RPMI-1640 supplemented with 10% heat-inactivated fetal bovine serum, 2 mmol/L L-glutamine, 100 U/mL penicillin, and 100 μg/mL streptomycin at 37°C in a 5% CO_2 atmosphere. Jurkat/wt and Jurkat/NTAL$^+$ cells show similar growth patterns in cell culture (data not shown).

Reagents and antibodies
The following reagents and antibodies were used: methylprednisolone (Solu-Medrol, Pharmacia Upjohn, Puurs, Belgium), U0126 monoethanolate, paraformaldehyde, tris(hydroxymethyl)aminomethane (Tris), sodium orthovanadate, sodium fluoride, glycerol, n-dodecyl β-D-maltoside (laurylmaltoside), phenylmethanesulfonyl fluoride (Sigma-Aldrich, St Louis, MO, USA), mouse monoclonal anti-CD3 Jurkat T-cell receptor antibody (clone C305; kindly provided by Arthur Weiss, University of California, San Francisco, CA, USA), phospho-Erk1/2 (phospho-p44/42 mitogen-activated protein kinase [MAPK]) (Thr202/Tyr204)-Alexa Fluor 647, phospho−stress-activated protein kinase/Jun N-terminal kinase (JNK) (Thr183/Tyr185)-Alexa Fluor 647, phospho-p38 MAPK (Thr180/Tyr182)-Alexa Fluor 647 (Cell Signaling Technology, Danvers, MA, USA), anti−CD69-phycoerythrin, Annexin V−Dy647, propidium iodide, Annexin V binding buffer (Exbio Praha, Vestec, Czech Republic), 4′,6-diamidino-2-phenylindole, dihydrochloride, Vybrant Dye Cycle Violet stain, LIVE/DEAD Fixable Dead Cell Stain kit (VIVID), mouse anti-NTAL IgG$_1$, anti−β-actin IgG$_1$, goat anti-mouse IgG+A+M−horseradish peroxidase antibody (Invitrogen, Carlsbad, CA, USA), rabbit phospho-p44/42 MAPK (ERK1/2) (Thr202/Tyr204), p44/42 MAPK (ERK1/2), phospho−SAPK/JNK (Thr183/Tyr185), SAPK/JNK, phospho-p38 MAPK (Thr180/Tyr182), p38 α-MAPK antibody (Cell Signaling Technology), goat anti-rabbit IgG (H+L)−horseradish peroxidase conjugate antibody (Bio-Rad, Philadelphia, PA, USA), RNeasy Mini Kit (Qiagen GmbH, Hilden, Germany), MoMLV Reverse Transcriptase (Gibco BRL, Carlsbad, CA, USA), and Protease Inhibitor Cocktail (Calbiochem/Merck, Darmstadt, Germany).

Methylprednisolone- and TCR-induced cell death assays
Jurkat/wt and Jurkat/NTAL$^+$ cells were seeded at a concentration of 0.5 or 1.0×10^6 cells/mL in six-well plates and cultured at 37°C in a 5% CO_2 atmosphere with a 1 mM concentration of methylprednisolone or methylprednisolone solvent as a negative control. The ERK inhibitor U0126 was added at the indicated time points at a concentration of 10 μM. After 24 and 48 hours, the cells were washed in phosphate-buffered saline (PBS) and resuspended in 50 μL Annexin V binding buffer with 2.5 μL Annexin V and 2.5 μL propidium iodide. The mixture was maintained for 30 minutes on ice, washed in Annexin V buffer and measured by flow cytometry. Live cells were defined as Annexin V−negative and propidium iodide−negative. Results are shown as the ratio of the live methylprednisolone-treated cells to control cells.

A similar method was used in the TCR-induced cell death experiment. Jurkat/wt and Jurkat/NTAL$^+$ cells were seeded at a concentration of 1.0×10^6 cells/mL in six-well plates and incubated with 5.25 μg/mL C305 antibody or RPMI alone as a negative control. The ERK inhibitor U0126 was added at the indicated time points at a concentration of 10 μM. After 3, 6, 12, and 24 hours, the cells were washed in PBS and resuspended in Annexin V binding buffer with 2.5 μL Annexin V. 4′,6-Diamidino-2-phenylindole, dihydrochloride was added before measurement instead of propidium iodide. Results are again shown as the ratio of the surviving methylprednisolone-treated cells to control cells.

Intracellular phosphospecific and surface CD69 flow cytometry
Jurkat/wt and Jurkat/NTAL$^+$ cells were seeded at a concentration of 2.0×10^6 cells/mL in 96-well V-bottom plates. Jurkat TCRs were activated by cross linking with 5.25 μg/mL C305 antibody. The VIVID stain diluted in dimethyl sulfoxide (1:10) was added to the cell suspension 15 minutes before fixation at a concentration of 0.5 μL/100 μL media. Cells were fixed with paraformaldehyde at a final concentration of 4%, incubated for 10 minutes at room temperature, and permeabilized with ice-cold methanol for 15 minutes on ice (final concentration: 50%). Cells were subsequently pelleted and resuspended in 200 μL PBS with 0.1% bovine serum albumin. Fifty microliters of the cell suspension was incubated for 30 minutes on ice with 5 μL phosphospecific antibody and then was washed and analyzed by flow cytometry. Analysis was performed on living cells, defined as VIVID-stain negative; staining of the phosphospecific antibodies is shown as the median fluorescent intensity.

The CD69 activation marker was analyzed after 24 hours of incubation of the Jurkat/wt and Jurkat/NTAL$^+$ cells with 5.25 μg/mL C305 antibody. Cells were washed in PBS, incubated for 30 minutes with the anti−CD69-phycoerythrin antibody and measured by flow cytometry. Results are shown as the percentage of CD69-positive cells.

Flow cytometry
All samples were measured with a BD LSRII flow cytometer (BD Immunocytometry Systems, San Jose, CA, USA). Data analysis was performed using FlowJo version 8.8.6 (TreeStar, Ashland, OR, USA).

Quantitative reverse transcription PCR
RNA from Jurkat/wt and Jurkat/NTAL$^+$ cells was isolated using the RNeasy Mini Kit and reverse transcribed into complementary DNA using MoMLV Reverse Transcriptase according to manufacturer's protocol. The quantitative reverse transcription PCR analysis was performed using the ABI 7700 system (Applied Biosystems, Foster City, CA, USA). NTAL primer and probe sequences were as follows, 5′-GGA CAT GGC ACC CAC AAG GA-3′; reverse primer, 5′-GGA ATT GGC ATC ATC ATC TTC TGG-3′; probe, 5′-(FAM) CTA TGT AGG CTT CCT CCG ACC CGT GTC TGC T-3′. For the amplification of LAT: forward primer, 5′-GAG AGC GCA GAA GCG TCT CT-3′; reverse primer, 5′-CAG TCT TAG CCG CTC CAG GAT-3′; probe, 5′-(FAM) ATG GCA GCC GGG AGT ATG TGA ATG TG. The housekeeping gene ABL was used for data normalization. PCR reaction and cycling conditions are described elsewhere [2].

Western blot
A total of 5.0×10^6 Jurkat/wt and Jurkat/NTAL$^+$ cells were lysed in 100 μL lysis buffer (20 mM Tris [pH 7.5] containing 50 mM sodium fluoride, protease inhibitor cocktail, 1 mM orthovanadate,
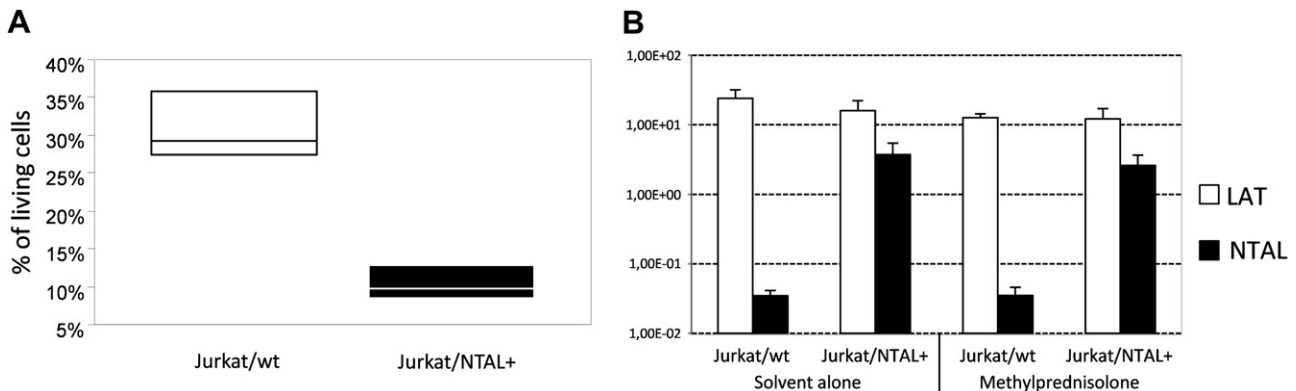
Figure 2. NTAL sensitizes leukemic cells to methylprednisolone treatment. (**A**) Jurkat/wt and Jurkat/NTAL^{+} cells treated 48 hours with methylprednisolone or solvent alone (control). The box-plots show the percentage of living Annexin V−negative, propidium iodide−negative Jurkat/wt (white), and Jurkat/NTAL[+] (black) cells. Results are representative of repeated experiments performed in triplicate ($p < 0.05$). (**B**) Expression of LAT (white) and NTAL (black) mRNA in Jurkat/wt and Jurkat/NTAL^{+} cells after the treatment with methylprednisolone or solvent alone (two experiments, quantitative reverse transcription PCR done in duplicate).

1 mM phenylmethanesulfonyl fluoride, 10 mM EDTA, 10% glycerol, and 1% laurylmaltoside) for 30 minutes on ice. The mixture was then centrifuged for 30 minutes, and the supernatant was mixed with sodium dodecyl sulfate−based loading buffer, boiled, sonicated, and used for the Western blot.

Statistical analysis
Mann−Whitney and Kruskal−Wallis tests were applied for statistical analyses performed using StatView software (SAS Institute, Cary, NC, USA). Experiments were done in triplicate or as indicated in repeated experiments.

Results

NTAL sensitizes leukemic cells to methylprednisolone treatment
In the Jurkat cell line (established from the peripheral blood of a 14-year-old boy with T-lineage ALL at first relapse) (Jurkat/wt), the NTAL protein is undetectable. To assess the role of the NTAL protein in malignant T-cell ALL blasts, we established a derivative Jurkat cell line that has stable NTAL expression (Jurkat/NTAL[+]) (Fig. 1). To delineate the effect of the NTAL protein in methylprednisolone-induced cell death in T-cell ALL, Jurkat/wt and Jurkat/NTAL^{+} cells were cultured with a 1-mM concentration of methylprednisolone or solvent alone (negative control). At the indicated time points, the rate of cell death was measured by flow cytometry. After 24 hours of treatment, we did not observe any changes in the number of living cells (mean: 88.5% in Jurkat/wt vs 88.5% in Jurkat/NTAL[+]). After 48 hours, Jurkat/wt cells showed significantly higher resistance to methylprednisolone than Jurkat/NTAL^{+} cells (mean: 31.3% ± 4.85% vs 10.5% ± 2.38% surviving cells; $p < 0.05$) (Fig. 2A). The expression of NTAL and LAT mRNA was stable during the experiment (Fig. 2B). This in vitro experiment accords with our observation that leukemic blasts of T-ALL patients with higher levels of NTAL mRNA are more sensitive to glucocorticoid treatment.

NTAL potentiates TCR-induced signaling, leading to increased phosphorylation of ERK
The impact of NTAL expression on leukocyte signaling is not completely defined. Moreover, the mechanism by which the NTAL molecule affects signal transmission in T-cell ALL is also unknown. NTAL has been hypothesized to inhibit leukocyte signaling via competition with LAT. To elucidate the role of NTAL in our experiment, we stimulated TCRs by cross linking with an anti-CD3 antibody, and we measured the phosphorylation of ERK, JNK, and p38 mitogen-activated protein kinase (MAPK) by flow cytometry and Western blot. In unstimulated Jurkat/wt and Jurkat/NTAL^{+} cells, the basal ERK, JNK, and p38 MAPK phosphorylation is comparable. After TCR stimulation, ERK becomes rapidly phosphorylated and reaches a maximum at 5 minutes after TCR cross linking; the phosphorylation then declines rapidly (Fig. 3A, B, C). The phosphorylation of ERK is 1.5-fold higher in Jurkat/NTAL^{+} cells than in Jurkat/wt cells at 5 minutes ($p < 0.05$) (Fig. 3B, C). In addition, Jurkat/NTAL^{+} cells express increased levels of the CD69 activation marker on the cell surface than Jurkat/wt cells at 24 hours after stimulation (mean: 77.4% ± 0.74% vs 90.5% ± 0.16%; $p < 0.05$) (Fig. 3D). A comparable increase of JNK phosphorylation of Jurkat/wt and Jurkat/NTAL^{+} cells was observed after TCR stimulation. In addition, we see a slower decrease of JNK phosphorylation in NTAL[+] cell that is compatible with higher engagement of ERK. Phosphorylation of p38 MAPK remained at the baseline level after TCR cross linking (Fig. 3C). These data suggest that NTAL potentiates the proximal signaling of malignant leukemic blasts, leading to increased ERK phosphorylation.
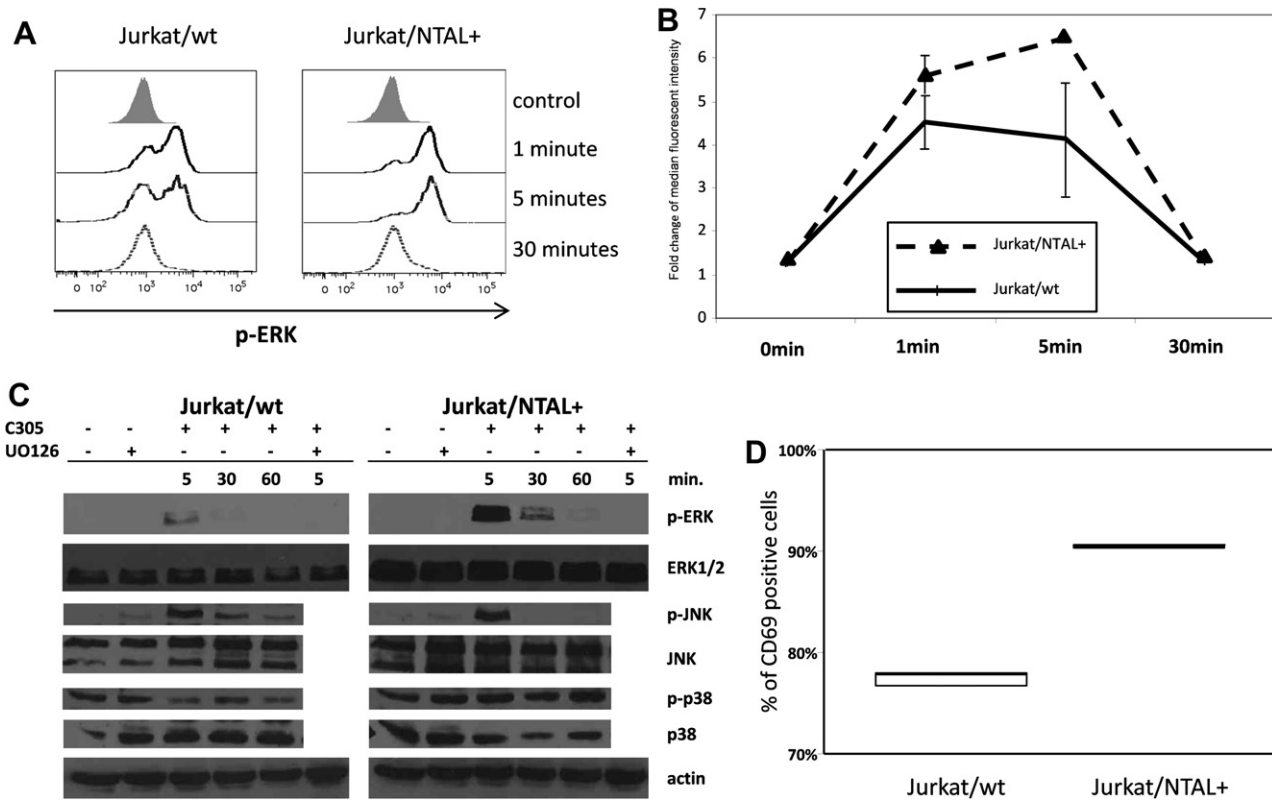
Figure 3. Jurkat/NTAL^{+} cells display higher activation after TCR-mediated stimulation. TCR was cross linked by the anti-CD3 antibody. (**A, B**) Intracellular expression of the phosphorylated ERK is higher 5 minutes after TCR stimulation in Jurkat/NTAL^{+} cells ($p < 0.05$) (experiment performed in triplicate). (**C**) Jurkat/wt and Jurkat/NTAL^{+} cells were incubated with anti-CD3 antibody and/or ERK inhibitor U0126 for indicated time points. Extracts of these cells were Western blotted with total protein or anti-phosphospecific ERK, JNK, and p38 MAPK antibodies. Actin levels were measured as a loading control. (**D**) Surface expression of the activation marker CD69 is higher in Jurkat/NTAL^{+} cells 24 hours after TCR cross linking ($p < 0.05$) (triplicate).

NTAL augments TCR-induced cell death, which can be blocked by inhibition of ERK phosphorylation

Next, we focused on the TCR-driven cell death. In the thymus, the differing intensity of TCR signals leads to either positive or negative selection of nonmalignant T-cell precursors. After TCR engagement, rapid and high ERK phosphorylation contributes to cell death, whereas delayed and prolonged ERK phosphorylation is anti-apoptotic [13,14]. Malignant Jurkat T cells die after strong signals induced by TCR cross linking and Jurkat/wt cells are less sensitive to TCR-induced cell death than Jurkat/NTAL[+] (mean: 86.8% ± 5.8% vs 70.9% ± 2.4% live cells at 6 hours; mean: 61.0% ± 2.3% vs 40.7% ± 2.8% live cells at 24 hours after TCR stimulation in Jurkat/wt vs Jurkat/NTAL^{+} cells, respectively ($p < 0.05$) (Fig. 4A, B). ERK phosphorylation can be blocked effectively with the specific ERK inhibitor U0126. When U0126 is added 120 minutes before the anti-CD3 antibody, cell death is almost completely blocked, although we still observe a difference between the Jurkat/wt and Jurkat/NTAL^{+} cells (mean: 89.3% ± 5.7% vs 85.9% ± 0.9% live cells at 6 hours; mean: 95.2% ± 1.1% vs 82.0% ± 0.2% live cells at 24 hours after TCR stimulation in Jurkat/wt vs Jurkat/NTAL[+]

cells, respectively ($p < 0.05$) (Fig. 4A). This difference could be caused by incomplete inhibition of ERK phosphorylation or by other ERK-independent mechanisms that contribute to cell death in NTAL^{+} cells. In contrast, when U0126 is added 30 minutes after the anti-CD3 antibody, the rate of cell death is only slightly decreased compared to anti-CD3 treatment alone (mean: 74.8% ± 5.5% vs 80.4% ± 7.8% at 6 hours; 72.1% ± 4.0% vs 53.4% ± 3.4% at 24 hours after TCR stimulation in Jurkat/wt vs Jurkat/NTAL^{+} cells, respectively, $p < 0.05$) (Fig. 4B). To conclude, as early as 30 minutes after TCR stimulation, the sequence of events leading to cell death has already started. Thus, ERK phosphorylation is probably mandatory for TCR-induced cell death. Inhibition of ERK phosphorylation significantly suppresses the positive effect of NTAL on TCR-induced cell death.

Sensitizing effect of NTAL to methylprednisolone treatment is reversed by inhibition of ERK phosphorylation

Finally, we investigated the effect of the ERK inhibitor U0126 on glucocorticoid-induced cell death. U0126 was
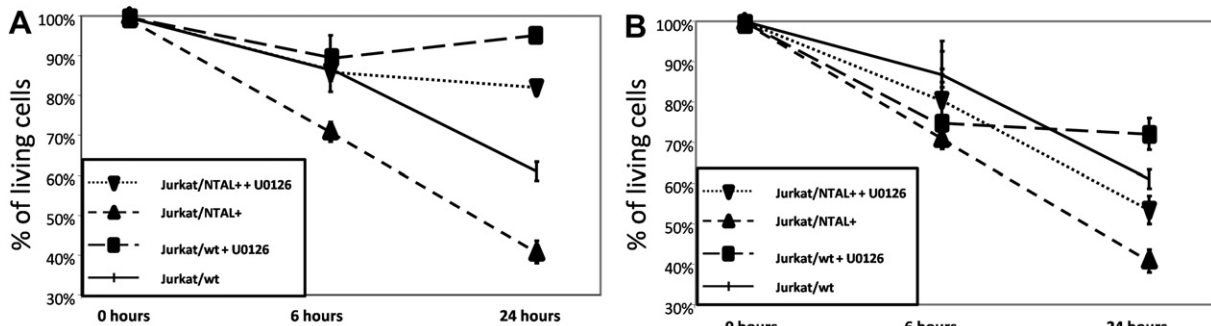
Figure 4. NTAL augments TCR-induced cell death, which can be blocked by inhibition of ERK phosphorylation. TCR was cross linked by the anti-CD3 antibody. (**A, B**) Percentage of living Annexin V−negative, propidium iodide−negative cells after TCR cross linking is higher in Jurkat/NTAL$^+$ cells ($p < 0.05$). (**A**) Addition of the ERK inhibitor U0126 120 minutes before the C305 antibody almost completely blocks TCR-induced cell death ($p < 0.05$) (triplicate). (**B**) Addition of U0126 30 minutes after the anti-CD3 antibody suppresses cell death only partially ($p < 0.05$) (triplicate).

added to the cell cultures of Jurkat/wt and Jurkat/NTAL$^+$ cells 30 minutes before methylprednisolone, and the cell death was measured at 48 hours by flow cytometry. Unlike in the original experiment with no intervention on the ERK phosphorylation (Fig. 2A), after ERK inhibition by U0126 the percentage of surviving cells was identical in Jurkat/wt and Jurkat/NTAL$^+$ cells (median: 29.9% ± 3.1% vs 29.3% ± 4.7% in Jurkat/wt and Jurkat/NTAL$^+$ cells; $p = 0.49$) (Fig. 5). Our experiments suggest that the mechanism leading to the higher sensitivity of NTAL$^+$ cells to methylprednisolone treatment is higher activation of the ERK kinase.

Discussion

The precise mechanism of regulation of glucocorticoid sensitivity or resistance is not yet fully understood. In our previous study, we have described, for the first time, the association between high expression of the adaptor protein NTAL and a better response to prednisone treatment in T-cell ALL [3]. In the present study, we confirmed these data in vitro and showed that the presence of the NTAL protein sensitizes T-ALL cells to the lethal effect of glucocorticoids. In addition, we attempted to reveal the mechanism by which NTAL contributes to prednisone-induced cell death.

Functional T-cell receptor signaling is the hallmark of T-cell ALL [4,5]. NTAL is nonenzymatic signaling molecule that is associated with the TCR. Therefore, we first focused on TCR-induced signaling. After TCR stimulation, cells expressing the NTAL protein display a more activated phenotype and have higher expression of the CD69 molecule on the cell surface than NTAL-negative cells. Moreover, NTAL augments TCR-induced cell death. We then focused on the intracellular signaling pathways. The proteins ERK, JNK, and p38 MAPK are key signaling molecules in lymphocytes. The basal phosphorylation of ERK, JNK, and p38 MAPK does not differ between Jurkat/wt and Jurkat/NTAL$^+$ cells. After TCR stimulation, we observed

only minor changes in the phosphorylation of JNK and no change in p38 MAPK, whereas ERK is phosphorylated considerably and very early. In addition, Jurkat/NTAL$^+$ cells display markedly higher ERK phosphorylation after TCR stimulation than Jurkat/wt cells. We conclude that NTAL augments the signaling via an enhancement of ERK activation. We can hypothesize that in T-cell ALL, NTAL is localized in lipid rafts, binds to the molecule GRB2, and (in cooperation with LAT) augments the activation of the RAS/RAF/MEK/ERK signaling cascade.

As the next step, we focused on the ERK molecule and its role in cell death. After TCR cross linking, early inhibition of ERK phosphorylation by the inhibitor U0126 blocks cell death. When U0126 is applied later (30 minutes after TCR stimulation by the anti-CD3 antibody), the cell death kinetics resemble those in the cells treated with anti-CD3 alone. We conclude that the events leading to cell death have already started within the first 30 minutes after TCR
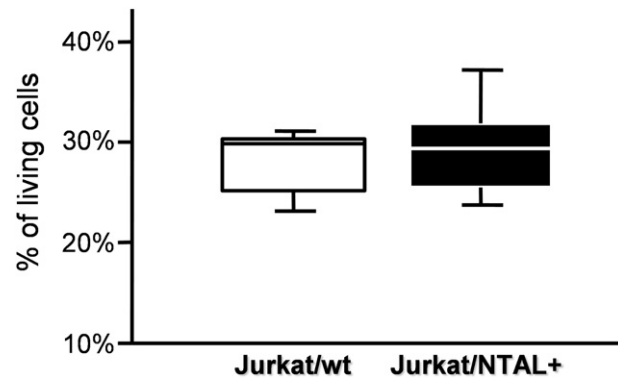
Figure 5. The sensitizing effect of NTAL to methylprednisolone-induced cell death is reversed by inhibition of ERK phosphorylation. U0126 was added 30 minutes before the addition of methylprednisolone, and the percentage of Annexin V−negative, propidium iodide−negative cells was assessed after 48 hours of co-incubation. ERK inhibition reverts the sensitizing effect of the NTAL molecule to methylprednisolone treatment in Jurkat/NTAL$^+$ cells (10-plicate) ($p = 0.49$).

stimulation. Thus, the early ERK phosphorylation initiates the events leading to the death of the Jurkat/NTAL$^+$ cells.

Finally, we cultured Jurkat/wt and Jurkat/NTAL$^+$ cells with methylprednisolone and ERK inhibitor U0126 together. We show that blocking of ERK phosphorylation results in an elimination of the difference between the Jurkat/wt and Jurkat/NTAL$^+$ cells, and the percentage of surviving cells is equal in the two cell lines.

Our results are in accord with the data from adult ALL, in which the phosphorylation of ERK has been described as a predictor of complete remission achievement [16]. We can speculate that in pediatric T-cell ALL, NTAL contributes to higher ERK phosphorylation and increases glucocorticoid sensitivity, and this mechanism leads to a better response to the leukemia treatment. We conclude that NTAL is a tumor suppressor that enhances the proximal signaling of leukemic blasts, and ERK is the key downstream molecule responsible for the biological effects.

Funding disclosure

Conflict of interest disclosure

No financial interest/relationships with financial interest relating to the topic of this article have been declared.

References

1. Stary J, Jabali Y, Trka J, et al. Long-term results of treatment of childhood acute lymphoblastic leukemia in the Czech Republic. Leukemia. 2010;24:425–428.
2. Riehm H, Reiter A, Schrappe M, et al. [Corticosteroid-dependent reduction of leukocyte count in blood as a prognostic factor in acute lymphoblastic leukemia in childhood (therapy study ALL-BFM 83)]. Klin Padiatr. 1987;199:151–160.
3. Svojgr K, Burjanivova T, Vaskova M, et al. Adaptor molecules expression in normal lymphopoiesis and in childhood leukemia. Immunol Lett. 2009;122:185–192.
4. Bellavia D, Campese AF, Checquolo S, et al. Combined expression of pTalpha and Notch3 in T cell leukemia identifies the requirement of preTCR for leukemogenesis. Proc Natl Acad Sci U S A. 2002;99: 3788–3793.
5. Talora C, Campese AF, Bellavia D, et al. Pre-TCR-triggered ERK signalling-dependent downregulation of E2A activity in Notch3-induced T-cell lymphoma. EMBO Rep. 2003;4:1067–1072.
6. Horejsi V, Zhang W, Schraven B. Transmembrane adaptor proteins: organizers of immunoreceptor signalling. Nat Rev Immunol. 2004;4: 603–616.
7. Brdicka T, Imrich M, Angelisova P, et al. Non-T cell activation linker (NTAL): a transmembrane adaptor protein involved in immunoreceptor signaling. J Exp Med. 2002;196:1617–1626.
8. Stork B, Engelke M, Frey J, et al. Grb2 and the non-T cell activation linker NTAL constitute a Ca(2+)-regulating signal circuit in B lymphocytes. Immunity. 2004;21:681–691.
9. Zhu M, Koonpaew S, Liu Y, et al. Negative regulation of T cell activation and autoimmunity by the transmembrane adaptor protein LAB. Immunity. 2006;25:757–768.
10. Janssen E, Zhu M, Zhang W, Koonpaew S, Zhang W. LAB: a new membrane-associated adaptor molecule in B cell activation. Nat Immunol. 2003;4:117–123.
11. Janssen E, Zhu M, Craven B, Zhang W. Linker for activation of B cells: a functional equivalent of a mutant linker for activation of T cells deficient in phospholipase C-gamma1 binding. J Immunol. 2004;172:6810–6819.
12. Chambard JC, Lefloch R, Pouyssegur J, Lenormand P. ERK implication in cell cycle regulation. Biochim Biophys Acta. 2007;1773:1299–1310.
13. Teixeiro E, Daniels MA. ERK and cell death: ERK location and T cell selection. FEBS J. 2010;277:30–38.
14. Daniels MA, Teixeiro E, Gill J, et al. Thymic selection threshold defined by compartmentalization of Ras/MAPK signalling. Nature. 2006;444:724–729.
15. Hobbs S, Jitrapakdee S, Wallace JC. Development of a bicistronic vector driven by the human polypeptide chain elongation factor 1alpha promoter for creation of stable mammalian cell lines that express very high levels of recombinant proteins. Biochem Biophys Res Commun. 1998;252:368–372.
16. Gregorj C, Ricciardi MR, Petrucci MT, et al. ERK1/2 phosphorylation is an independent predictor of complete remission in newly diagnosed adult acute lymphoblastic leukemia. Blood. 2007;109:5473–5476.

Regulation of Src Family Kinases Involved in T Cell Receptor Signaling by Protein-tyrosine Phosphatase CD148[*][S]

Ondrej Stepanek[‡1]**, Tomas Kalina**[§]**, Peter Draber**[‡1]**, Tereza Skopcova**[‡]**, Karel Svojgr**[§]**, Pavla Angelisova**[‡]**, Vaclav Horejsi**[‡]**, Arthur Weiss**[¶]**, and Tomas Brdicka**[‡2]

From the [‡]*Institute of Molecular Genetics, Academy of Sciences of the Czech Republic, 142 20 Prague, Czech Republic,* [§]*Childhood Leukemia Investigation Prague and Department of Pediatric Hematology and Oncology, 2nd Faculty of Medicine, Charles University, 150 06 Prague, Czech Republic, and the* [¶]*Howard Hughes Medical Institute and Department of Medicine, University of California San Francisco, San Francisco, California 94143*

CD148 is a receptor-like protein-tyrosine phosphatase known to inhibit transduction of mitogenic signals in non-hematopoietic cells. Similarly, in the hematopoietic lineage, CD148 inhibited signal transduction downstream of T cell receptor. However, it also augmented immunoreceptor signaling in B cells and macrophages via dephosphorylating C-terminal tyrosine of Src family kinases (SFK). Accordingly, endogenous CD148 compensated for the loss of the main SFK activator CD45 in murine B cells and macrophages but not in T cells. Hypothetical explanations for the difference between T cells and other leukocyte lineages include the inability of CD148 to dephosphorylate a specific set of SFKs involved in T cell activation or the lack of CD148 expression during critical stages of T cell development. Here we describe striking differences in CD148 expression between human and murine thymocyte subsets, the only unifying feature being the absence of CD148 during the positive selection when the major developmental block occurs under CD45 deficiency. Moreover, we demonstrate that similar to CD45, CD148 has both activating and inhibitory effects on the SFKs involved in TCR signaling. However, in the absence of CD45, activating effects prevail, resulting in functional complementation of CD45 deficiency in human T cell lines. Importantly, this is independent of the tyrosines in the CD148 C-terminal tail, contradicting the recently proposed phosphotyrosine displacement model as a mechanism of SFK activation by CD148. Collectively, our data suggest that differential effects of CD148 in T cells and other leukocyte subsets cannot be explained by the CD148 inability to activate T cell SFKs but rather by its dual inhibitory/activatory function and specific expression pattern.

Protein tyrosine phosphorylation plays an important role in transducing many cellular signals. The tyrosine phosphoryla-tion status of individual proteins is regulated by opposing actions of protein-tyrosine kinases and PTPs.[3] The effects of PTP activity on signal transduction can be both stimulatory and inhibitory, depending on the individual PTP specificity. In TCR signaling, some PTPs (*e.g.* SHP-1) have a largely negative impact on signal propagation, whereas the CD45 PTP appears to have a dual function. It enables the activation of SFKs by dephosphorylating their inhibitory C-terminal phosphoty-rosine (Tyr-505 in Lck and Tyr-528 in Fyn) and is, thus, indispensable for the initiation of TCR signal transduction. However, CD45 also plays a direct or indirect role in the dephosphorylation of SFKs at their catalytic sites (Tyr-394 for Lck), which negatively influences their activity (1). Another PTP expressed in the immune system, CD148, also appears to produce both activating and inhibitory effects.

CD148 (DEP-1, PTPRJ) is an R3 family receptor-like PTP with a large highly *N*-glycosylated extracellular segment containing multiple fibronectin III-like repeats, a transmembrane domain, and a single intracellular protein-tyrosine phosphatase domain followed by a short C-terminal tail containing three conserved tyrosine residues (1–5).

CD148 is a broadly expressed PTP found in non-hematopoietic tissues such as epithelia and fibroblasts as well as in leukocytes (2, 4, 6). In peripheral blood, CD148 is expressed on all white blood cell populations, including T cells, and platelets in humans (5–8). CD148 is further up-regulated on T cells after activation with mitogens (5, 6, 8). Less is known about CD148 expression on thymocytes. Immunohistochemical staining of human thymi revealed that CD148-positive T cells are localized in medulla, suggesting its expression in mature thymocytes (5, 9). This was supported by flow cytometry that detected CD148 only on CD3-positive thymocytes (5). However, examination of CD148 expression at defined stages of thymocyte development has not been reported.

Similar to human cells, the majority of murine peripheral leukocyte subsets are also CD148-positive. However, naïve T cells are a notable exception, exhibiting very weak CD148 expression (10). This also seems to be reflected in contrasting data obtained with murine and human thymi as only mouse

[3] The abbreviations used are: PTP, protein-tyrosine phosphatase; SFK, Src-family kinase; SP, single positive; APC, allophycocyanin; DN, double negative; DP, double positive; iSP, immature single positive; PB, Pacific Blue; TCR, T cell receptor; aa, amino acids; PLC, phospholipase C; LAT, linker for activation of T cells.

Expression and Function of CD148 in T Cells

CD4$^-$CD8$^-$ double negative thymocytes, representing the earliest stage of T cell thymic development, exhibited low level CD148 positivity (10).

A wide range of evidence suggests that CD148 acts as a tumor suppressor in non-hematopoietic tissues (11–17), likely by dephosphorylating and negatively regulating receptor tyrosine kinases (16, 18–21) and/or downstream signal transducers (13, 22). On the other hand, CD148 also plays an activating role via dephosphorylation of the inhibitory tyrosine in Src (19, 23).

CD148 function has been studied in hematopoietic lineage cells by using CD148$^{-/-}$ mice, where partially blocked B cell receptor and macrophage FcR signaling was observed (24). Double- deficient CD148$^{-/-}$CD45$^{-/-}$ mice revealed overlapping functions of these PTPs in B cells and macrophages. Double-deficient cells were unable to signal via B cell receptor and FcR due to the inactivation of SFKs, which were hyperphosphorylated at their inhibitory tyrosines (24). In platelets, which do not express CD45, CD148 inactivation alone was sufficient to block signaling through glycoprotein VI and αIIbβ3 integrin, again most likely due to the inability of CD148-deficient platelets to activate SFKs (25).

It has been speculated that conserved tyrosine residues in the C-terminal tail of CD148 may be critical for SFK activation by CD148 (26). In members of R4 PTP family, similar tyrosines have been shown to play a major role in this process via displacing SFK inhibitory tyrosine from the SH2 domain, thus making it available for dephosphorylation (27). However, this model has never been tested on any R3 family member including CD148.

In T cells, no specific effect of CD148 deficiency was observed on wild type or CD45$^{-/-}$ genetic backgrounds in mice (1, 24). However, this may be explained by the lack of CD148 on murine thymocytes (beyond DN stage) as well as naïve T cells. The function of CD148 in human T cells has been studied using two approaches; that is, CD148 cross-linking with a specific antibody and CD148 ectopic expression in CD148 negative Jurkat T cell line. Cross-linking of CD148 induced calcium influx and tyrosine phosphorylation in human peripheral blood leukocytes (7, 28) and enhanced peripheral T cell proliferation induced by anti-CD3 antibody *in vitro* (7, 8). Although it is not clear how the cross-linking affects CD148 function, these data clearly show that modulation of endogenous CD148 activity and/or localization impacts peripheral T cell signaling. Forced expression of CD148 in Jurkat cells inhibited both proximal and distal effects of TCR engagement probably via inhibition of LAT and PLCγ1 phosphorylation (29–31). This was observed even at physiologically relevant levels of CD148 expression (29). Taken together, studies to date suggest that CD148 is a negative regulator of TCR signaling, which is in apparent contradiction with data obtained from other leukocyte populations.

To better understand the role of CD148 in human T cell development and function, we analyzed the expression of CD148 during T cell development in mice and humans as well as the ability of CD148 to activate SFKs in human T cells. We describe striking differences in CD148 expression on different human and mouse thymocyte subsets. Moreover, we show that CD148 is capable of SFK activation and complements CD45 deficiency in human T cells.

EXPERIMENTAL PROCEDURES

Antibodies—For Western blotting and cell activation, the following antibodies were used anti-phosphotyrosine (clone 4G10, mouse origin (Upstate Biotechnologies, Lake Placid, NY), human Lck and human Fyn (rabbit, kindly provided by A. Veillette, Clinical Research Institute of Montreal, Canada), human Lck (mouse, Exbio, Vestec, Czech Republic), human Erk2 (rabbit, Santa Cruz Biotechnology, Santa Cruz, CA), Jurkat TCRβ (clone C305 (32)), human CD3 (MEM92, mouse, Exbio), human LAT (rabbit, kindly provided by L. Samelson, Center for Cancer Research, Bethesda, MA), human PLCγ1, Myc tag (mouse), phospho-p42/44 MAPK (Erk1/2) (Thr-202/Tyr-204), phospho-Src family (Tyr-416), phospho-Src (Tyr-527), non-phospho-Src (Tyr-527, all three chicken Src numbering), phospho-Lck (Tyr-505), phospho-PLCγ1 (Tyr-783) (rabbit, Cell Signaling, Danvers, MA), phospho-LAT (Tyr-191, rabbit, Upstate Biotechnology). For flow cytometry, mouse antigens were CD148 (clone 8A-1, hamster (10)), TCRβ-FITC, CD8α-PB, CD11b-APC, CD11c-APC, Thy1.1-FITC (eBioscience, San Diego, CA), TCR$\gamma\delta$-Alexa Fluor 680, CD45-FITC, NK1.1-APC, CD19-DyLight 647, CD45-PB (Exbio), CD19-PB, CD4-PerCP/Cy5.5 (BioLegend, San Diego, CA). For flow cytometry, human antigens were CD148-PE (clone 143–41, R&D Systems, Minneapolis, MN), TCR$\alpha\beta$-PB (BioLegend), CD19-APC, CD44-PB, CD69-FITC, CD1a-APC, CD8-Alexa Fluor 700 (Exbio), CD27-FITC, CD45RA-PE-Cy7, CD3-APC-H7, CD34-PerCP-Cy5.5 (BD Biosciences), CD4-ECD (Immunotech, Marseille, France), and CD45-PO (PO, Pacific Orange) (Invitrogen). Secondary antibodies were goat anti-mouse-HRP IgG-specific (Sigma), goat anti-rabbit-HRP (Bio-Rad), goat anti-mouse-HRP light chain specific (Jackson ImmunoResearch, West Grove, PA), goat anti-mouse-IRDye 680 and goat anti-rabbit-IRDye 800CW (LI-COR Biosciences, Lincoln, NE), goat anti-hamster-DyLight 549 (Rockland, Gilbertsville, PA), donkey anti-goat-DyLight 549 (Jackson ImmunoResearch), and goat anti-mouse-Alexa Fluor 488 (Invitrogen). Monoclonal antibodies against human CD148 were generated by standard techniques. Briefly, F$_1$ (BALB/c $\times$ B10.A) hybrid mice were immunized intrasplenically with the bacterially expressed and Talon purified (Clontech Laboratories, Mountain View, CA) His-tagged N-terminal fragment (aa 36–452) of human CD148. Hybridomas were prepared and selected by standard techniques using Sp2/0 myeloma cells as fusion partners.

cDNA Constructs, Cloning, and Mutagenesis—The construct encoding the Myc-tagged version of human CD148 was generated using fusion PCR to insert the Myc-tag coding sequence (EQKLISEEDL) downstream of the leader peptide between amino acids Gly-38 and Thr-39 of the CD148 precursor protein, and the resulting product was cloned into MSCV-IThy1.1 vector (NotI/SalI), kindly provided by P. Marrack (National Jewish Health, Denver, CO). The C1239S mutant of CD148 has been described previously (29). The MSCV-IThy1.1 version of this construct was generated by restriction cloning. 2YF and 3YF mutants, where tyrosines 1311/1320 or 1311/1320/1335, respectively, were replaced with phenylalanines, were generated with the QuikChange site-directed mutagenesis kit (Stratagene, La Jolla, CA) according to the manufacturer's instruc-

tions. A similar procedure was also used to generate substrate trapping mutant of CD148 where aspartate 1205 was replaced with alanine. The CD148-SHP-1 chimera consisting of aa 1–1018 of CD148 (containing the Myc tag described above) followed by aa 214–595 from SHP-1 was generated using fusion PCR. Myc-CD45 in MSCV-IThy1.1 encoding a protein composed of CD148 signal peptide (aa 1–38), Myc tag, and CD45RABC-coding sequence was generated from the Myc-CD148 construct by replacing all of the CD148 coding sequence downstream of the Myc tag with aa 26–1304 of CD45RABC. All the constructs were verified by sequencing.

Cell Lines and Primary Cells—JS-7 (33), Jurkat with inducible CD148 TetOn expression (29), CD45$^-$HPB-ALL (34) (kindly provided by P. Beverley, The Jenner Institute, Compton, UK), and J45.01 (35) T cell lines and Phoenix Ampho cells (Origene, Rockville, MD) were cultivated in RPMI 1640 or DMEM, respectively, supplemented with 10% FBS, 2 mM glutamine, 20 μg/ml gentamycin, 50 μg/ml streptomycin, and 10^4 units/ml penicillin at 37 °C in 5% CO$_2$. Murine blood and thymi were collected from healthy C57Bl/6j mice 2–16 weeks old (obtained from IMG Animal Facility). A single-cell thymocyte suspension was prepared followed by erythrocyte lysis in ACK buffer (150 mM NH$_4$Cl, 0.1 mM EDTA (disodium salt), 1 mM KHCO$_3$). Human peripheral blood mononuclear cells were isolated from buffy coats (obtained from Thomayer University Hospital, Prague, Czech Republic) or from fresh blood of healthy donors using Ficoll gradient centrifugation. Human thymic tissue was obtained from material discarded during cardiac surgery of 9-day to 4-year-old children. Single cell suspensions of thymocytes were prepared. Erythrocytes were lysed in BD Lysing Solution (BD Biosciences). Where applicable, the procedures were performed after obtaining an informed consent from the donors or their guardians and in accordance with local ethical guidelines and declaration of Helsinki. They were also approved by the Institutional Review Board and Animal Care and Use Committee of Institute of Molecular Genetics as well as the Institutional Review Board of University Hospital in Motol, Prague.

Cell Activation—JS-7 cells were activated with 4 μg/ml soluble C305 antibody. The activation was stopped by rapid cell lysis in SDS-PAGE sample buffer. To analyze CD69 up-regulation, cells were activated overnight by plate-bound C305 antibody. CD69 expression was analyzed by flow cytometry.

Biochemical Procedures—To obtain whole cell SDS lysates, cells in serum-free RPMI or PBS (50 million/ml) were lysed by adding equal volume of 2× concentrated SDS-PAGE sample buffer followed by sonication. These lysates were used to quantify the phosphorylation status of SFKs by immunoblotting using IRDye 680- or IRDye 800CW-conjugated secondary antibodies, Odyssey Infrared Imaging System (LI-COR), and AIDA image analyzer software (Raytest, Straubenhardt, Germany). For analysis of other phosphorylation events, standard peroxidase-based ECL techniques and exposure to x-ray films was used. For immunoprecipitation experiments, 7.5×10^7 cells were lysed in 1.5 ml of ice-cold laurylmaltoside lysis buffer (1% dodecylmaltoside, 1 mM Pefabloc, 5 mM iodoacetamide, 1 mM sodium orthovanadate, 100 mM NaCl, 50 mM NaF, 10% glycerol v/v, 20 mM Tris, pH 7.5) and incubated for 30 min on ice. Nuclei

and debris were removed by centrifugation, and the resulting lysate was subjected to immunoprecipitation with anti-Myc antibody (3.3 μg/ml) followed by incubation with Protein A/G PLUS-Sepharose (Santa Cruz Biotechnology). Immunoprecipitates were eluted with SDS-PAGE sample buffer and subjected to immunoblotting as indicated. For substrate trapping experiments with Myc-CD148 D1205A, ice-cold phosphate buffer without phosphatase inhibitors (0.2% dodecylmaltoside, 1 mM Pefabloc, 50 mM NaCl, 10% glycerol v/v, 100 mM phosphate, pH 7.5) was used for cell lysis.

Flow Cytometry—Cells lines were stained with the indicated antibodies. Murine leukocytes were stained in PBS, 1% BSA, 20% mouse serum for 30 min on ice. The 8A-1 hamster antibody recognizing mouse CD148 gives only a very low signal using standard staining procedure (10). Thus, we used a sequential double secondary antibody staining (goat anti-hamster DyLight 549 and donkey anti-goat DyLight 549) to increase the specific signal intensity. Human peripheral blood mononuclear cells were stained in PBS, 1% BSA, 20% human AB serum on ice for 30 min. Human thymocytes were stained for 30 min in PBS with 2 mM EDTA at 4 °C. For calcium response measurements, JS-7 cells and their derivatives were loaded with 2 μg/ml Fluo-4 dye (Invitrogen) and analyzed by flow cytometry at 37 °C for 30 s at rest and then activated with 0.2 μg/ml C305 antibody, and the fluorescence was followed for another 3–4 min. The calcium response index was calculated as the percentage of cells with Fluo-4 fluorescence higher than the 95th percentile of resting cells during the time interval between 10 and 20 s. An LSR II (BD Biosciences) flow cytometer was used for analysis of surface markers. A FACSCalibur (BD Biosciences) flow cytometer was used for calcium flux measurements. Data were analyzed using FlowJo software (TreeStar, San Carlos, CA).

Cell Sorting and Quantitative RT-PCR—Thymocytes from 2 mice (4–6 weeks old) were pooled and stained with the indicated antibodies in Hanks' balanced salt solution, 25% goat serum on ice for 45 min, and sorted using an Influx cell sorter (BD Biosciences). Of $\alpha\beta$T cell developmental stages (gated as CD45$^+$/CD11b$^-$/CD11c$^-$/CD19$^-$/NK1.1$^-$/$\gamma\delta$TCR$^-$), 0.5–2 × 10^6 cells of DN (CD3$^-$/CD4$^-$/CD8$^-$), iSP (CD3$^-$/CD4$^-$CD8$^+$), DP (CD4$^+$/CD8$^+$), SP8 (CD3$^+$/CD4$^-$/CD8$^+$), and SP4 (CD3$^+$/CD4$^+$/CD8$^-$) subpopulations were collected. RNA was isolated using a Quick-RNA MiniPrep kit (Zymo Research Corp., Irvine, CA). Reverse transcription was performed with RevertAid reverse transcriptase (Fermentas, Thermo Fisher Scientific, Waltham, MA) using a combination of random pentadecamer and anchored oligo(dT)$_{20}$ primers. Quantitative PCR was performed using a LightCycler 480 SYBR Green I Master chemistry (Roche Applied Science) in duplicate with following primers: CD148-for 5′-ctgatggtgcagacagagga-3′, CD148-rev ctcactggctcgaggttttc, Actbb-for ctaaggccaaccgtgaaaag, Actb-rev accagaggcatacagggaca, Tbp-for ggcggtttggctaggttt, Tbp-rev gggttatcttcacacaccatga, Tubb2A-for aaccagatcggcgctaagt, Tubb2A-rev tgccagcagcttcattgta, Hprt1-for tcctcctcagaccgcttttt, Hprt1-rev cctggttcatcatcgctaatc, Eef1a1-for acacgtagattccggcaagt, an dEef1a1-rev aggagcccttttcccatctc. Primer efficiencies were determined on diluted cDNA from DN cells. Relative mRNA amounts were calculated from measured Ct
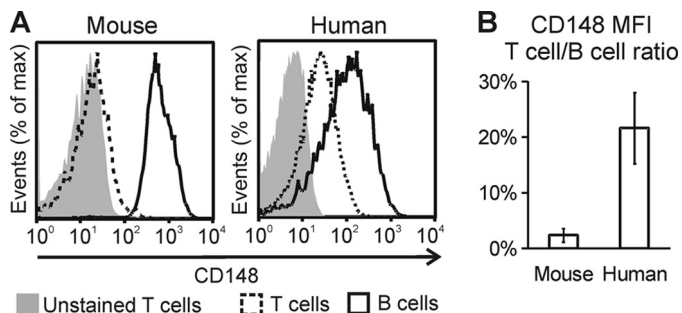
FIGURE 1. **CD148 expression on peripheral $\alpha\beta$T cells differs between mice and humans.** Murine or human peripheral blood leukocytes were stained with anti-CD19, anti-$\alpha\beta$TCR, and anti-CD148 antibodies. *A*, shown are CD148 levels on blood $\alpha\beta$T cells (CD19$^-\alpha\beta$TCR$^+$, *dashed line*) and B cells (CD19$^+\alpha\beta$TCR$^-$, *solid line*). $\alpha\beta$T cells stained with secondary antibody only are provided as a negative control (*gray-filled histogram*). *B*, shown is CD148 signal intensity (mean fluorescence intensity) on $\alpha\beta$T cells shown as a percentage of CD148 signal intensity on B cells in murine or human blood. Data are the mean $\pm$ S.D. of five (mouse) or four (human) donors.

values, and primer efficiencies with DN mRNA levels were arbitrarily set as 1. CD148 mRNA level was normalized to a geometric mean of all five or four (excluding Eef1a1) reference genes.

Retroviral Infection—Phoenix Ampho cells were transfected with retroviral MSCV-IThy1.1 vector using Lipofectamine 2000 (Invitrogen) according to the manufacturer's instructions. Virus-containing supernatant was supplemented with 10 μg/ml Polybrene (Sigma) and added to JS-7 cells. The mixture was centrifuged for 90 min (1250 $\times$ g). Positive cells were sorted by auto-MACS Pro Separator (Miltenyi, Bergisch Gladbach, Germany) after staining with anti-Thy1.1-FITC antibody on ice and subsequently with anti-FITC microbeads (Miltenyi) at 4 °C.

RNA Interference—CD148 knockdown in JS-7 cells was performed by electroporation (700 V/cm, 60 ms) of 5×10^5 cells with 100 pmol of siRNA1 (ID s230207, Ambion, Austin, TX) or siRNA2 (ID s230208) in 100 μl of Opti-MEM media (Ambion) using a BTX electroporator (Harvard Apparatus, Holliston, MA). Cells were used for analysis 2 days after electroporation.

Statistics—For calculation of statistical significance, a two-tailed Student's *t* test (unequal variance) was used.

RESULTS

CD148 Is Differentially Expressed on Human and Murine T Cells—Published data on CD148 expression appeared to be partially inconsistent. Although CD148 was not detected on murine peripheral T cells (10), human T cells were repeatedly shown to be CD148-positive (5–7). Moreover, murine thymocytes were almost CD148-negative with a weak signal only at early stages (10). In contrast, the limited data available on human thymi suggested that the regulation of CD148 expression on human thymocytes may be very different, with CD148 expression appearing at the later stages of T cell development (5, 9). However, no detailed subset analysis has been carried out.

When analyzed by flow cytometry, human blood T cells exhibited substantial levels of CD148, albeit somewhat lower than B cells. In contrast, CD148 was hardly detectable on murine blood T cells (Fig. 1*A*). To compare signals given by two different antibodies (to human and murine CD148), we calcu-

lated the T cell intensity as a percentage of the B cell mean fluorescence intensity (Fig. 1*B*). Thus, the expression of CD148 on peripheral T cells relative to B cells was much higher in humans than in mice. Next, we analyzed the expression of CD148 during particular thymocyte developmental stages in mice and humans by flow cytometry (supplemental Figs. S1 and S2). An improved staining procedure enabled us to measure the expression of murine CD148 more reliably than before (see "Experimental Procedures"). In mice, CD148 is expressed at the DN stage but sharply drops through the DP stage to the SP stage cells, which exhibited only very low CD148 amounts (Fig. 2, *A* and *C*). Staining of human thymocytes revealed a completely inverse pattern as DN cells were CD148-negative and only a relatively low number of DPs displayed CD148 positivity (Fig. 2, *B* and *D*). On the other hand, a substantial percentage of SP cells exhibited high CD148 expression.

To rule out the possibility that the loss of anti-CD148 staining on murine thymocytes during the development could be caused by the loss of the epitope on CD148 (*e.g.* due to alternative glycosylation or splicing), we performed quantitative RT-PCR on sorted thymic populations. Using primers specific for conserved intracellular part of CD148 molecule, we detected the highest level of CD148 mRNA in DN cells with a gradual decline during the maturation, thus confirming the flow cytometry data (Fig. 2*E*).

Completely different CD148 expression in thymus between mice and humans provides an explanation for differences in CD148 expression in peripheral T cells. Loss of CD148 during transition of murine thymocytes to DP and SP stages is consistent with CD148 negativity of mature peripheral T cells. In contrast, human thymocytes gain CD148 expression at later thymocyte developmental stages and retain it in the periphery.

CD148 Is Expressed on Mature CD1a$^-$, CD27$^+$, CD44$^+$ Thymocytes in Humans—DP and SP cells in human thymus contained both CD148-negative and -positive cells (Fig. 2, *B* and *D*); thus, we performed analysis of thymic CD148 expression in more detail. CD1a is a marker of cortical immature thymocytes. Its expression is lost during maturation of single-positive cells and is accompanied with transition to a terminal thymocyte stage (36). Expression of CD148 negatively correlated with expression of CD1a in the whole thymus (Fig. 3*A*), suggesting that CD148 could be expressed exclusively by the most mature human thymocytes. Further analysis was focused on DP and SP cells (excluding iSPs). The maturation status of these cells was assessed based solely on the expression of CD1a and CD44 (36–38). This approach simplified the gating process as well as the data representation in the manner complementary to the strategy used in Fig. 2. Development from early DP cells into mature SPs starts at CD44$^-$CD1a$^+$-stage progresses through a CD44$^+$CD1a$^+$ stage and terminates at CD44$^+$CD1a$^-$ stage (Fig. 3*B*). Classification according to CD44 and CD1a expression correlated well to DP/SP transition. CD44$^-$CD1a$^+$ cells consisted mainly of DP cells, and the CD44$^+$CD1a$^+$ population contained comparable numbers of DP and SP, predominantly CD4$^+$ SP, and finally, CD44$^+$CD1a$^-$ thymocytes represented almost exclusively SP cells, highly positive for CD3 (Fig. 3*C* and not shown). Cells expressing markers of successful positive selection, CD27 and CD69, appeared at CD44$^+$CD1a$^+$ stage
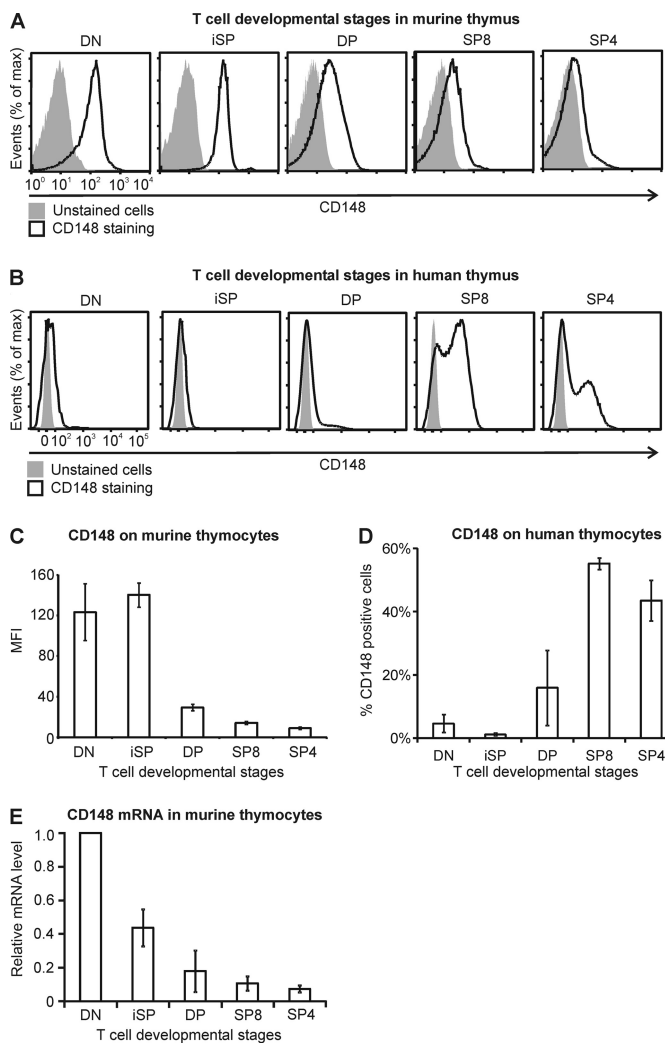
FIGURE 2. **CD148 expression is down-regulated in mice but up-regulated in humans during thymic $\alpha\beta$T cell development.** *A*, murine thymocytes from 2–16-week-old mice were stained with antibodies to CD4, CD8, CD11c, CD19, CD148, $\alpha\beta$TCR, $\gamma\delta$TCR, and NK1.1. Cells of non-T cell lineage were gated out, and the remaining cells were divided into five developmental stages: DN, iSP, DP, SP8, and SP4 (see supplemental Fig. 1 for details). CD148 fluorescence intensity (*solid black line*) as well as background signal (*gray*) of particular thymocyte subpopulations from a representative thymus (of five) is shown. *B*, human thymocytes were stained with antibodies to CD3, CD4, CD8, CD34, CD45, and CD148. Thymocytes were divided into five developmental stages similarly as for mouse thymus: DN, iSP, DP, SP8, and SP4 (supplemental Fig. 2). CD148 fluorescence intensity as well as the background signal of particular thymocyte subpopulations from a representative thymus (of six) is shown. *C*, quantification of CD148 expression in murine T cell subsets is shown as mean fluorescence intensity because CD148 was homogenously expressed in all individual subpopulations. Data are the mean $\pm$ S.D., $n = 3$. *D*, some human subsets (DP and SP) exhibited a bimodal distribution of CD148 signal; therefore, the percentage of CD148-positive cells at a particular developmental stage is shown. Data are the mean $\pm$ S.D., $n = 3$. *E*, murine thymocytes from 4–6-week-old mice were stained with antibodies to CD4, CD8, CD11a, CD11b, CD19, CD45, $\alpha\beta$TCR, $\gamma\delta$TCR, and NK1.1 and FACS-sorted. RNA was isolated and subjected to RT-quantitative PCR with primers specific for CD148, actinβ, tubulinβ2A, TATA-box binding protein, HPRT1, or eEF-1α1. The relative amount of CD148 mRNA was determined after normalization using the geometric mean of mRNA levels of all used reference genes. The CD148 mRNA level in DN subpopulation was arbitrarily set as 1. Data are the mean $\pm$ S.D., $n = 4$.

and constituted a majority of CD44$^+$CD1a$^-$ cells (Fig. 3*C*). Interestingly, CD148 up-regulation was delayed after CD27 and CD69 markers as CD148 was rarely expressed before the cells reached a CD44$^+$CD1a$^-$ terminal stage (Fig. 3*C*). Expression of
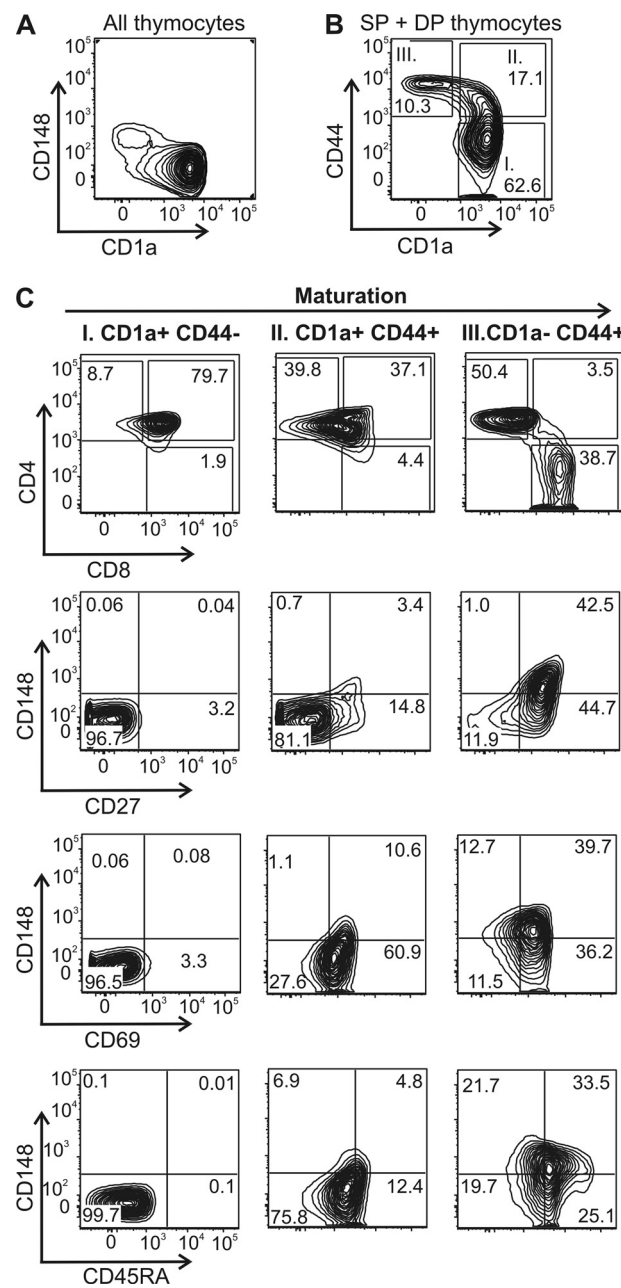

FIGURE 3. **CD148 is expressed exclusively on mature thymocytes in humans.** Human thymocytes were investigated by polychromatic flow cytometry after staining with antibodies to CD1a, CD3, CD4, CD8, CD44, CD45, CD148, and CD27 or CD45RA or CD69. A representative thymus (of three) is shown. *A*, staining of the entire thymocyte pool with CD148 and CD1a shows inverse correlation between the expressions of these two surface proteins. *B*, CD1a *versus* CD44 staining of SP+DP thymocyte pool (CD4$^+$ and/or CD8$^+$) shows three subsets representing three maturation stages from CD1a$^+$CD44$^-$ (here termed *I*) through CD1a$^+$CD44$^+$ (*II*) to CD1a$^-$CD44$^+$ (*III*). *C*, shown is expression of CD4 *versus* CD8 and CD148 *versus* CD27, CD69, or CD45RA of particular maturation stages gated as shown in *B*.

CD45RA splice isoform followed a similar kinetics as CD148. Interestingly, CD45RA and CD148 exhibited rather an inverse correlation on mature CD44$^+$CD1a$^-$ thymocytes (Fig. 3*C*).

Thus, CD148 is expressed mainly on CD44$^+$CD1a$^-$ SP thymocytes, representing the terminal stage of thymic T cell development. CD148 was also detected on an unusual subpopulation of DP thymocytes characterized by CD44$^+$CD1a$^-$ mature phenotype.
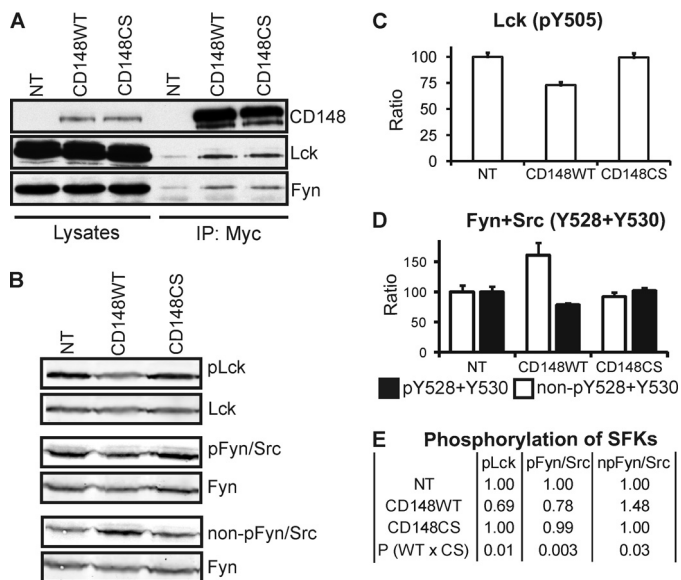
FIGURE 4. **CD148 binds Lck and Fyn and dephosphorylates their C-terminal tyrosines.** JS-7 cells transduced with CD148-WT or CD148-CS inactive mutant and non-transduced cells (*NT*) were used to study the ability of CD148 to bind and activate SFKs in T cells. *A*, Myc-tagged CD148-WT or CS mutant were immunoprecipitated from transduced JS-7 cell lysates with anti-Myc antibodies. Lysates and immunoprecipitates (*IP*) were analyzed by immunoblotting using anti-Lck, anti-Fyn, and anti-CD148 antibody. Non-transduced JS-7 cells were used as a negative control. A representative experiment (of five) is shown. *B*, cells were lysed, and levels of the phosphorylated form of Lck (Tyr(P)-505 (pLck)), total Lck, the phosphorylated forms of Fyn+Src (Tyr(P)-528 at Fyn, Tyr(P)-530 at Src (pFyn/Src)), the non-phosphorylated forms of Fyn+Src (Tyr-528 at Fyn, Tyr-530 at Src (non-pFyn/Src)), and total Fyn were detected via immunoblotting with specific antibodies. *C* and *D*, quantification of phosphorylated Lck and phosphorylated and non-phosphorylated levels of Fyn+Src normalized for total Lck and Fyn level, respectively, are shown. The quantification of immunoblots was performed by Odyssey infrared imaging system. Data represent the mean ± S.D. of triplicates of one representative experiment (of at least three). *E*, shown are relative levels of phosphorylated Lck, phosphorylated Fyn+Src, and non-phosphorylated Fyn+Src (normalized to total Lck and Fyn expression, respectively) in the CD148-WT and CD148-CS expressing cells compared with non-transduced cells. Data represent the mean from three independent experiments. *p* values for the significance of the difference between CD148-WT- and CD148-CS-expressing cells are also shown.

CD148 Dephosphorylates Src-family Kinases in T Cells—The positive role in signal transduction and selective ability of endogenous murine CD148 to complement CD45 deficiency in B cells and macrophages but not in T cells (24) could be explained by the lack of CD148 expression in DP stage where the major developmental block in CD45-deficient mice was observed. Alternatively, CD148 could play an opposite role in T cells. This hypothesis is supported by the observation that forced expression of physiologically relevant levels of CD148 in the human T cell line Jurkat resulted in inhibition of T cell signaling (29, 31). To determine whether CD148 is capable of activation of SFKs involved in TCR signaling, we ectopically expressed CD148 in JS-7 cells (33). JS-7 is a T cell line derived from Jurkat and was chosen because it does not express CD45 (33) and (like majority of leukemic T cell lines but in contrast to human peripheral T cells) contains only a low level of CD148 (supplemental Fig. 3), which results in defects in TCR signaling in these cells.

We retrovirally transduced JS-7 to express N-terminal Myc-tagged wild type CD148 (CD148-WT) and the C1239S phosphatase-dead mutant of CD148 (CD148-CS). The proteins

were surface-localized with proper transmembrane orientation (supplemental Fig. 3). Interestingly, Myc-CD148-WT or CS co-precipitated with Lck and Fyn (Fig. 4*A*), suggesting an interaction of CD148 with these SFKs in T cells, independent of CD148 phosphatase activity.

To assess the effect of CD148 expression on the activation state of SFKs in resting cells, we monitored phosphorylation status of SFKs using specific antibodies recognizing Lck phosphorylated at Tyr-505, Src phosphorylated at Tyr-530, or Src non-phosphorylated at Tyr-530 (numbers correspond to human Src protein) via immunoblotting. The latter two antibodies also stain an Src-related kinase Fyn when phosphorylated or non-phosphorylated at Tyr-528 (not shown); therefore, we detected an aggregate pool of Fyn and Src proteins (Fyn+Src) phosphorylated or not at their C-terminal inhibitory tyrosines. Expression of CD148-WT, but not catalytically inactive CS mutant, was associated with reduced phosphorylation of Tyr-505 on Lck (Fig. 4, *B*, *C*, and *E*). Similarly, Fyn and/or Src were also hypophosphorylated at the respective tyrosines in CD148-WT-expressing cells as revealed by the anti-pSrc and anti-non-pSrc antibody stainings (Fig. 4, *B*, *D*, and *E*). Staining with two complementary antibodies to non-phosphorylated and phosphorylated Src enabled us to estimate the ratio of phosphorylated Fyn+Src molecules in resting JS-7 cells and its change after CD148 expression (supplemental Fig. 4). Approximately one-third of Fyn+Src molecules were non-phosphorylated at C-terminal tyrosine in JS-7 cells. The expression of CD148 changed the amount of non-phosphorylated forms of Fyn+Src nearly to one-half of the total Fyn+Src pool. Lck Tyr-505 phosphorylation seemed to be even more affected by CD148 expression (Fig. 4*E*); unfortunately, the lack of antibody to non-phosphorylated Lck Tyr-505 prevented us from conducting a similar quantification in this case.

CD148 Is Able to Complement CD45 Deficiency in T Cells—Co-precipitation of Lck and Fyn with CD148 and the impact of CD148 expression on the phosphorylation status of SFKs in resting JS-7 cells suggested that Lck and Fyn and/or Src are recognized by CD148 as substrates. Because of CD45 deficiency, TCR triggering in JS-7 cells leads to only a weak response, especially under limiting TCR stimulation conditions. However, in contrast to other CD45-deficient T cell lines, JS-7 is still capable of some signaling, probably due to the presence of the Syk kinase (33, 39). The weaker TCR-mediated response of JS-7 enabled us to test the effects of ectopically expressed CD148-WT, CD148-CS, and CD45 (supplemental Fig. 3) on the TCR signaling capacity in these cells.

Activation via anti-TCR antibody induced a global increase of protein tyrosine phosphorylation in JS-7 cells that was substantially enhanced by expression of either CD148-WT or CD45 but not CD148-CS (Fig. 5*A*). CD148 and CD45 also induced phosphorylation of the activation loop tyrosines in SFKs both in resting and TCR-stimulated cells (Fig. 5*B*). Accordingly, TCR-induced Erk phosphorylation was higher in cells expressing CD148-WT or CD45 (Fig. 5*C*). Calcium increase was also positively regulated by CD148 and CD45 in JS-7 cells after the TCR engagement (Fig. 5*D*). CD69, an activation marker whose expression depends on Ras signaling pathways in T cells, was used for analysis of long term effects of TCR
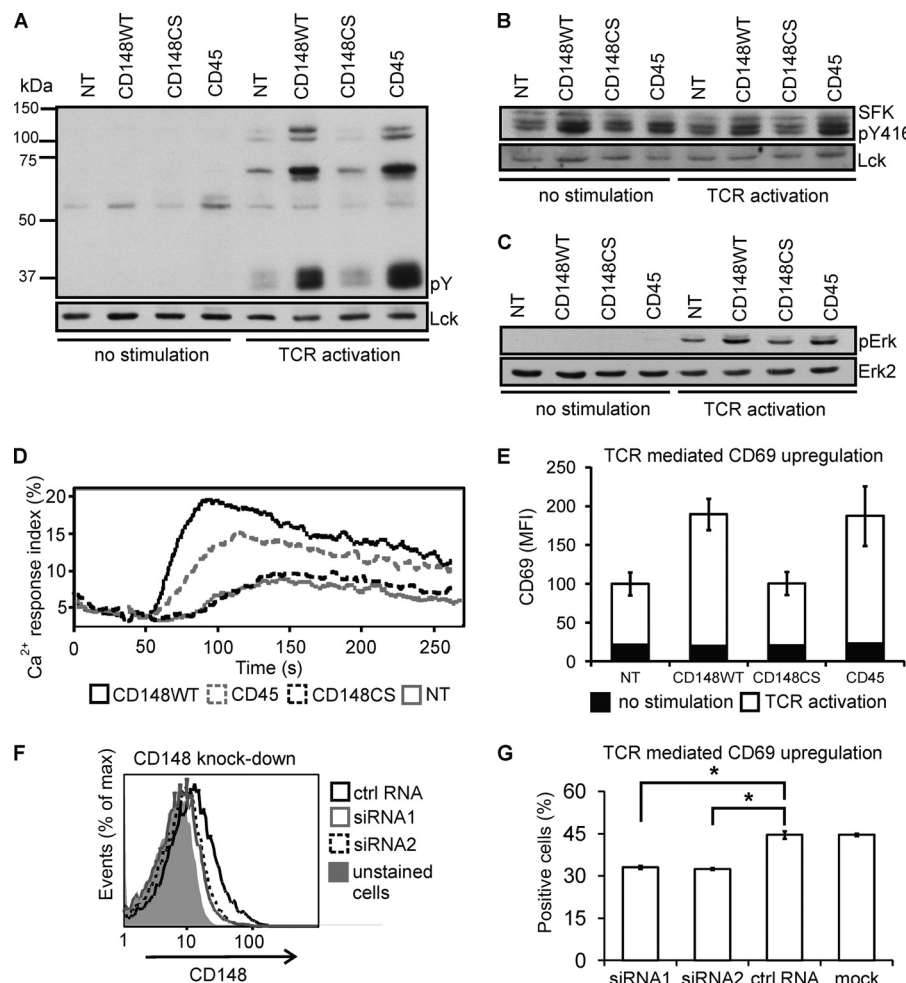
FIGURE 5. **CD148 complements CD45 deficiency of JS-7 cells.** JS-7 cells transduced with CD148-WT, CD148-CS inactive mutant, or CD45 and non-transduced cells (*NT*) were analyzed for intracellular signaling responses after TCR triggering (*A–E*), and the effects of CD148 knockdown on TCR signaling in JS-7 cells were examined (*F* and *G*). *A*, transgenic JS-7 cells and non-transduced cells were stimulated with 4 μg/ml anti-TCR-specific antibody for 30 s and immunoblotted after lysis. Anti-phosphotyrosine (*pY*) antibody was used to detect overall tyrosine phosphorylation in activated and non-activated cells. Re-probing the membrane with anti-Lck rabbit antibody served as a loading control. The phosphorylated bands in the non-stimulated samples probably represent Src family kinases that migrate in the corresponding molecular weight range. *B*, transgenic JS-7 cells and non-transduced cells were stimulated with 4 μg/ml anti-TCR-specific antibody for 30 s or left non-stimulated and immunoblotted after lysis. The blots were stained with the antibody to the activation loop tyrosine of SFKs (Tyr(P)-416 (*pY416*), numbered according to chicken Src). Re-probing the membrane with antibody to total-Lck served as a loading control. *C*, transgenic JS-7 cells and non-transduced cells were stimulated with 4 μg/ml anti-TCR specific antibody for 1 min and immunoblotted after lysis. Anti-phospho-Erk1/2 (Thr(P)-202/Tyr(P)-204 (pErk)) antibody was used to detect Erk activation in stimulated and non-stimulated cells. Re-probing the membrane with anti-Erk2 antibody was used as a loading control. *D*, JS-7 cells ectopically expressing CD148-WT (*solid black line*), CD148-CS mutant (*dashed black line*), or CD45 (*dashed gray line*) and non-transduced JS-7 cells (*solid gray line*) were analyzed by flow cytometry after Fluo4 loading. Anti-TCR antibody (200 ng/ml) was added 30 s after beginning the measurement. One representative experiment (of four) is shown. *E*, transduced JS-7 cells and non-transduced cells were activated via immobilized anti-TCR antibody overnight and examined for CD69 expression. *Black bars* represent the CD69 signal of non-stimulated cells (including autofluorescence), and *white bars* represent CD69 up-regulation after TCR stimulation. Data are the mean ± S.D. Data originate from triplicates from one representative experiment (of five). *F*, shown are the effects of CD148 silencing by electroporation of specific interfering RNA oligonucleotides on CD148 surface level in JS-7 cells. *G*, CD148 silenced and control JS-7 cells were examined for up-regulation of CD69 after plate-bound anti-TCR antibody stimulation via flow cytometry. *, $p < 0.005$. Data are the mean ± S.D. Data originate from triplicates from one representative experiment (of four).

stimulation. In agreement with the amplification of the proximal signaling pathways, CD69 expression was enhanced by CD148 and CD45 in activated but not resting cells (Fig. 5*E*).

The low but detectable level of CD148 in JS-7 cells allowed us to further reduce CD148 expression using small interfering RNA (Fig. 5*F*). Silencing of CD148 reduced the outcome of TCR triggering measured as the number of CD69 up-regulating cells (Fig. 5*G*).

Examination of the response of JS-7 cells to TCR activation provided us with solid evidence that CD148 is able not only to globally decrease the C-terminal tyrosine phosphorylation of

SFKs, but it can positively regulate those SFKs involved in TCR signal transduction. A similar role of CD148 in promoting TCR signaling was observed in two other CD45-deficient T cell lines also; that is, Jurkat cell-derived J45.01 and CD45⁻HPB-ALL, a cell line unrelated to Jurkat cells (Fig. 6).

CD45 Activity Determines the Net Effect of CD148 on LAT and PLCγ1 Phosphorylation after TCR Triggering—An inhibitory function of CD148 in the CD45-sufficient Jurkat T cell line was demonstrated previously using doxycycline-inducible expression. It has been shown that in these cells, CD148-WT, but not the CS mutant, inhibits TCR-induced phosphorylation

A

B
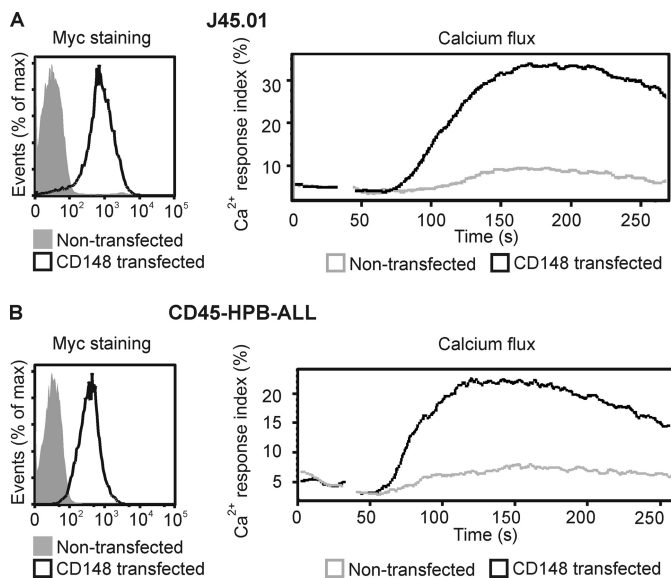
FIGURE 6. **CD148 complements CD45 deficiency in two additional T cell lines.** J45.01 cells (*A*) and CD45-HPB-ALL (*B*) were transduced with N-terminal Myc-tagged CD148-WT. Expression of CD148 was verified by extracellular anti-Myc staining followed by flow cytometry analysis. Calcium influx was measured by flow cytometry after Fluo4 loading. Anti-TCR antibody (2 μg/ml, for J45.01) or anti-CD3 antibody (40 μg/ml, for CD45⁻ HPB-ALL) was added 30 s after beginning the measurement. One representative experiment (of three) is shown.

of LAT and PLCγ1, leading to a hypothesis that these components of TCR signal transduction pathways are direct substrates of CD148 (29). We used the same Jurkat clones inducibly expressing CD148 WT or the inactive C1239S mutant (Fig. 7*A*), and we observed a similar negative effect of CD148 on LAT and PLCγ1 phosphorylation (Fig. 7*B*). In contrast, expression of CD148 in CD45-deficient JS-7 cells resulted in substantially enhanced phosphorylation of both LAT and PLCγ1 after TCR triggering (Fig. 7*C*). These results suggest that the positive effects of CD148 on SFKs over-balanced the potential negative effect on LAT and PLCγ1 phosphorylation in JS-7 cells.

CD148 Dephosphorylates Both C-terminal and Activation Loop Tyrosine in T Cells—We induced expression of CD148-WT or CD148-CS in the CD45-sufficient Jurkat cells and monitored changes in the phosphorylation status of Lck using the Odyssey infrared imaging system. Both tyrosines were significantly hypophosphorylated after the induction of CD148 wild type but not CS mutant expression (Fig. 7, *D* and *E*). This indicated that CD148 was able to dephosphorylate the C-terminal inhibitory tyrosine of Lck in T cells even in the presence of endogenous CD45. More importantly, our data indicate that the SFK activation loop phosphotyrosines are also substrates for CD148.

To further confirm that Lck is a direct substrate of CD148, we generated a substrate trapping D1205A (CD148-DA) mutant that covalently binds its substrates but is unable to catalyze the dephosphorylation reaction (21). Immunoprecipitation from cells transduced with CD148-WT and CD148-DA revealed that similar amounts of Lck co-precipitated with both constructs (Fig. 7*F*). However, the Lck co-precipitated with the trapping mutant exhibited much higher level of phosphorylation at both activating and inhibitory residues, indicating that both

tyrosines were trapped by the mutant and protected from dephosphorylation. Collectively, these data suggest that both activatory and inhibitory tyrosines of SFKs are substrates of CD148.

Selectivity of CD148 PTP Domain Does Not Depend on the Presence of the C-terminal Tyrosines—CD148 contains three tyrosines near its C terminus, one of which (Tyr-1320) is conserved not only among different vertebrate species but also among members of R3 subtype of receptor-like PTPs (26). C-terminal Tyr-789 of unrelated phosphatase PTPRA plays a crucial role in binding and recognition of Fyn in a phosphorylation-dependent manner (27). Although flanked by different residues than PTPRA Tyr-789, the C-terminal tyrosines corresponding to CD148 Tyr-1320 in three R3 subtype members were reported to bind Fyn after pervanadate-induced phosphorylation (40). To study the role of CD148 C-terminal tyrosines in recognition and dephosphorylation of SFKs, we generated Y1311F/Y1320F double tyrosine mutant (CD148−2YF) and Y1311F/Y1320F/Y1335F triple tyrosine mutant (CD148−3YF) (supplemental Fig. 5). Surprisingly, both CD148 tyrosine mutants were able to rescue TCR signaling in JS-7 cells, similarly to the wild type phosphatase (Fig. 8, *A–C*). To further study the mechanism by which CD148 interacts with SFKs, we generated a chimeric receptor-like PTP that contained extracellular, transmembrane, and submembrane parts of CD148 and the phosphatase domain of another phosphatase, SHP-1. CD148/SHP1 chimera-transduced JS-7 cells (supplemental Fig. 5) were unable to rescue signaling as measured in a number of different assays (Fig. 8, *A*, *B*, and *D*). Moreover, TCR-induced CD69 up-regulation was slightly weakened by the expression of the chimera, suggesting it was catalytically functional with an SHP-1-like inhibitory effect (Fig. 8*B*).

Considering these data, we hypothesize that C-terminal tyrosines of CD148 are not necessary for interaction of CD148 with SFKs in T cells. However, the inability of CD148/SHP1 chimera to promote TCR signaling in JS-7 cells suggests some level of selectivity of CD148 and SHP1 catalytic domains or their proximal structures.

DISCUSSION

CD148 has been previously shown to play a positive role in surface receptor signal transduction via dephosphorylation of inhibitory tyrosines of SFKs in B cells, macrophages, platelets, and some non-hematopoietic tissues (19, 23–25). On the other hand, CD148 has been reported to act as a negative regulator of signal transduction in many non-hematopoietic biological systems as well as in TCR signaling in human T cell line Jurkat (29–31). Moreover, endogenous CD148 is obviously unable to rescue T cell development in CD45-deficient mice and humans (41–44). To bring more clarity to these somewhat contradictory functions, we carried out a more thorough analysis of CD148 expression during T cell development in mice and humans and also tested the ability of CD148 to positively regulate SFKs involved in TCR signal transduction. We found striking differences in CD148 expression between human and murine thymocytes as well as peripheral T cells. Moreover, we were able to show that CD148 had the ability to positively reg-
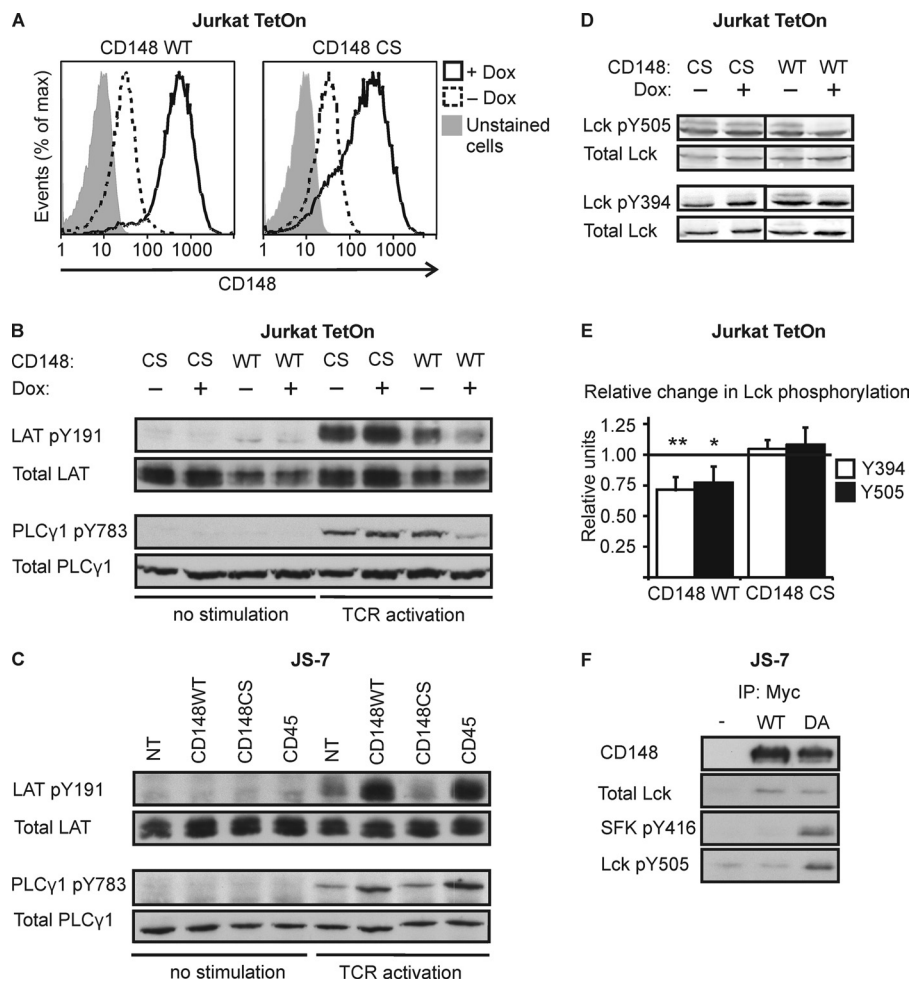
FIGURE 7. **Effects of CD148 on phosphorylation of its potential substrates in TCR signal transduction pathway.** *A*, expression of CD148- WT or C1239S mutant was induced with doxycycline (*Dox*) and analyzed by flow cytometry. *B*, expression of CD148-WT or CD148-CS was induced in Jurkat TetOn cells with doxycycline. Subsequently, the cells were stimulated with 4 μg/ml anti-TCR specific antibody for 30 s or left non-stimulated and immunoblotted after lysis. The phosphorylation status of LAT Tyr-191 and PLCγ1 Tyr-783 was detected with specific antibodies. Re-staining the membranes with antibodies to total LAT or PLCγ1, respectively, served as loading controls. *C*, non-transduced JS-7 cells (*NT*) and transgenic JS-7 cells expressing CD148 -WT, CD148-CS, or CD45 were stimulated with 4 μg/ml anti-TCR-specific antibody for 30 s or left non-stimulated and immunoblotted after lysis. The phosphorylation status of LAT Tyr-191 and PLCγ1 Tyr-783 was detected with specific antibodies. Re-probing the membranes with antibodies to total LAT or PLCγ1, respectively, served as loading controls. *D*, Jurkat cells inducibly expressing CD148-WT or CD148-CS were lysed, and phosphorylation of Lck inhibitory tyrosine 505 and Lck activation loop tyrosine 394 was detected by antibodies to Lck Tyr(P)-505 and Src Tyr(P)-416, respectively. Total Lck was used as a loading control. One representative experiment (of three) is shown. *E*, relative change in phosphorylation of both key Lck tyrosines normalized to total Lck after the induction of CD148-WT or CS expression was quantified using the Odyssey infrared imaging system. The level of phosphorylation in cells untreated with doxycycline was arbitrarily set as 1 (*black line*). Data are the mean $\pm$ S.D. ($n = 4$ for WT and 3 for CS). *, *p* (WT *versus* CS) < 0.05; **, *p* (WT *versus* CS) < 0.01. *F*, JS-7 cells expressing Myc-CD148-WT or Myc-CD148-DA and non-transduced cells were lysed in phosphate buffer without phosphatase inhibitors and subjected to immunoprecipitation (*IP*) via anti-Myc-tag antibody. The precipitates were immunoblotted and stained with antibodies to total Lck, Tyr(P)-416 of Src (SFK pY416), and Tyr(P)-505 of Lck.

ulate Src family kinase functions mediating TCR signal transduction in human T cell lines.

CD45-deficient mice exhibit a severe developmental block during thymocyte development (1) that sharply contrasts with developmental consequences in B cells and macrophages (24). Three published cases of CD45-deficient patients revealed an indispensable role of CD45 in the development of mature peripheral T cells also in humans (41–43). Here we clearly show that although murine thymocytes lose CD148 expression at early stages, human thymocytes gain CD148 positivity at the terminal phase. However, both humans and mice express very low levels of CD148 at the DP stage when positive selection takes place and when the development is blocked in the absence of CD45, potentially explaining the inability of CD148 to compensate for the loss of CD45 in T cell development. The limited

number of T cells that escape from thymus to the periphery in CD45-deficient mice and humans exhibit a strong functional defect (42, 44). However, the maturation status as well as the level of CD148 on these cells was not studied in the rare human cases.

Our data pointed to the restricted expression of CD148 to CD1a$^-$CD27$^+$CD44$^+$ terminal maturation stage of human thymocytes. CD1a is a commonly used diagnostic marker for T cell neoplasia. CD1a-positive cortical precursor T cell acute lymphoblastic leukemia cases were repeatedly reported to exhibit a better treatment response and survival prognosis in comparison with CD1a-negative T cell acute lymphoblastic leukemia both in children and adults (45, 46). Additionally, expression of CD1a correlated with susceptibility to *in vitro* induced apoptosis in childhood T cell acute lymphoblastic leu-
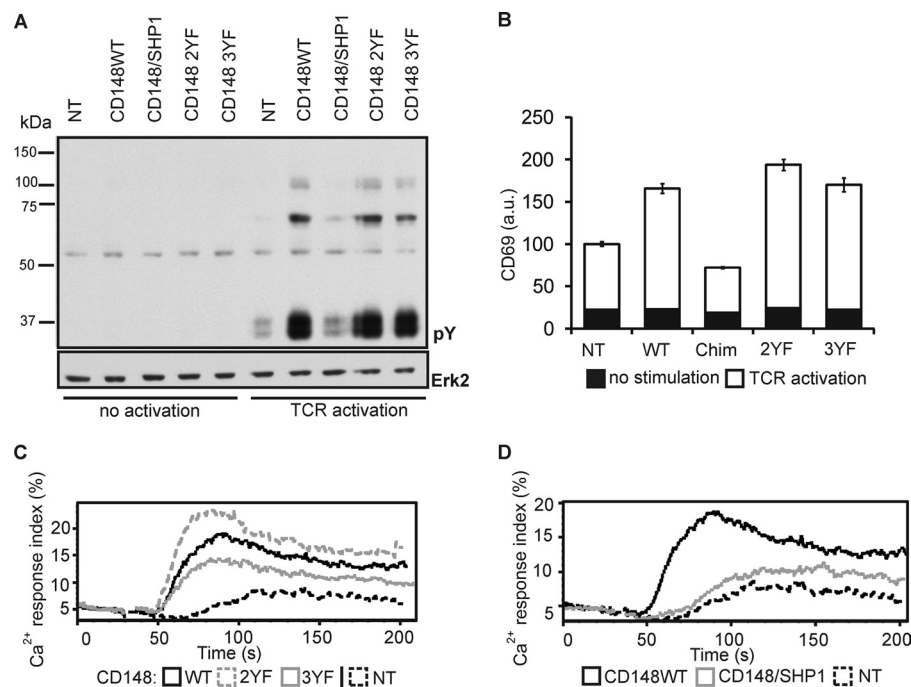
FIGURE 8. **Catalytic domain of CD148 but not the C-terminal tyrosines is required for SFK recognition as a substrate.** JS-7 cells transduced with CD148-WT, CD148–2YF mutant, CD148–3YF mutant, or CD148/SHP1 chimera and non-transduced cells (*NT*) were analyzed for intracellular signaling response after TCR triggering. *A*, transgenic JS-7 cells and non-transduced cells were stimulated with 4 μg/ml anti-TCR antibody for 30 s and immunoblotted. Anti-phosphotyrosine antibody was used to detect overall tyrosine phosphorylation in activated and non-activated cells. Re-probing the membrane with anti-Erk2 antibody was used as a loading control. *B*, transgenic JS-7 cells and non-transduced cells were activated via plate-bound anti-TCR antibody overnight and examined for CD69 expression via flow cytometry. *Black bars* represent CD69 signals in non-stimulated cells (including autofluorescence), whereas *white bars* represent CD69 up-regulation after TCR stimulation. Data are the mean ± S.D. Data originate from triplicates from one representative experiment (of four). *a.u.*, arbitrary units; *Chim*, chimera. *C*, JS-7 cells ectopically expressing CD148-WT (*solid black line*), CD148–2YF mutant (*dashed gray line*), or CD148–3YF mutant (*solid gray line*), and non-transduced JS-7 cells (*dashed black line*) were analyzed by flow cytometry after Fluo4 loading. Anti-TCR antibody (200 ng/ml) was added 30 s after beginning of the measurement. One representative experiment (of five) is shown. *D*, shown is the same experiment as in *C* with JS-7 cells ectopically expressing CD148-WT (*solid black line*) or CD148/SHP1 chimera (*solid gray line*) and non-transduced JS-7 cells (*dashed black line*). One representative experiment (of five) is shown.

kemia cells (47). Given the potential of CD148 to serve as an additional marker of mature T cell subset as well as the tumor suppressor properties of CD148 described in malignancies of solid tissues (11–14), it would be of high interest to analyze CD148 expression in T cell leukemia.

The absence of CD148 on mature peripheral T cells is in agreement with the lack of any described T cell phenotype of CD148 knock-out mice (24). However, a role for CD148 in mouse T cell biology cannot be completely excluded, as murine T cells up-regulate CD148 after activation (10). CD148 expression in human mature thymocytes and peripheral T cells implies that the function of CD148 in human T cells cannot be easily uncovered using a mouse model. We showed that expression of either CD148 or CD45 promotes TCR signaling in CD45-deficient human T cell lines, which reveals a level of redundancy between CD148 and CD45 in T cells not appreciated so far. Unavailability of CD45- or CD148-deficient humans restricted our functional analysis to cell lines. However, because we observed similar effects of CD148 on TCR signaling in three different CD45-negative T cell lines as well as in a knockdown experiment, we believe that our observations revealed a general mechanism rather than a particular cell line and/or overexpression-specific effect and were sufficient to prove that CD148 is capable of activating a T cell-specific set of SFKs, most notably Lck. Although Lck is also expressed in other cell types, it is really critical only in T cells, and the effect of

CD148 on the activity of this particular kinase has not been tested before. Our data thus broadened the spectrum of SFKs known to be activated by CD148 and suggest that selectivity of CD148 for specific members of this family may be limited. Moreover, we bring evidence that in addition to the C-terminal inhibitory phosphotyrosine, the activation loop phosphotyrosine in SFKs is also a substrate of CD148 in living cells. This finding is also supported by previous observations that recombinant CD148 phosphatase domain dephosphorylated activation loop tyrosines in SFKs *in vitro* (23, 48).

Our initial observations seemingly contradicted previous work that described the inhibitory effects of ectopically expressed CD148 in CD45-sufficient Jurkat T cells (29, 31). In our hands, CD148 had inhibitory effects in CD45-expressing Jurkat, whereas at the same time we observed activating effects in the CD45-deficient Jurkat clone JS-7. The most plausible explanation was that CD148 could impact TCR signaling both in a positive and negative manner. In CD45-negative JS-7 cells, CD148 expression led to reduced phosphorylation of the inhibitory tyrosine in Lck accompanied by enhanced activity of Lck and autophosphorylation of the activating tyrosine. In contrast, in CD45-positive cells both key tyrosines were hypophosphorylated when CD148 was expressed, probably as a consequence of substantially higher phosphatase activity resulting from concerted action of both CD45 and CD148. According to Nika *et al.* (49), the activity of Lck is mainly determined by the phosphor-

ylation status of the activation loop tyrosine, thus explaining reduced kinase activity when both tyrosines are dephosphorylated. We concluded that CD148 influences the activity of Lck negatively via dephosphorylation of the activation loop phosphotyrosine and positively through dephosphorylation of the C-terminal phosphotyrosine. This is consistent with the inhibitory impact of CD148 on TCR signaling in CD45-positive T cells, and it is also very similar to the observed effects of altering the CD45 expression level in murine thymocytes (50, 51).

Thus, our data indicate that CD148 regulates SFKs in T cells in a similar manner as CD45 and suggest that the activity of CD45 is the decisive factor determining whether the net effect of CD148 expression is an enhancement or an inhibition of TCR signal transduction. Importantly, this can be dependent not only on the regulation of SFKs but also on direct dephosphorylation of other proteins, such as PLCγ or LAT, as suggested before (27).

Although the canonical TCR pathway has been intensively studied, less is known about TCR signaling in particular biological contexts, characterized by different T cell life stages of differentiation (*e.g.* thymic stages, naïve mature, activated, or memory T cells), T cells lineages (*e.g.* CD8$^+$ or CD4$^+$, Th1, Th2, Th17, or regulatory T cells), or conditions (tonic or ligand dependent). Importantly, CD148 expression and CD45 splicing differ among particular T cell subsets (our data and Refs. 6, 8, 10, and 44). Furthermore, it has been shown that CD45 differentially regulates basal and inducible TCR signaling in murine thymocytes (50). Thus, the effects of CD148 activity could vary substantially depending on particular T cell developmental stage, lineage, and other circumstances. Recently, several mouse genetic models with varied CD45 expression level or activity have been developed and intensively studied to improve the understanding of the complex behavior of CD45 in T cells (50, 51). Given the differential expression of CD148 on T cells together with the ability of CD148 to regulate SFKs in a similar manner as CD45, CD148 activity should be taken into account when applying such findings to humans.

Phosphorylation of a SFK C-terminal tyrosine inhibits the catalytic activity by stabilizing it in the closed conformation via intramolecular interaction with SH2 and SH3 domains. To explain how a PTP can access the nested phosphotyrosine, a phosphotyrosine displacement model was suggested (27). According to this model, a C-terminal tyrosine of the PTP gets phosphorylated and subsequently competitively binds to the SH2 domain of the SFK, resulting in the release of the closed conformation and access of the PTP to the phosphorylated C-terminal site of the kinase. Although the experimental evidence supporting this model comes from studies done on PTPs of R4 subtype, other unrelated receptor-like phosphatases including CD148 also usually contain at least one tyrosine at their C-terminal region. Moreover, phosphatases PTPRO, SAP-1 (PTPRH), and VE-PTP (PTPRB) related to CD148 were shown to bind Fyn after pervanadate-induced phosphorylation via their C-terminal tyrosine, indicating the phosphotyrosine displacement model can be valid also for PTPs of R3 subtype (26, 40). However, this model was never directly tested using a member of R3 family. Here we show that mutation of all three CD148 C-terminal tyrosines to phenylalanines does not inhibit

its ability to enhance TCR signaling. These results led us to conclude that the phosphotyrosine displacement model for CD148 does not apply. On the other hand, the finding that the CD148/SHP-1 swap chimera, containing the SHP-1 catalytic domain, failed to enhance TCR signaling suggests a specific interaction mechanism between CD148 and SFKs.

Our investigation demonstrated that CD148 is able to activate SFKs involved in TCR signal transduction. This could be most clearly observed in CD45 deficient environment. In CD45-sufficient T cell line, the proactivatory effect on the Lck inhibitory tyrosine is overbalanced by dephosphorylating the activation loop tyrosine of Lck and/or other substrates essential for TCR signal transduction leading to the net inhibitory effect of CD148 (29, 31). Together with the analogous dual role of CD45 (50, 51), our study suggests that dual inhibitory/stimulatory function may be a common principle governing the signaling by different receptor-like PTPs. The net outcome of their action may depend on cellular or biochemical context.

REFERENCES

1. Hermiston, M. L., Zikherman, J., and Zhu, J. W. (2009) *Immunol. Rev.* **228,** 288–311
2. Honda, H., Inazawa, J., Nishida, J., Yazaki, Y., and Hirai, H. (1994) *Blood* **84,** 4186–4194
3. Kuramochi, S., Matsuda, S., Matsuda, Y., Saitoh, T., Ohsugi, M., and Yamamoto, T. (1996) *FEBS Lett.* **378,** 7–14
4. Zhang, L., Martelli, M. L., Battaglia, C., Trapasso, F., Tramontano, D., Viglietto, G., Porcellini, A., Santoro, M., and Fusco, A. (1997) *Exp. Cell Res.* **235,** 62–70
5. Autschbach, F., Palou, E., Mechtersheimer, G., Rohr, C., Pirotto, F., Gassler, N., Otto, H. F., Schraven, B., and Gaya, A. (1999) *Tissue Antigens* **54,** 485–498
6. Schraven, B., Hegen, M., Autschbach, F., Gaya, A., Schwartz, C., and Meuer, S. (1997) in *Leukocyte Typing VI* (Kishimoto, T., ed) pp. 576–580, Garland Publishing, Inc., New York
7. de la Fuente-García, M. A., Nicolás, J. M., Freed, J. H., Palou, E., Thomas, A. P., Vilella, R., Vives, J., and Gayá, A. (1998) *Blood* **91,** 2800–2809
8. Tangye, S. G., Phillips, J. H., Lanier, L. L., de Vries, J. E., and Aversa, G. (1998) *J. Immunol.* **161,** 3249–3255
9. Gayà, A., Pirotto, F., Palou, E., Autschbach, F., Del Pozo, V., Solé, J., and Serra-Pages, C. (1999) *Leuk. Lymphoma* **35,** 237–243
10. Lin, J., Zhu, J. W., Baker, J. E., and Weiss, A. (2004) *J. Immunol.* **173,** 2324–2330
11. Ruivenkamp, C. A., van Wezel, T., Zanon, C., Stassen, A. P., Vlcek, C., Csikós, T., Klous, A. M., Tripodis, N., Perrakis, A., Boerrigter, L., Groot, P. C., Lindeman, J., Mooi, W. J., Meijjer, G. A., Scholten, G., Dauwerse, H., Paces, V., van Zandwijk, N., van Ommen, G. J., and Demant, P. (2002) *Nat. Genet.* **31,** 295–300
12. Trapasso, F., Iuliano, R., Boccia, A., Stella, A., Visconti, R., Bruni, P., Baldassarre, G., Santoro, M., Viglietto, G., and Fusco, A. (2000) *Mol. Cell. Biol.* **20,** 9236–9246
13. Massa, A., Barbieri, F., Aiello, C., Arena, S., Pattarozzi, A., Pirani, P., Corsaro, A., Iuliano, R., Fusco, A., Zona, G., Spaziante, R., Florio, T., and Schettini, G. (2004) *J. Biol. Chem.* **279,** 29004–29012
14. Ruivenkamp, C., Hermsen, M., Postma, C., Klous, A., Baak, J., Meijer, G., and Demant, P. (2003) *Oncogene* **22,** 3472–3474
15. Trapasso, F., Yendamuri, S., Dumon, K. R., Iuliano, R., Cesari, R., Feig, B.,

Seto, R., Infante, L., Ishii, H., Vecchione, A., During, M. J., Croce, C. M., and Fusco, A. (2004) *Carcinogenesis* **25,** 2107–2114

16. Balavenkatraman, K. K., Jandt, E., Friedrich, K., Kautenburger, T., Pool-Zobel, B. L., Ostman, A., and Böhmer, F. D. (2006) *Oncogene* **25,** 6319–6324

17. Keane, M. M., Lowrey, G. A., Ettenberg, S. A., Dayton, M. A., and Lipkowitz, S. (1996) *Cancer Res.* **56,** 4236–4243

18. Kovalenko, M., Denner, K., Sandström, J., Persson, C., Gross, S., Jandt, E., Vilella, R., Böhmer, F., and Ostman, A. (2000) *J. Biol. Chem.* **275,** 16219–16226

19. Chabot, C., Spring, K., Gratton, J. P., Elchebly, M., and Royal, I. (2009) *Mol. Cell. Biol.* **29,** 241–253

20. Grazia, Lampugnani, M., Zanetti, A., Corada, M., Takahashi, T., Balconi, G., Breviario, F., Orsenigo, F., Cattelino, A., Kemler, R., Daniel, T. O., and Dejana, E. (2003) *J. Cell Biol.* **161,** 793–804

21. Palka, H. L., Park, M., and Tonks, N. K. (2003) *J. Biol. Chem.* **278,** 5728–5735

22. Tsuboi, N., Utsunomiya, T., Roberts, R. L., Ito, H., Takahashi, K., Noda, M., and Takahashi, T. (2008) *Biochem. J.* **413,** 193–200

23. Pera, I. L., Iuliano, R., Florio, T., Susini, C., Trapasso, F., Santoro, M., Chiariotti, L., Schettini, G., Viglietto, G., and Fusco, A. (2005) *Oncogene* **24,** 3187–3195

24. Zhu, J. W., Brdicka, T., Katsumoto, T. R., Lin, J., and Weiss, A. (2008) *Immunity* **28,** 183–196

25. Senis, Y. A., Tomlinson, M. G., Ellison, S., Mazharian, A., Lim, J., Zhao, Y., Kornerup, K. N., Auger, J. M., Thomas, S. G., Dhanjal, T., Kalia, N., Zhu, J. W., Weiss, A., and Watson, S. P. (2009) *Blood* **113,** 4942–4954

26. Matozaki, T., Murata, Y., Mori, M., Kotani, T., Okazawa, H., and Ohnishi, H. (2010) *Cell. Signal.* **22,** 1811–1817

27. Zheng, X. M., Resnick, R. J., and Shalloway, D. (2000) *EMBO J.* **19,** 964–978

28. Palou, E., de la Fuente-García, M. A., Nicolás, J. M., Vilardell, C., Vives, J., and Gayá, A. (1997) *Immunol. Lett.* **57,** 101–103

29. Baker, J. E., Majeti, R., Tangye, S. G., and Weiss, A. (2001) *Mol. Cell. Biol.* **21,** 2393–2403

30. Tangye, S. G., Wu, J., Aversa, G., de Vries, J. E., Lanier, L. L., and Phillips, J. H. (1998) *J. Immunol.* **161,** 3803–3807

31. Lin, J., and Weiss, A. (2003) *J. Cell Biol.* **162,** 673–682

32. Weiss, A., and Stobo, J. D. (1984) *J. Exp. Med.* **160,** 1284–1299

33. Peyron, J. F., Verma, S., de Waal Malefyt, R., Sancho, J., Terhorst, C., and Spits, H. (1991) *Int. Immunol.* **3,** 1357–1366

34. Shiroo, M., Goff, L., Biffen, M., Shivnan, E., and Alexander, D. (1992)

EMBO J. **11,** 4887–4897

35. Koretzky, G. A., Picus, J., Schultz, T., and Weiss, A. (1991) *Proc. Natl. Acad. Sci. U.S.A.* **88,** 2037–2041

36. Res, P., Blom, B., Hori, T., Weijer, K., and Spits, H. (1997) *J. Exp. Med.* **185,** 141–151

37. Patel, D. D., Hale, L. P., Wichard, L. P., Radcliff, G., Mackay, C. R., and Haynes, B. F. (1995) in *Leukocyte Typing V* (Schlossman, S. F., ed) pp. 1725–1727, Oxford University Press, New York

38. Stauder, R., Terpe, H. J., Stark, H., Thaler, J., Mackay, C., and Gunthert, U. (1995) in *Leukocyte Typing V* (Schlossman, S. F., ed) pp. 1719–1723, Oxford University Press, New York

39. Chu, D. H., Spits, H., Peyron, J. F., Rowley, R. B., Bolen, J. B., and Weiss, A. (1996) *EMBO J.* **15,** 6251–6261

40. Murata, Y., Mori, M., Kotani, T., Supriatna, Y., Okazawa, H., Kusakari, S., Saito, Y., Ohnishi, H., and Matozaki, T. (2010) *Genes Cells* **15,** 513–524

41. Cale, C. M., Klein, N. J., Novelli, V., Veys, P., Jones, A. M., and Morgan, G. (1997) *Arch. Dis. Child* **76,** 163–164

42. Kung, C., Pingel, J. T., Heikinheimo, M., Klemola, T., Varkila, K., Yoo, L. I., Vuopala, K., Poyhonen, M., Uhari, M., Rogers, M., Speck, S. H., Chatila, T., and Thomas, M. L. (2000) *Nat. Med.* **6,** 343–345

43. Tchilian, E. Z., Wallace, D. L., Wells, R. S., Flower, D. R., Morgan, G., and Beverley, P. C. L. (2001) *J. Immunol.* **166,** 1308–1313

44. Hermiston, M. L., Xu, Z., and Weiss, A. (2003) *Annu. Rev. Immunol.* **21,** 107–137

45. Schabath, R., Ratei, R., and Ludwig, W. D. (2003) *Best Pract. Res. Clin. Haematol.* **16,** 613–628

46. Marks, D. I., Paietta, E. M., Moorman, A. V., Richards, S. M., Buck, G., DeWald, G., Ferrando, A., Fielding, A. K., Goldstone, A. H., Ketterling, R. P., Litzow, M. R., Luger, S. M., McMillan, A. K., Mansour, M. R., Rowe, J. M., Tallman, M. S., and Lazarus, H. M. (2009) *Blood* **114,** 5136–5145

47. Wuchter, C., Ruppert, V., Schrappe, M., Dörken, B., Ludwig, W. D., and Karawajew, L. (2002) *Blood* **99,** 4109–4115

48. Ellison, S., Mori, J., Barr, A. J., and Senis, Y. A. (2010) *J. Thromb. Haemost.* **8,** 1575–1583

49. Nika, K., Soldani, C., Salek, M., Paster, W., Gray, A., Etzensperger, R., Fugger, L., Polzella, P., Cerundolo, V., Dushek, O., Höfer, T., Viola, A., and Acuto, O. (2010) *Immunity* **32,** 766–777

50. Zikherman, J., Jenne, C., Watson, S., Doan, K., Raschke, W., Goodnow, C. C., and Weiss, A. (2010) *Immunity* **32,** 342–354

51. McNeill, L., Salmond, R. J., Cooper, J. C., Carret, C. K., Cassady-Cain, R. L., Roche-Molina, M., Tandon, P., Holmes, N., and Alexander, D. R. (2007) *Immunity* **27,** 425–437
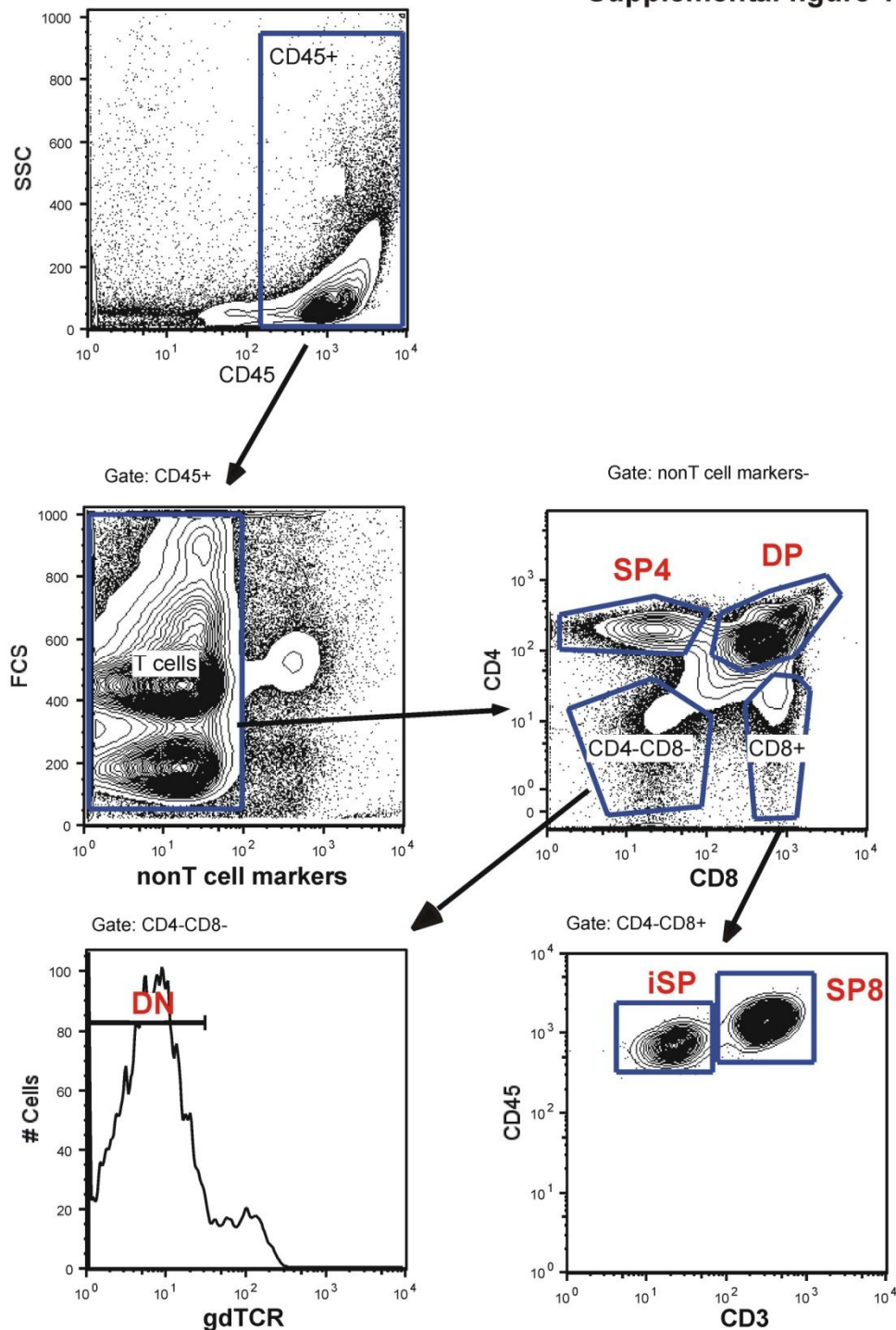
FIGURE S1. Gating strategy used for murine thymocytes. T cells were gated as $CD45^+CD19^-$ $NK1.1^-CD11c^-$ thymocytes. T-cell subpopulations were defined as follows: DN ($CD4^-CD8^-$ $\gamma\delta TCR^-$), iSP ($CD3^-$, $CD4^-$, $CD8^+$), DP ($CD4^+CD8^+$), SP8 ($CD4^-CD8^+CD3^+$), and SP4 ($CD4^+CD8^-$).
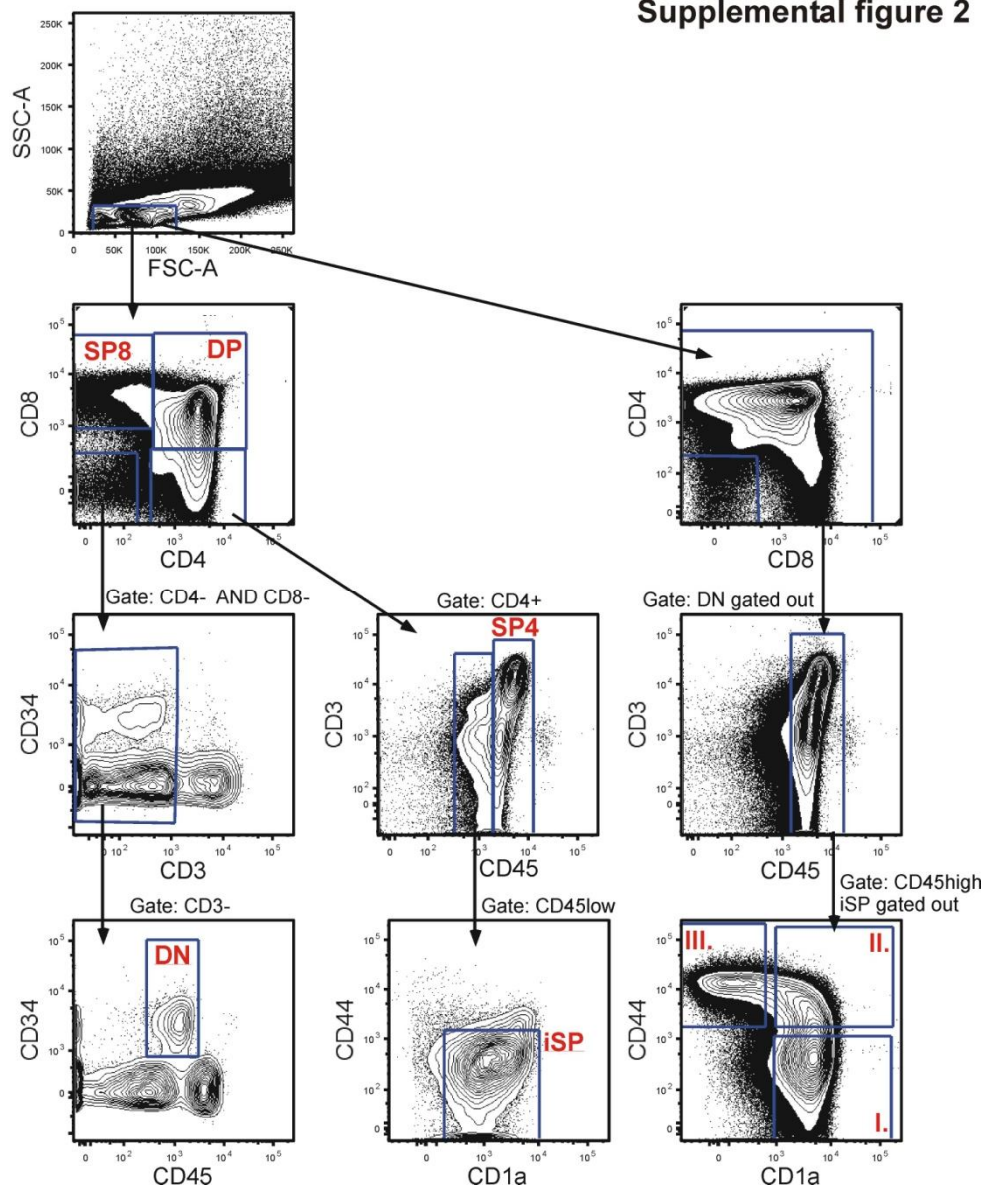
FIGURE S2. Gating strategy used for human thymocytes. DN cells were defined as CD4$^-$CD8$^-$CD3$^-$CD34$^+$CD45^{dim}, iSP as CD4$^+$ CD45^{dim}, DP as CD8$^+$CD4$^+$, SP8 as CD4$^-$CD8$^+$, and SP4 as CD4$^+$CD8$^-$CD45$^+$ thymocytes. Gating of DP+SP4+SP8 cells for CD1a vs CD44 analysis is also provided.

Supplemental figure 3
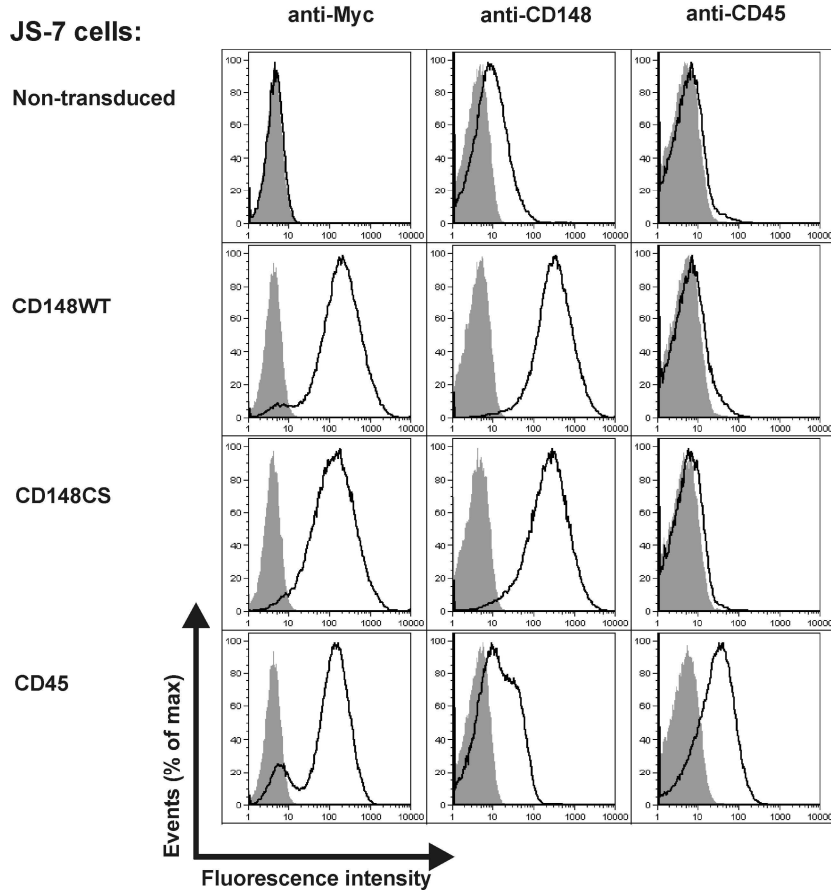
FIGURE S3. Expression of CD148 and CD45 constructs in JS-7 transfectants I. JS-7 cells transduced with Myc-tagged CD148-WT, CD148-CS, or CD45 and non-transduced cells were examined for expression of CD148, CD45, and extracellular Myc-tag by flow cytometry (solid black line). Unstained controls are shown as filled grey histograms.

Supplemental figure 4

A

	NT	CD148
Relative pSrc Y530 signal	1	*a*
Relative non-pSrc Y530 signal	1	*b*

B

	NT	CD148
Phosphorylated molecules (ratio)	*x*	*x-d*
Non-phosphorylated molecules (ratio)	*1-x*	*1-x+d*

C

I. $a = (x-d)/x$

II. $b = (1-x+d)/(1-x)$

**D**

$x = (b-1)/(b-a)$

$d = (a+b-a*b-1)/(b-a)$

E

	NT	CD148
Phosphorylated molecules (ratio)	$(b-1)/(b-a)$	$(a*b-a)/(b-a)$
Non-phosphorylated molecules (ratio)	$(1-a)/(b-a)$	$(b-a*b)/(b-a)$

F

	NT	CD148
Phosphorylated molecules	69%	53%
Non-phosphorylated molecules	31%	47%

FIGURE S4. Calculation of the percentage of C-terminal tyrosine phosphorylated Fyn+Src molecules in JS-7 cells and its change after expression of CD148. (A) Definition of input parameters a, b. Mean signals from pSrc Y530 and non-pSrc Y530 antibody stainings of non-transduced JS-7 cell lysates were set as 1, while mean signals obtained from staining of CD148-WT transduced cell lysates were set as "a" and "b" for pSrc Y530 and non-pSrc Y530, respectively. (B) Definition of calculated variables x, d. "x" represents a fraction of phosphorylated Fyn+Src molecules in non-transfected JS-7 cells and "d" represents decrease in "x" after expression of CD148 phosphatase. (C) The system of two simultaneous equations describes the relation between "a", " b" and "x", "d". (D) Solution of the equations for x and d. (E) The table shows the fractions of phosphorylated and non-phosphorylated Fyn+Src molecules in non-transduced and CD148 expressing cells after substituting the values determined from the equations for the variables in the table in (B). (F) Calculated results for

Supplemental Figure 5
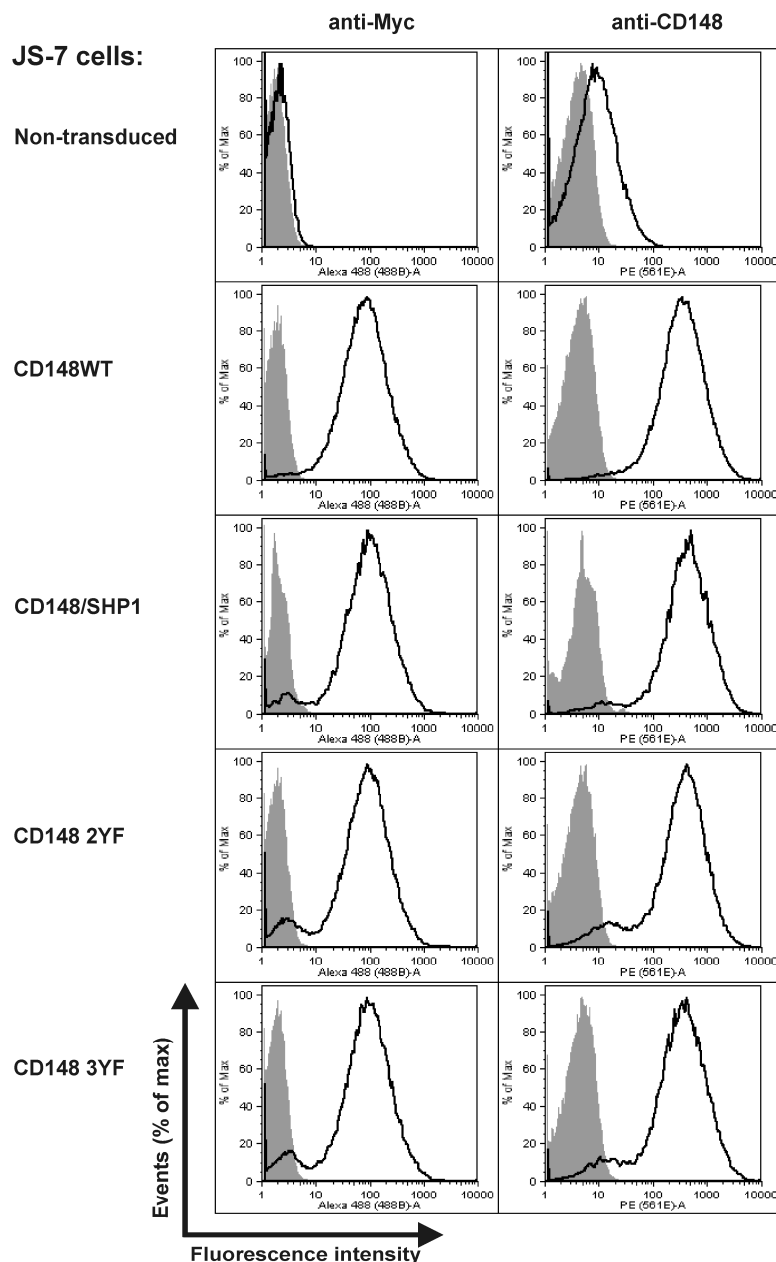
FIGURE S5. Expression of CD148 constructs in JS-7 transfectants II. JS-7 cells transduced with Myc-tagged CD148-WT, CD148/SHP1 chimera, CD148-2YF, or CD148-3YF and non-transduced cells were examined for expression of CD148 and extracellular Myc-tag by flow cytometry (solid black line). Unstained controls are shown as filled grey histograms.